Stimulation of CD8 T cells with membrane vesicles prepared from antigen presenting cells

Author:
Jin, Dongbin

Publication Date:
2015

DOI:
https://doi.org/10.26190/unsworks/18250

Stimulation of CD8 T cells with membrane vesicles prepared from antigen presenting cells

Dongbin Jin

A thesis submitted for the degree of
Doctor of Philosophy
in the Faculty of Medicine, University of New South Wales

Immunology Division
Garvan Institute of Medical Research
Darlinghurst, Sydney, Australia

March 2015

THE UNIVERSITY OF NEW SOUTH WALES

Thesis/Dissertation Sheet

Surname or Family name: **Jin**

First name: **Dongbin** Other name/s:

Abbreviation for degree as given in the University calendar: **Ph.D**

School: **Clinical School - St. Vincents** Faculty: **Medicine**

Title: **Stimulation of CD8 T cells with membrane vesicles prepared from antigen presenting cells**

Abstract 350 words maximum: (PLEASE TYPE)

Immunotherapy has emerged as a promising tool to treat diseases via enhancing or suppressing immune responses of T cells. For infectious diseases and cancer, inducing expansion of antigen–specific CD8 T cells has proved effective in preclinical and clinical studies for eliminating infected or malignant cells. In this thesis a subcellular vaccine prepared by sonication of disrupted mature dendritic cells (DCs) followed by loading with specific peptides was developed and used to stimulate naïve CD8 T cells. To achieve this, a new culture method was developed to prepare large numbers of mature DCs from mouse bone marrow (BM). Cell disruption and sonication of these BMDCs yielded membrane vesicle nano-particles that were immunogenic for CD8 T cells both *in vitro* and *in vivo*. Notably, the *in vivo* immunogenicity of the vesicles was considerably increased when co-delivered with anti-CD9 antibodies and CpG oligodeoxynucleotides, especially when given in multiple injections. Preliminary experiments demonstrated the potential of membrane vesicles for cancer immunotherapy in murine models.

FOR OFFICE USE ONLY **Date of completion of requirements for Award:**

THIS SHEET IS TO BE GLUED TO THE INSIDE FRONT COVER OF THE THESIS

ORIGINALITY STATEMENT

'I hereby declare that this submission is my own work and to the best of my knowledge it contains no materials previously published or written by another person, or substantial proportions of material which have been accepted for the award of any other degree or diploma at UNSW or any other educational institution, except where due acknowledgement is made in the thesis. Any contribution made to the research by others, with whom I have worked at UNSW or elsewhere, is explicitly acknowledged in the thesis. I also declare that the intellectual content of this thesis is the product of my own work, except to the extent that assistance from others in the project's design and conception or in style, presentation and linguistic expression is acknowledged.'

Signed .....

Dongbin Jin

Date 26 March 2015

COPYRIGHT STATEMENT

'I hereby grant to the University of New South Wales or its agents the right to archive and to make available my thesis or dissertation in whole or part in the University libraries in all forms of media, now or hereafter known, subject to the provisions of the Copyright Act 1968. I retain all proprietary rights, such as patent rights. I also retain the right to use in future works (such as articles or books) all or part of this thesis or dissertation. I also authorise University Microfilms to use the abstract of my thesis in Dissertations Abstract International (this is applicable to doctoral theses only). I have either used no substantial portions of copyright material in my thesis or I have obtained permission to use copyright material; where permission has not been granted I have applied/will apply for a partial restriction of the digital copy of my thesis or dissertation.'

Signed .....

Dongbin Jin

Date 26 March 2015

AUTHENTICITY STATEMENT

'I certify that the Library deposit digital copy is a direct equivalent of the final officially approved version of my thesis. No emendation of content has occurred and if there are any minor variations in formatting, they are the result of the conversion to digital format.'

Signed .....

Dongbin Jin

Date 26 March 2015

ACKNOWLEDGEMENTS

Many thanks to my supervisor, Prof. Jonathan Sprent for providing continued guidance and support throughout the course of this project. Thank you to my co-supervisors A/Prof. Cecile King and Dr. Jae-Ho Cho for their invaluable comments and help.

Thank you to Sprent Lab members of past and present. Special thanks go to Amanda for excellent research assistance, encouragements and much more. Thank you to Rachel for transferring techniques related to this project. Thank you to Heeok for help with immunoblotting. Thank you to Kylie, Theresa, Jessica, and Gabriela for kind help and advice.

Thanks to all the support from the Immunology Division and the Garvan Facilities, particularly the Flow Cytometry and the BTF. Special thanks go to Dipti and Joanna for providing kind assistance for some of my experiments.

Lastly, thank you to my family (Jing, Gloria, Shenqi and Ailin) and my parents for their love, encouragement and patience.

Experiments that were not the sole work of the author

All experiments were performed by the author at the Garvan Institute of Medical Research, with the following exceptions:

Amanda Hong performed TCR transgenic mice genotyping.

Amanda Hong and **Joanna Warren** provided help for single cell preparations of mouse spleen and lymph nodes for some experiments.

Dr. Dipti Vijayan provided technical help for Immunofluorescence Microscopy.

Dr. Heeok Kim provided technical help for Immunoblotting.

TABLE OF CONTENTS

LIST OF FIGURES

ABBREVIATIONS

aAPC	Artificial antigen presenting cell
Ab	Antibody
AIDS	Acquired immunodeficiency syndrome
APC	Antigen presenting cell
BCR	B cell receptor
Bcl-2	B cell lymphoma-2
BD	Becton Dickinson
BM	Bone marrow
BMDC	Bone marrow derived dendritic cell
BSA	Bovine serum albumin
CCR	C-C chemokine receptor
CD	Cluster of differentiation
cDC	Conventional dendritic cell
CFSE	Carboxyfluorescein succinimidyl ester
CLR	C-type lectin receptor
cTEC	Cortical epithelial cells
CTL	Cytotoxic T lymphocyte
CTLA-4	Cytotoxic T lymphocyte antigen-4
CpG	Cytosine-phosphate-Guanine
c.p.m	Counts per minutes
CXCR	CXC chemokine receptors
DC	Dendritic cell
DN	Double negative thymocytes
DNA	Deoxyribonucleic acid
DN	Double negative thymocytes
DP	Double positive thymocytes
ELISA	Enzyme-linked immunosorbent assay
EBV	Epstein–Barr virus
ER	Endoplasmic reticulum
FACS	Flourescence activated cell sorting
Fc	Fragment crystallizable region
FcR	Fc receptor
FCS	Fetal calf serum
FDA	Food and Drug Administration
FDC	Follicular DC
FITC	Fluorescein isothiocyanate
Foxp3	Forkhead box P3
FSC	Forward scatter
GMCSF	Granulocyte macrophage colony stimulating factor
IFNγ	Interferon-gamma
ICAM-1	Intercellular adhesion molecule 1
IDO	Indoleamine 2,3-dioxygenase
Ig	Immunoglobulin
IL	Interleukin
ILC	Innate lymphoid cell
IRF	Interferon regulatory factor

IS	Immunological synapse
I.T.	Intra-tumour
iTreg	Induced T regulatory cells
I.V.	Intravenous
LFA-1	Lymphocyte function-associated antigen 1
LN	Lymph node
LPS	Lipopolysaccharide
mAb	Monoclonal antibody
MACS	Magnetic activated cell sorting
MAPK	Mitogen-activated protein kinases
MHC	Major histocompatibility complex
NFκB	Nuclear factor-kB
NK	Natural killer
NKT	Natural killer T
NLR	NOD-like receptor
nTreg	Natural T regulatory cells
ODN	Oligodeoxynucleotides
OVA	Ovalbumin
PALS	Peri-arteriolar lymphoid sheath
PAPM	Pathogen-associated molecular pattern
PBS	Phosphate buffered saline
PD-1	Programmed death-1
pDC	Plasmacytoid dendritic cell
PDL-1	Programmed death ligand-1
pMHC	Peptide/MHC complexes
PRR	Pattern recognition receptors
pV	Peptide pulsed membrane vesicles
RBC	Red blood cell
RLR	RIG-I-like receptor
RNA	Ribonucleic acid
RT	Room temperature
SAv-HRP	Streptavidin-Horseradish Peroxidase
S.C.	Subcutaneous
SD	Standard deviation
SDS	Sodium dodecyl sulfate
SLO	Secondary lymphoid organ
SMAC	Supramolecular activation cluster
SP	Single positive thymocytes
TCR	T-cell receptor
Tfh	T follicular helper
Th	T helper
TGFβ	Transforming growth factor beta
TLR	Toll like receptor
TNF	Tumor necrosis factor
TIL	Tumour-infiltrating lymphocytes
Treg	Regulatory T cells
TRP-2	Tyrosinase related protein-2

1 Introduction

1.1 The immune system

The immune system is a complex network of multiple organs, cells and molecules that protects the host from invading pathogens and malignant cells whilst maintaining tolerance to healthy self-tissues and beneficial commensal organisms. This process needs to be tightly controlled to prevent self-tissue destruction and the development of autoimmune diseases, while ensuring a robust immune response against pathogens and abnormal tissue.

Immune defence is achieved through the coordination of two arms of the immune system, known as the innate and adaptive immune systems (Figure 1). The innate immune system provides both anatomical barriers and immediate responses by promptly initiating a local inflammatory reaction. The adaptive immune system responds to specific antigens, which are targets for the receptors of the adaptive immune response, and provides long-lasting protection against subsequent antigenic challenges by the generation of immunological memory.

1.1.1 Innate immune responses

The innate immune system is a non-specific defence mechanism that functions in a fully functional form encoded by germline genes of the host. The innate immune system provides the host with the first line of defence against invading pathogens through physiologic and chemical barriers, such as epithelial cell layers, the mucociliary apparatus and low pH or bacteriolytic secretions. The importance of physical barriers against infection is evidenced by patients with severe cutaneous burns or primary ciliary dyskinesia who are extremely susceptible to infections and have increased morbidity (Meeks and Bush, 2000; Turvey and Broide, 2010). Once pathogens invade the host, their presence induces inflammation through a cascade of events including synthesis of pro-inflammatory cytokines, production of acute-phase proteins such as C-reactive protein, and activation of serum proteins of the complement system which will

bind to and mark pathogens as dangerous. Some soluble complement fragments recruit effector cells of the innate immune system that will take up the complement-bound pathogens by phagocytosis and destroy the pathogen in the phagolysosomes by enzymes and free radicals (Parham and Janeway, 2009).

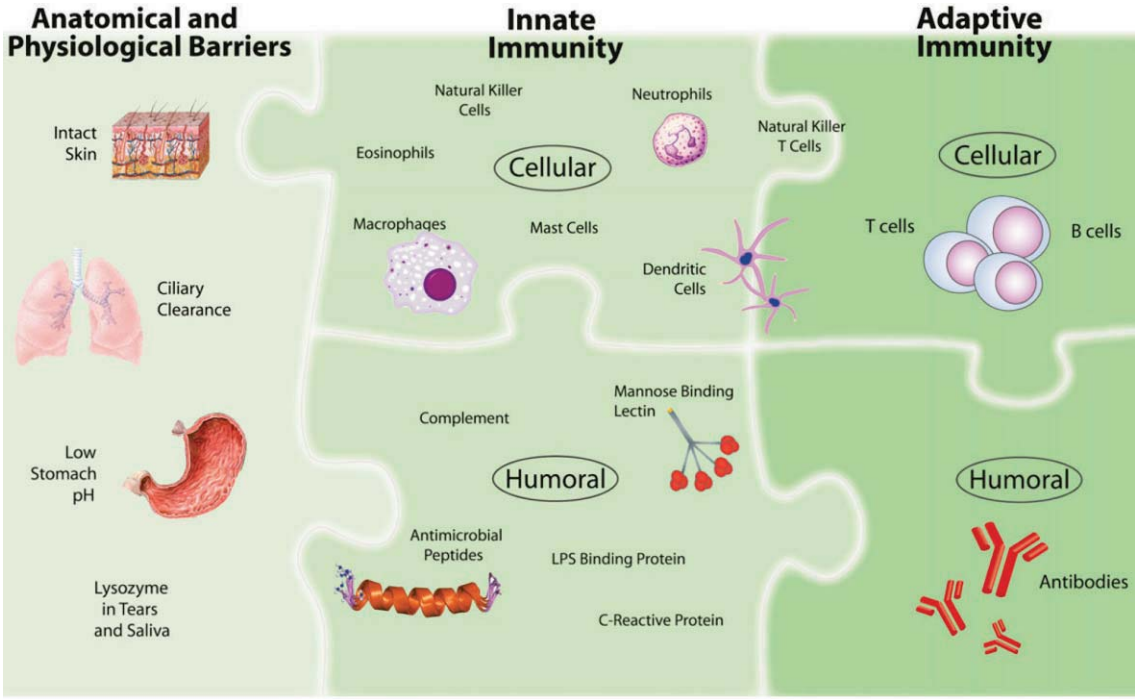

Figure 1. The immune system. The mammalian immune system can be viewed as consisting of 3 main levels: (1) anatomic and physiologic barriers (often included as part of innate immunity); (2) innate immunity; and (3) adaptive immunity. In common with many classification systems, some elements of the immune system are difficult to categorise. For example, NK T cells and dendritic cells could be classified as being at the border of innate and adaptive immunity rather than being firmly in one camp. (Figure reproduced from (Turvey and Broide, 2010)).

The innate immune system has different types of effector cells. One group of cells are granulocytes, which include neutrophils, eosinophils, basophils, and mast cells. Neutrophils are the most abundant granulocyte and are specialised in phagocytosis of pathogens. Eosinophils and basophils are mainly involved in immune responses against parasites (Behm and Ovington, 2000). Mast cells are involved in wound healing and they are key initiators of immediate hypersensitivity responses (Chaplin, 2010).

Another group of innate immune cells are monocytes, macrophages, and dendritic cells (DCs). Monocytes circulate in the blood, and upon infection, they proliferate and differentiate into macrophages and DCs. Macrophages are, like neutrophils, efficient phagocytes and they can be found in all tissues and work as scavengers to remove dead cells and invading pathogens. Macrophages are generally the first cells that sense the danger of infection and they secrete cytokines and recruit other immune cells to the site of infection. DCs have many characteristics in common with macrophages but they are especially efficient in antigen presentation and the induction of adaptive immune responses (Parham and Janeway, 2009; Steinman and Cohn, 1973).

The final group of innate immune cells are innate lymphoid cells (ILCs) which lack recombined antigen receptors. This is an emerging area with more and more innate-like B and T cells being identified that blur the boundaries between the innate and adaptive immune systems. The prototypical ILCs are natural killer (NK) cells and they are important in anti-viral and anti-tumour immune responses. NK cells recognise and kill cells that have lost or have reduced expression of major histocompatibility complex (MHC) class I molecules (Karre et al., 1986). Natural killer T (NKT) cells share characteristics of both NK cells and T cells, and recognise lipid antigens presented on CD1d molecules. Other ILCs include $\gamma\delta$ T cells, B1 B cells and marginal zone B cells. These innate B and T cells have a relatively restricted repertoire of antigen receptors and are enriched in mucosal tissues and respond rapidly to infections (Lanier, 2013).

Activities of innate immune cells are largely governed by pattern recognition receptors (PRRs) which include Toll-like receptors (TLRs), NOD-like receptors (NLRs), RIG-I-like receptors (RLRs) and C-type lectin receptors (CLRs). Each of these PRRs detects distinct pathogen-conserved components termed pathogen-associated molecular patterns (PAMPs). The prototypical PAMP is lipopolysaccharide (LPS, also called endotoxin) found on the bacterial cell membrane, which is recognised by TLR-4. Other common PAMPs include double-stranded RNA (recognised by TLR-3), bacterial flagellin (recognised by TLR-5), and un-methylated CpG DNA motifs (recognised by TLR-9) (Blander and

Sander, 2012). The detection of pathogens through the interactions of PRRs and PAMPs activates intracellular signalling, including nuclear factor-kB (NFκB), mitogen-activated protein kinases (MAPKs) and interferon regulatory factors (IRFs). This results in the release of pro-inflammatory cytokines, chemokines and cytotoxic factors that initiate local inflammatory responses and remove pathogens (Blander and Sander, 2012; Kaisho and Akira, 2006).

Cells of the innate immune system do not have the ability to alter the reactivity of their receptors, and, except for NK cells (Min-Oo et al., 2013), generally do not develop immunologic memory. However, the innate immune system provides the host with early and immediate protection that works so efficiently that in fact most animal species survive solely by relying on innate immune responses. Only vertebrates, including humans, have the added benefits of the adaptive immune system, which combats the few pathogens that evade innate immune clearance. Although innate and adaptive immune responses are different arms of the host immune system, they are not mutually exclusive. In fact, adaptive immune responses are initiated and activated by signals delivered by the innate immune system, notably during presentation of antigen to T cells (see below).

1.1.2 Antigen presenting cells

Antigens are recognised by specific antigen receptors on cells of the adaptive immune system. B cells recognise 3-dimensional structures of native antigens, usually in the form of proteins, through B cell receptors (BCR, also called immunoglobulins or antibody when they are secreted from B cells). By contrast, T cells can only recognise antigens when they are processed into short linear peptide epitopes and bound to MHC molecules on antigen-presenting cells (APCs) (Chaplin, 2006). There are two classes of MHC molecules: MHC class I and class II, which present peptide antigens at the APCs surface to CD8 and CD4 T cells, respectively. Processing and presentation of pathogen or tumour cell-derived antigens is essential for mounting protective T cell responses. Likewise, T cell recognition of self-antigens in the form of self-

peptide/MHC complexes (pMHC) is critical for maintenance of self-tolerance and is also important for the survival and homeostasis of naïve T cells (Blum et al., 2013; Sprent and Surh, 2011).

Generally, intracellular antigens originate from the cytosol or nucleus and are processed and presented on MHC class I, while exogenous antigens are processed through different pathways and presented on MHC class II. Exogenous antigens can also be presented on MHC class I via cross-presentation which allows the APCs to activate CD8 T cells without being directly infected with pathogens (Kurts et al., 2010; Neefjes et al., 2011). All nucleated cells express MHC class I and can therefore act to a varying degree as APCs, though initial activation of naïve CD8 T cells is controlled almost exclusively by DCs. However, MHC class II is primarily expressed by professional APCs, such as dendritic cells, macrophages and B cells. Of these, DCs are the most potent APCs for both CD4 and CD8 T cells, and DCs have the unique ability to cross-present antigens for priming CD8 T cells (Jung et al., 2002).

DCs are a heterogeneous group of cells that are categorised into four main subsets: conventional (or classical) DCs (cDCs), Langerhans cells, plasmacytoid DCs (pDCs), and monocyte-derived DCs (Belz and Nutt, 2012; Satpathy et al., 2012). cDCs are the predominant subset of DCs under steady conditions and they are highly phagocytic and specialised in antigen processing and presentation. cDCs can be further divided into migratory and lymphoid tissue-resident DCs. Migratory cDCs develop from early precursors in the peripheral tissues, where they sample antigens and then migrate via afferent lymphatics to the T cell zones of lymph nodes (LNs) to activate antigen-specific T cells. Lymphoid tissue-resident cDCs do not traffic from or to other tissues and they develop from DC precursors and exert their functions within lymphoid tissues. Among lymphoid tissue-resident cDCs, $CD8\alpha^+$ DCs are effective in cross-presentation and inducing CTL responses (Belz et al., 2004; Pooley et al., 2001) while $CD4^+$ DCs and $CD4^-CD8\alpha^-$ DCs are efficient at triggering T helper responses (den Haan and Bevan, 2002; Mount et al., 2008).

In contrast to cDCs, Langerhans cells normally reside in the skin and

resemble tissue-resident macrophages in the steady state, but acquire many features of migratory cDCs after activation (Miller et al., 2012). pDCs, in turn, resemble B cells with surface expression of B220 and distinct spherical morphology. Compared to cDCs, they are less phagocytic and inefficient in antigen presentation in the steady state. However, after sensing foreign nucleic acids, such as CpG DNA, they massively secrete type I interferon and become efficient APCs to activate T cells (Reizis et al., 2011).

In the steady state, DCs remain non-activated and present self-antigens to T cells and maintain immune tolerance. However, after infection, the recognition of pathogens through PRRs will induce the activation and maturation of DCs, which is accompanied by increased cross-presentation of antigen, higher expression of co-stimulatory molecules and secretion of pro-inflammatory cytokines. Presentation of pathogen-derived antigens along with strong co-stimulatory and inflammatory signals induces clonal expansion and effector functions of antigen-specific T cells (Hammer and Ma, 2013). Because of their distribution throughout the body, expression of various PRRs to detect pathogens and their unique ability to prime naïve T cells, DCs act as messengers between the innate and the adaptive immune systems.

1.1.3 Adaptive immune responses

Unlike the innate mechanisms of host defence, adaptive immune responses are antigen specific. As described above, adaptive immune responses are based on both T cell recognition of antigen through TCR and B cell recognition of antigen through BCR. Millions of antigen receptors with unique specificity are generated through random somatic rearrangement of germline-encoded gene elements which provide the host with a broad array of protection against almost any possible pathogen that might be encountered. In addition to specificity, immunologic memory is another unique feature of adaptive immunity. For memory generation, antigens and other pathogen-associated signals delivered by APCs induce clonal expansion and differentiation of antigen specific T and B cells into effector cells. After clearance of the pathogen by various effector

mechanisms, a small proportion of the responding T and B cells will survive as long-lived memory cells with improved function, thereby providing the host with faster and stronger protection for subsequent encounter with the same pathogen (Bonilla and Oettgen, 2010).

After developing in the primary lymphoid organs (T cells in thymus and B cells in bone marrow), T and B cells traffic to secondary lymphoid organs (SLOs; LNs, spleen and Peyer's patches) which provide an optimal environment for cell survival and the generation of adaptive immune responses to pathogens. Adaptive immune responses originate in these areas under the influence of innate immune system signals provided either directly by circulating pathogens or indirectly by pathogen-activated cutaneous or mucosal APCs migrating to the secondary lymphoid organs. B cell responses are mainly exerted by the secretion of antibodies which travel through the bloodstream to exert effector functions. By contrast, T cells function by migrating directly to sites of infection guided by expression of various homing molecules, such as CD62L, CCR7 and LFA-1. T cell migration is highly dependent on the differentiation state of T cells (Masopust and Schenkel, 2013). Naïve T cells constantly recirculate from blood to lymph through defined "T cell areas" of the lymphoid tissues, the para-cortical regions of LNs and Peyer's patches and the periarteriolar lymphocyte sheaths (PALS) of spleen. Migration through these sites enables specific T cells to contact antigen displayed on the surface of APCs. After activation and differentiation, effector T cells enter the bloodstream (leaving LN via efferent lymph and then the venous system) and then disseminate throughout the body, including the site of infection, to exert contact-dependent effector functions (Masopust and Schenkel, 2013).

B cells arise from stem cells in the bone marrow by a series of steps that involve immunoglobulin (Ig) VDJ gene rearrangement to produce a diverse repertoire of pre-B, immature B and then mature B cells expressing surface immunoglobulin IgM and IgD. Mature B cells then leave the marrow and recirculate through defined "B cell area" of the SLOs. After encounter with cognate antigens in these areas and collaborative interactions with T helper

cells, B cells undergo Ig isotype switching and affinity maturation through the process known as Ig somatic hypermutation which results in the production of antibodies of different isotypes (IgG, IgA and IgE) or subtypes (e.g. IgG1, IgG3) with the same antigenic specificity. B cells with membrane bound Igs internalise and process antigens for T cell responses, and therefore act as APCs for T helper cells after these cells have been activated by DCs (Parkin and Cohen, 2001). After further differentiation of B cells into plasma cells, Igs are secreted as effector molecules, which are antibodies. Along with complement proteins and antimicrobial peptides, antibodies are the key mediator of the humoral immune response. The effector functions of antibodies include neutralising toxins, opsonisation of pathogens for phagocytosis, activation of complement, preventing organisms adhering to mucosal surfaces, and sensitisation of tumour and infected cells for antibody-dependent cytotoxic attack. The majority of plasma cells are short-lived, but small numbers of these cells survive for prolonged periods in the bone marrow where they provide constant synthesis of specific antibody to guard against re-infection by the pathogen concerned (Radbruch et al., 2006). In parallel with plasma cell generation, less-differentiated responding B cells differentiate into long-lived, antigen-specific memory B cells. Like specific antibody, these cells provide long-lasting protection against pathogen re-infection (McHeyzer-Williams et al., 2012).

T cells develop in the thymus from bone marrow-derived hematopoietic precursors (Starr et al., 2003). Unlike typical thymocytes, T cell precursors entering the thymus do not express CD4 and CD8 molecules and are termed "double-negative" (DN) thymocytes. These cells initially lack antigen-specific T cell receptors (TCRs) and progress through several developmental stages: they first express pre-TCR molecules, and then acquire rearranged TCR $\alpha\beta$ heterodimers by V(D)J recombination together with up-regulation of CD4 and CD8 expression to form the majority population of "double-positive" (DP) thymocytes. The fate of DP thymocytes is determined by their interaction with a broad array of self-peptides bound to MHC class I and class II molecules on

cortical epithelial cells (cTEC) (Koch and Radtke, 2011). Most DP cells have negligible TCR affinity for self pMHC on cTEC and these cells die *in situ* "by neglect". Around 1-2% of DP cells have strong TCR affinity for self pMHC and these cells receive a strong TCR signal that leads to death by "negative selection". A few DP cells, ~1%, have low but significant TCR affinity for self pMHC. These cells receive a low-level TCR signal which protects the cells from death (positive selection) and causes the cells to differentiate into "single-positive" (SP) $CD4^+8^-$ or $CD4^-8^+$ cells as a consequence of recognition of pMHC II and pMHC I, respectively (Germain, 2002; Koch and Radtke, 2011). Mature CD4 and CD8 T cells are then released from the thymus to form the pool of long-lived recirculating T cells.

1.1.4 CD4 T cells

Naïve CD4 T cells are resting cells, maintained by contact with self pMHC II and IL-7, and are marked by a low density of CD44 and high expression of LN homing receptors, CCR7 and CD62L (Sprent and Surh, 2011). Through the binding specificity of CD4 molecules for MHC II, CD4 T cells are programmed to respond to pMHC II ligands. When activated by antigen, CD4 T cells are classically designated as T helper (Th) cells as they provide help for both humoral and cellular responses. Depending on the nature of the cytokines present at the site of activation, Th cells differentiate into functionally distinct subsets: Th1, Th2, Th9, Th17, follicular helper T (Tfh) cells, and regulatory T (Treg) cells (Nakayamada et al., 2012).

Th1 cells are characterised by T-bet expression and provide help for CD8 T cells through interleukin-2 (IL-2) synthesis and display effector function via interferon-γ (IFNγ) production. Th2 cells express GATA3 and mediate effector function through several cytokines, especially IL-4, IL-5 and IL-13 (Nakayamada et al., 2012). Th9 cells produce IL-9 and defend the host against helminth infections (Tan and Gery, 2012). Th17 cells express RORγt and produce IL-17 and IL-21. Th17 cells play important roles in clearing pathogens but can also

cause pathologic inflammation and contribute to autoimmune disease (Yang et al., 2014). Tfh cells are characterised by the expression of Bcl6 and particular chemokine receptors, CXCR5, which allows Tfh cells to enter B cell zones to form germinal centres; here, Tfh cells provide cognate help for B cells through IL-21 synthesis and induce specific B cells to differentiate into plasma cells and memory cells (Tangye et al., 2013).

In addition to these positive effects on the immune response, some CD4 cells have a suppressive function. These T regulatory cells (Treg) are typically $CD4^+CD25^+FoxP3^+$ and arise predominantly in the thymus as natural Treg (nTreg) cells, although some Tregs can arise from naïve CD4 cells responding to antigen in the presence of TGFβ in the gut as induced Treg (iTreg) cells (Ohkura et al., 2013). Through their immunosuppressive function, which is mediated in part via IL-10 synthesis, Treg play an important role in inducing peripheral tolerance and minimising the deleterious effects of immune-mediated inflammation. Conversely, Tregs can have a negative effect by suppressing immune responses to tumours (Josefowicz et al., 2012).

There is increasing evidence that in some situations Th cell function is reversible. For instance, under certain conditions Treg cells can lose FoxP3 expression to become Th1-like cells producing pro-inflammatory cytokines (Dominguez-Villar et al., 2011; Oldenhove et al., 2009). Likewise, phenotypic changes are also observed in Th1, Th2, Th17 and Tfh cells, suggesting that Th cell phenotypes are often plastic rather than fixed, which has important implications for therapeutic intervention (Nakayamada et al., 2012).

1.2 CD8 T cells

Like CD4 cells, naïve CD8 T cells are long-lived resting cells with a $CD44^{lo}$, $CD62L^+$, $CCR7^+$ phenotype (Sprent and Surh, 2011). These cells are kept alive in interphase through weak TCR signalling resulting from continuous CD8-dependent contact with self pMHC I ligands combined with interaction with IL-7 and also IL-15. Through their capacity to become cytotoxic T lymphocytes (CTL)

after activation by foreign antigens, CD8 T cells are key players in adaptive immune responses and play an essential role in eliminating pathogen-infected target cells. Likewise, the CTL function of CD8 T cells is vital for destroying tumour cells. Since my thesis focuses on the role of CD8 T cells in cancer immunotherapy, the properties and functions of CD8 T cells are described below in some detail.

1.2.1 CD8 T cell activation

In the periphery, during their recirculation through SLOs naïve CD8 T cells are constantly searching for pathogens in the form of cognate peptides presented by MHC class I (pMHC) on APCs. In mice, it is estimated that 10^2 - 10^3 naïve CD8 T cells have TCR specificity for any single given pMHC I complex (Moon et al., 2007; Obar et al., 2008). Considering that mice contain billions of total cells, searching for rare antigen-presenting cells by each clone of CD8 T cells would seem challenging. Nevertheless, because naïve T cells constantly circulate through the sites of antigen localization in defined regions of the SLOs, virtually all specific T (and B) cells are able to make contact with antigen within a few days of infection or immunization (Masopust and Schenkel, 2013; Sprent et al., 1971). Antigens can reach SLOs either directly or indirectly by being first taken up by peripheral immature DCs at the initial site of infection. DC recognition of pathogens by the interaction of PRRs and PAMPs activates these cells and augments their phagocytic function and prolongs the half-life of surface MHC molecules, allowing the cells to remain immunogenic after migration to the T cell zones in SLOs. (Blander and Medzhitov, 2006). Activated mature DCs also express higher levels of co-stimulatory molecules and secrete chemokines and cytokines, especially IL-12, which are important for optimal CD8 T cell activation.

In the SLOs, after finding cognate pMHC through transient interactions with many DCs, CD8 T cells become arrested and stably interact with the antigen-presenting DC to form an immunological synapse (IS). The IS mediates

efficient intercellular signalling between T cells and APCs. On T cells, the IS is characterised by a highly-organised supramolecular activation cluster (SMAC) with central accumulation of TCR-peptide-MHC and co-stimulatory molecules (e.g. CD28-CD80/CD86), termed the cSMAC, surrounded by a ring of interacting adhesion molecules such as LFA-1–ICAM-1, plus a distal region enriched with F-actins (Dustin, 2014; Huppa and Davis, 2003). In the IS, the interaction of TCRs with cognate peptide-MHC class I complexes delivers a TCR signal, which is often called Signal 1. An additional signal (Signal 2) is provided by interactions between co-stimulatory molecules on T cells with complementary ligands on APCs. Although there are many co-stimulatory molecules, CD28 expressed by T cells is the major co-stimulatory receptor, and this receptor interacts selectively with B7-1 (CD80) and B7-2 (CD86) which are highly expressed by activated DCs (Greenwald et al., 2005). The combination of Signal 1 and Signal 2 is often potent enough to drive clonal expansion and differentiation of CD8 T cells. However, the presence of inflammatory cytokines (e.g. IL-12, type I IFNs) secreted by DCs, termed Signal 3, may be required for full activation of CD8 T cells and the acquisition of effector functions (Curtsinger et al., 2003a; Curtsinger et al., 2003b).

1.2.2 CD8 T cell differentiation and memory generation

When optimally activated, CD8 T cells undergo massive expansion through multiple cell divisions and generate a large army of effector cells, notably CTLs, which are able to rapidly eradicate pathogen-infected cells (Figure 2). During differentiation into effector cells, responding CD8 T cells decrease their expression of the IL-7 receptor and of lymphoid tissue-homing receptors, CD62L and CCR7, but upregulate CD44 and various chemokine receptors, thereby enabling the cells to leave the lymphoid tissues and migrate to peripheral tissues to search for target cells to exert their effector functions (Bromley et al., 2005). Upon antigen-dependent recognition of a target cell, CTLs form an IS with the target cell (similar to the IS formed between naïve T cells and DCs)

and deliver cytotoxic granules such as perforin and granzymes to the target cell, therefore causing these cells to die rapidly by apoptosis (de Saint Basile et al., 2010). Activated CD8 T cells can also kill target cells via Fas/Fas-ligand interaction and secrete cytokines such as IFNγ and TNF which cause local inflammatory responses; cytokine secretion ceases when CTLs lose contact with antigen, thereby preventing unnecessary damage to the host (Slifka and Whitton, 2000).

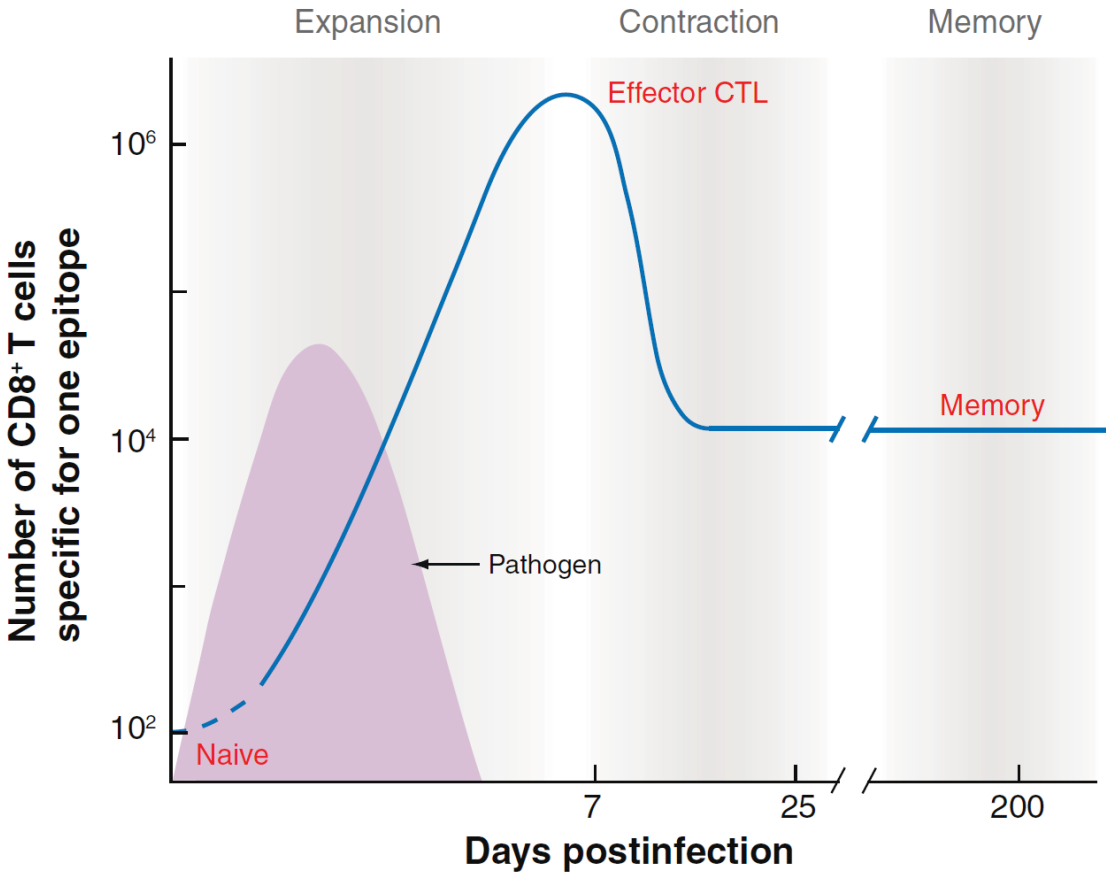

Figure 2. Kinetics of the CD8 T cell responses. Graphic illustration of the kinetics of the massive proliferative response of naive CD8 T cells following infection of a mouse with a virulent pathogen such as *Listeria monocytogenes*, lymphocytic choriomeningitis virus, vesicular stomatitis virus, or vaccinia. By some estimates, a mouse contains 10^2 – 10^3 naive CD8 T cells specific for any one epitope. After a lag of about 24 hours, these precursors go through 15 – 20 cell divisions and generate millions of effector cytotoxic T lymphocytes (CTLs) by day 7 – 8 postinfection. When a pathogen is cleared, the majority of the effectors die, leaving behind a pool of CD8 memory T cells. (Figure reproduced from (Williams and Bevan, 2007)).

After killing infected target cells, most CTLs die and only 5% to 10% of responding CD8 T cells survive to become long-lived memory cells (Figure 2); memory CD8 T cells tend to be drawn from less-differentiated precursors which show only limited down-regulation of the IL-7 receptor (Kaech et al., 2003). Once formed, memory CD8 T cells can be divided into effector memory cells ($CD62L^{low}CCR7^{low}$), central memory cells ($CD62L^{hi}CCR7^{hi}$) and tissue-resident memory cells ($CD103^{hi}CD69^{hi}CD27^{low}$) (Mueller et al., 2013). Central memory CD8 T cells reside in SLOs and, via up-regulation of CD122, these cells divide intermittently through contact with IL-15. Effector memory CD8 T cells reside in non-lymphoid tissues and are important for responding to pathogens that localise in these sites. Tissue-resident memory CD8 T cells reside in the skin, brain and mucosal tissues (Kaech and Cui, 2012). Because memory CD8 T cells are present at a high frequency relative to naïve cells and are strategically distributed throughout the body, these cells provide the host with potent life-long protection against recurrent infections (Kaech and Cui, 2012; Williams and Bevan, 2007).

Although the expansion and effector generation of CD8 T cells is necessary for effective pathogen clearance, this event needs to be tightly controlled in order to avoid normal tissue damage. The immune system uses multiple regulatory mechanisms to prevent overt CD8 T cell responses, such as antigenic competition between CD8 T cells, limiting persistent contact with antigens by CTL-mediated killing of infected APCs, negative regulation of CD8 T cell responses by CTLA-4 and PD-1, and Treg-mediated immune suppression (Arens and Schoenberger, 2010). Some of these mechanisms are also associated with immune evasion of pathogens and cancer (see below), which poses both significant challenges and opportunities for effective therapeutic interventions, such as vaccines.

1.3 Vaccines for optimal CD8 T cell stimulation

Vaccination remains the most successful public health intervention ever developed, as evidenced by the elimination or great reduction of several important infectious diseases and markedly increased life expectancy after its extensive application over the past century. However, effective vaccines against chronic human infectious pathogens (e.g. human immunodeficiency virus, Mycobacterium tuberculosis and hepatitis C) and cancer do not yet exist (Andre et al., 2008; Sallusto et al., 2010). Considering the major role of CD8 T cells in the control of virus infection and malignancy progression, much of current vaccine research is focused on effective stimulation of antigen-specific CD8 T cells (Appay et al., 2008; Fridman et al., 2012; Yewdell, 2010). Apart from efficacy, safety is the most important requirement for vaccines, especially for prophylactic vaccines. For this reason, subunit vaccines with molecularly defined antigens are preferred over live pathogen-based vaccines, although the latter can induce more potent immune responses. However, many characteristics of live pathogens can be utilised and incorporated into subunit vaccination for enhanced immunogenicity while maintaining its safety profile. Many of the successful approaches were inspired by studies on natural immunity against pathogen infections (Bachmann and Jennings, 2010; Irvine et al., 2013; Jennings and Bachmann, 2007).

1.3.1 Shape and size

Pathogens such as viruses and bacteria are particulate, their size ranging from about 20 nanometres to a few micrometres, and have surfaces with dense repetitive displays of proteins. These characteristics are associated with enhanced uptake and efficient cross-presentation by host APCs. Therefore, compared to soluble protein or peptide antigens, antigens linked to or incorporated into nano- or microparticles (such as in the form of virosomes, virus-like particles and liposomes) are more efficiently taken up by APCs and effectively processed for the MHC class I pathway to cross-prime CD8 T cells (Harding and Song, 1994; Kourtis et al., 2013; Kovacsovics-Bankowski et al.,

1993; Kovacsovics-Bankowski and Rock, 1995; Reddy et al., 2007). The immune system can effectively process antigens from both virus and bacteria-sized particles (Di Bonito et al., 2009; Pfeifer et al., 1993). However, it has been shown that only particles smaller than 200 nanometres can directly drain to lymph nodes through the lymphatic system, while larger particles need to be first taken up by tissue-resident dendritic cells (Manolova et al., 2008). As only lymphoid tissue-resident CD8α^+ cDCs are effective in cross-presentation (at least in steady state conditions), nanoparticles may be more advantageous than microparticles for effective cross-priming of CD8 T cells *in vivo* (Bachmann and Jennings, 2010; Fifis et al., 2004).

1.3.2 Adjuvants

As mentioned earlier, activation of the innate immune system is controlled by recognition of PAMPs by a number of PRRs. Interactions of PRRs with PAMPs induce the activation of innate immune cells, especially DCs, and result in the secretion of pro-inflammatory cytokines (e.g. IL-12, TNF) and migration to secondary lymphoid organs to present pathogen-derived antigens to T and B cells. Most adjuvants work in this manner, i.e. by enhancing vaccine-induced adaptive immune responses as the result of triggering PRR-related signaling and subsequent activation of innate immune cells (Coffman et al., 2010). Synthetic analogs of some PAMPs, such as CpG oligodeoxynucleotides (ODN) and Poly I:C, are extensively used for subunit vaccines which by themselves are poorly immunogenic. While adjuvants can help vaccines to induce potent immune responses, care must be taken to avoid non-specific strong innate immune activation which is usually associated with adjuvant-related side effects. Indeed, severe side effects can be observed in mice injected with a mixture of antigens plus CpG ODN. However, when antigen and CpG ODN are incorporated into the same nanoparticles, potent CD8 T cell responses are induced with no measurable side effects (Bourquin et al., 2008; Storni et al., 2004). This is due to the focused activation of innate immune cells. Thus, CpG ODN activation of the cells that take up and present antigens lowers the dose of antigen required

for effective stimulation of CD8 T cells. Therefore, vaccination of antigens and adjuvants in a physically-linked form may be an optimal way to induce potent immune responses while reducing the risk of side effects.

1.3.3 Duration of antigen contact

Effective immune responses against virulent infections are characterised by the unique kinetics of antigen load. As pathogens replicate, they will produce exponentially increasing concentrations of antigens along with PAMPs, which is followed by a gradual decrease in antigen concentration after the onset of immune-mediated pathogen clearance. Most antigen persistence/presentation and initial CD8 T cell activation/proliferation takes place within the first 3 days of infection, after which CD8 T cells start to acquire effector functions and kill pathogen-infected cells, including antigen-presenting dendritic cells (Williams and Bevan, 2007; Wong and Pamer, 2003). CD8 T cells generally continue to expand until about one week post-infection. Thereafter, antigen concentration wanes, and CD8 T cell expansion is followed by a contraction phase where most of the responding cells die, leaving only a small proportion of cells to survive to form long-lived memory cells.

Although very brief (6 to 12 hour) exposure to antigen is sufficient to induce a fully-functional CD8 T cell response, longer antigenic stimulation is needed to increase the magnitude of CTL responses (Prlic et al., 2006). Furthermore, there is some evidence that CD8 T cell differentiation into memory cells requires prolonged antigen encounter (Bachmann et al., 2006; Williams and Bevan, 2004). Therefore, optimal generation of potent CTL responses and a pool of memory CD8 T cells require prolonged antigen presentation plus the adjuvant effect of innate immune stimulation. On this point, some vaccine adjuvants such as aluminum salts and immunostimulatory complexes function largely by prolonging antigen presentation, although innate immune stimulation also plays a role (Coffman et al., 2010). An alternative approach is to deliver subunit vaccines repeatedly. Interestingly, Johansen et al. found that, with a fixed cumulative dose of antigen, injecting mice exponentially with increasing

doses of both peptide and CpG ODN over four days was superior in stimulating CTL responses than a single high dose or multiple equal doses (Johansen et al., 2008). This approach of injecting antigen in exponential doses mimics the situation in a typical virus infection.

Taken together, vaccines that mimic the multiple characteristics of pathogen infections, including particulate shape with repetitive displays of antigens, PAMPs-induced activation of APCs, and perhaps administration of antigen in exponential doses, may serve as an optimal approach to induce strong CD8 T cell responses against the infection. This scenario applies to prophylactic vaccines for typical acute infections where the immune response causes total or near-complete elimination of the pathogen concerned. With chronic infections, however, the failure to eliminate the pathogen causes persistence of the immune response, thus posing the risk of severe pathology as the result of chronic inflammation (Speiser et al., 2014). To avoid this problem, chronic immune responses are regulated by T cell expression of inhibitory receptors, notably PD-1 and CTLA4. As discussed below, expression of these and other inhibitory molecules by T cells severely curtails the immune response to cancer.

1.4 Cancer and immunotherapy

1.4.1 Cancer therapy

Cancers arise as the result of genetic mutations in oncogenes and tumour suppressor genes that lead to uncontrolled growth, invasion, and sometimes metastasis of neoplastic cells (Futreal et al., 2004). Since cancer is a leading cause of death worldwide, there has been an enormous amount of research devoted to the development of effective cancer therapies, notably new methods of surgery, chemotherapy, radiotherapy, and immunotherapy. The therapies used vary depending upon the location and grade of the tumour and the stage of the disease, as well as the general state of a patient's health. Complete removal of the cancer without damage to the rest of the body is the obvious goal of cancer therapy. Sometimes this can be accomplished by surgery alone, but often cancers relapse later as tumour cells spread locally or enter lymphatic

and blood vessels to metastasise to distant sites in the body. Chemotherapy and radiotherapy are often effective against cancer but their lack of specificity leads to serious side effects, including suppression of ongoing immune responses (Melenhorst and Barrett, 2011).

1.4.2 Immune responses against cancers

There is ample evidence that the immune system plays a prominent role in preventing tumour development. Mice lacking essential components of the innate or adaptive immune system are more susceptible to the development of spontaneous or chemically-induced tumours (Dunn et al., 2004). Also in humans, patients with immune deficiencies such as acquired immunodeficiency syndrome (AIDS) develop tumours, e.g. EBV lymphoma, that rarely occur in healthy individuals (Marin-Muller et al., 2009; Ramirez-Olivencia et al., 2009). Indeed, the immune system has multiple components that have the potential to eliminate cancers, such as antibodies, macrophages, NK cells and tumour antigen-specific T cells (Sahin et al., 1997; Whiteside, 2010). Thus, in patients with colorectal carcinoma, the presence of pro-inflammatory cytokines in the tumour and the high ratio of both Th1 and CD8 T cells in tumour-infiltrating lymphocytes (TILs) were found to correlate with reduced metastatic invasion and increased survival of the patients (Galon et al., 2006; Pages et al., 2005).

Why cancers develop in the presence of an apparently normal immune system is still poorly understood. There are several possibilities. First, most (though not all) antigens on tumour cells are self-antigens that are either overexpressed or modified post-transcriptionally. Hence, many T cells with the potential to recognise tumour antigens are eliminated during ontogeny in the thymus through contact with self pMHC ligands, leaving only cells with relatively low TCR affinity to mount anti-tumour responses (Schmid et al., 2010); this scenario, however, may not apply to recognition of mutated tumour antigens. Another problem is that tumour cells lack PAMPs and therefore generally do not activate APCs. Hence, many of the APCs that present tumour antigens to T cells (including tumour cells themselves) provide only weak co-stimulatory signals

and therefore tend to induce tolerance instead of immunity (Whiteside, 2010). The tumour microenvironment can also be immunosuppressive. Thus, immune responses to tumours are dampened by various immunoinhibitory mechanisms, such as tumour antigen loss, local synthesis of immunosuppressive factors (IDO, IL-10 and TGF-β), Fas ligand expression leading to T cell death, T cell expression of inhibitory membrane proteins (PD-L1/PD-1, CTLA-4), and suppression of T cell function by contact with Tregs and tolerogenic APCs (macrophages and myeloid-derived suppressor cells) in the tumour (Baitsch et al., 2012). There is also the problem that tumours are genetically unstable and can be replaced by genetic variants that are resistant to immune responses (Schreiber et al., 2011). Finally, the power of tumour immune surveillance declines with ages, leading to a higher incidence of cancer in the elderly, which has stimulated the use of immune-potentiating agents to treat elderly cancer patients (Goronzy and Weyand, 2013; Provinciali, 2009).

Natural immune responses against cancer are clearly not optimal but nevertheless, after therapeutic intervention, functional tumour-specific T cells can often be detected in the circulating blood, suggesting that most T cells are rendered hypo-responsive in the tumour microenvironment rather than systemically (Baumgaertner et al., 2012; Zippelius et al., 2004). Furthermore, recent findings that administration of PD-1 mAb or other forms of checkpoint inhibitor blockade can overcome immune-suppression in the tumour microenvironment and induce an overt immune response, leading to tumour stabilization and improved patients survival, have given new hope for the success of cancer immunotherapy (Postow et al., 2015; van den Boorn and Hartmann, 2013).

1.4.3 Immunotherapy for cancer

As mentioned above, natural T cell responses against tumour cells are restricted by both T cell intrinsic and extrinsic mechanisms, notably low-affinity TCR reactivity and expression of checkpoint inhibitors by T cells, and immunosuppression by the tumour microenvironment. Early efforts to enhance

anti-tumour immune responses included systemic administration of cytokines such as IL-2 and interferons, and reinfusion of *ex vivo* activated TILs (Rosenberg et al., 1994). In certain cases these early studies provided significant survival benefits to cancer patients; however, their use is limited by off-target toxicities (e.g. vascular leak syndrome associated with IL-2 therapy) and challenges with manufacturing (Boyman and Sprent, 2012; Maus et al., 2014; Rosenberg, 2004). More recently, adoptive transfer of genetically-engineered T cells with high-affinity TCRs for tumour antigens and antibody-mediated blockade of immune checkpoints (e.g. CTLA-4, PD-1/PD-L1) are producing even more promising clinical efficacy with minimal toxicity for a variety of malignancies. These protocols may provide even greater benefit when used in combinatorial regimens (Postow et al., 2015; Quezada and Peggs, 2013), e.g. by simultaneous blockade of CTLA-4 and PD-1 (Wolchok et al., 2013). Likewise, immune checkpoint blockade can also be combined with chemotherapy, radiotherapy, and other immunotherapies, such as tumour antigen-loaded vaccines.

As described earlier, to induce effective CD8 T cell responses, naïve T cells require contact with MHC I-bound peptide and co-stimulatory molecules on professional APCs, especially DCs. For this reason, since the 1990s, antigen-pulsed DCs have been used as a therapeutic cancer vaccine in clinical studies, leading to approval of DC-based therapy, Sipuleucel-T, by the US Food and Drug Administration (FDA) in 2010 for the treatment of late-stage prostate cancer; this treatment has provided a 4-month survival benefit. Clinical use of DCs has proved to be safe with only minor adverse side effects. However, when DCs are used as a monotherapy in clinical studies, anti-tumour immune responses have typically been limited and objective tumour response rates have been disappointingly low (Anguille et al., 2014). And, even for the US FDA-approved Sipuleucel-T, many concerns have been raised regarding the production, design, and the survival benefit of DC immunotherapy (Huber et al., 2012). After more than 40 years of extensive research on DCs since their initial discovery by Steinman et al (Steinman and Cohn, 1973), we are still not clear about how to

optimally prepare DCs for immunotherapy, and preparation methods established so far are expensive and inconsistent in terms of quality. Furthermore, it is difficult to keep DCs alive during their preparation *in vitro*, and after injection, the majority of cells die by apoptosis and induce tolerance instead of immune responses (Josien et al., 2000; Kim et al., 2009; Kushwah and Hu, 2010; Miga et al., 2001). Moreover, DCs home poorly after injection and thus often fail to make contact with T cells in the lymphoid tissues.

Problems associated with cell-based vaccines, including those noted above, have facilitated the development of non-cellular vaccines, such as virus-like particles, liposomes and exosomes (Eggermont et al., 2014; Kushnir et al., 2012). Exosomes are 30 – 100 nm sized, late endosome-derived membrane vesicles released by most cell types, including DCs and tumours (Pitt et al., 2014). The report by Zitvogel et al showing tumour growth retardation in mice treated with antigen-pulsed DC exosomes has sparkled great interest in exosomes (Zitvogel et al., 1998). Tumour exosomes have also been shown to induce a CD8 T-cell dependent anti-tumour immune response through transferring tumour antigens to DCs (Hao et al., 2006). However, they do not spontaneously induce anti-tumour responses and may even induce immune suppression *in vivo* (Clayton et al., 2007; Liu et al., 2006; Wieckowski et al., 2009). Therefore, exosomes can have either activating or inhibitory effects *in vivo* and the nature of the exosome-induced immune response may depend upon the physiological state of the donor cells which may influence the composition of exosomes. Specifically, tolerogenic exosomes may express inhibitory molecules such as FasL (Andreola et al., 2002) or TGF-β (Clayton et al., 2007), whereas immune-activating exosomes probably express stimulatory molecules and factors (Gastpar et al., 2005; Thery et al., 2009). While the use of exosomes for tumour immunotherapy has considerable promise, its therapeutic use is constrained by poor secretion of exosomes from mature DCs (Segura et al., 2005). The release of exosomes is higher from immature DCs, but since immature DCs express only low levels of costimulatory and adhesion molecules, they are less immunogenic and can even be immunosuppressive

(Viaud et al., 2010). To date, clinical trials have demonstrated the safety of exosome-based therapy. However, the therapeutic effect and the activating effects on the immune system were found to be limited (Gehrmann et al., 2014).

1.5 Project aim

The suboptimal efficacy of exosomes has prompted research into finding alternative and better subcellular vaccines. Previously, in murine studies our group found that exosomes shed from artificial APCs prepared from a transfected *Drosophila* cell line (Hwang et al., 2003) and membrane vesicles prepared from a DC cell line following sonication (Hwang et al., 2003; Kovar et al., 2006) are both highly immunogenic as the result of joint expression of antigen/MHC, B7 and ICAM-1. Like exosomes from DCs, membrane vesicles from mature DC lines are more immunogenic than those from immature DCs. Importantly, when compared to exosomes, membrane vesicles from DC lines are much more potent and obtainable in much larger quantities (Kovar et al., 2006). Therefore, membrane vesicles could be a very promising substitute for DCs and exosomes as a next-generation cancer vaccine. This approach is still at an early development stage, however, and in particular it has yet to be shown that it is practical to prepare membrane vesicles from normal DCs in quantities sufficient for therapeutic administration.

With this background, the overall aim of my PhD project was to prepare large quantities of highly-immunogenic membrane vesicles from bone marrow-derived dendritic cells (BMDCs) and use these vesicles loaded with specific peptides to stimulate CD8 T cells for cancer immunotherapy. To achieve this goal, I first optimised BMDC expansion and maturation *in vitro* and made purified preparations of membrane vesicles from mature DCs in the cultures. Then, after loading with peptide, I used the vesicles to stimulate naïve CD8 T cells under various conditions, first *in vitro* and then *in vivo.* Measurement of effector function included preliminary studies on anti-tumour immunity.

2 Materials and Methods

2.1 Buffers, media and solution

Buffer/Solution	**Components**	**Suppliers**
S2 cell media	Schneider's Drosophila medium	Gibco
	10% Fetal Bovine Serum	Gibco
	0.5 mg/ml Geneticin	Gibco
CFSE buffer	0.1% BSA	Gibco
	5 μM CFSE	InVitrogen
	PBS (1x)	Gibco
Complete media	10% Fetal Bovine Serum	Gibco
	50 Units/ml penicillin	Gibco
	50 μg/ml streptomycin	Gibco
	1 mM Sodium Pyruvate	Gibco
	50 μM 2-Mercaptoethanol	Gibco
	1x MEM NEAA	Gibco
	500 mL RPMI-1640	Gibco
DC media	20 ng/ml murine GMCSF	PeproTech
	Complete media	
ELISA coating buffer	7.13g $NaHCO_3$	Merck
	1.59g Na_2CO_3	Merck
	q.s. to 1.0L	
	pH to 9.5 with 10 N NaOH	Garvan
ELISA wash buffer	PBS	Gibco
	0.05% Tween-20	ICN Biomedicals
ELISA assay diluent	10% Fetal Bovine Serum	Gibco
	PBS	Gibco
ELISA stop solution	2 N H_2SO_4	Ajax FineChem

FACS buffer	0.1% NaN_3 0.5% bovine serum albumin (BSA) 1x PBS	Amersham Gibco Gibco Gibco
Homogenization buffer	10mM Tris-Cl, pH7.5 0.5mM $MgCl_2$	Garvan Garvan
1x Perm/Wash solution	10% 10x Perm/Wash buffer 90% Distilled H_2O	BD Garvan
RBC lysis buffer	8.26g NH_4Cl 1g $KHCO_3$ 0.037g EDTA 1L Distilled H_2O	Merck Merck Gibco Garvan
10% sodium dodecyl sulfate (SDS)	10% SDS	Garvan
Tonicity buffer	1.694 M NaCl Homogenization buffer	Garvan

2.2 Antibodies

Target	Clone	Source
CD16/32 (Fc block)	2.4G2	BD
CD69	H1.2F3	eBioscience
CD25	PC61.5	eBioscience
TCRβ	H57-597	eBioscience
CD11c	N418	eBioscience
H-2K^b (MHC I)	AF6-88.5.5.3	eBioscience
I-A^b (MHC II)	AF6-120.1	BD
CD80 (B7-1)	16-10A1	eBioscience
CD86 (B7-2)	GL1	BD
CD45R (B220)	RA3-6B2	BD
Ly6G	RB6-8C5	eBioscience
H-2L^d (MHC I)	30-5-7S	Cedarlane
Pan-Cadherin	Polyclonal	Cell Signalling
Calnexin	Polyclonal	Abcam
COX-IV	Polyclonal	Cell Signalling
Lamin A/C	Polyclonal	Cell Signalling
β-2-Microglobulin	Polyclonal	SantaCruz
CD3	17A2	eBioscience
CD8	53-6.7	eBioscience
CD90.1 (Thy1.1)	HIS51	eBioscience
CD45.1 (Ly5.1)	A20	eBioscience
CD9	KMC8	BD
Perforin	EBioOMAK-D	eBioscience
Granzyme-B	GB11	BD
IFNγ	XMG1.2	eBioscience
F4/80	BM8	BioLegend
FcγR II/III	93	eBioscience

2.3 Mice

C57BL/6 mice were obtained from the Animal Resources Centre (ARC), Perth, WA, Australia. Source of OT-1.Thy1.1(CD90.1) and 2C.Thy1.1 TCR-transgenic mice (both on a C57BL/6 background) were described previously (Cho et al., 2013) and were obtained from the breeding colony at Australian BioResources (ABR), Moss Vale, NSW, Australia. All mice were maintained under specific pathogen-free conditions and used at 6 – 12 weeks of age, according to protocols approved by the Animal Experimental Ethics Committee at the Garvan Institute of Medical Research, which comply with the Australian code of practice for the care and use of animals for scientific purposes.

2.4 Transfected Drosophila cell culture

Transfected *Drosophila* S2 cells expressing murine L^d MHC class I alone, or along with murine B7-1 and ICAM-1 molecules were generated previously (Cai et al., 1996), and cultured with S2 cell media in a humidified 28°C incubator. 24 hours before use, the transfected gene expression was induced by addition of $CuSO_4$ to a final concentration of 1 mM. These cells were used as artificial antigen-presenting cells (aAPCs).

2.5 Cell surface staining and flow cytometry

Single cell suspension was transferred to a 96 well V-bottom plate (GBO, Germany) and then centrifuged at 1500 rpm (440 x g) for 5 minutes. Cell pellet was resuspended in FACS buffer (50 μl/sample) and treated with Mouse BD Fc Block (anti-CD16/32; 1 μg/sample) for 10 minutes. Fluorochrome-conjugated antibodies against surface molecules were then added and incubated for another 30 minutes. Finally, stained cells were resuspended in FACS buffer after removing un-bound antibodies by repeated FACS buffer washing and centrifugation. All procedures were performed at 4°C or on ice. Immediately prior to data acquisition on flow cytometry (FACSCanto II with Diva software, BD), stained cells were transferred to 5 ml round-bottom tubes (BD) by filtering

through 35 μm cell-strainer cap. Acquired data were later analysed with FlowJo software (Tree Star).

2.6 CD8 T cell isolation

Lymph nodes (LNs) from naïve 2C or OT-1 TCR-transgenic mice ($CD90.1^+$) were pooled and used for single cell preparation with a tissue grinder and complete media. CD8 T cells were then purified from the single cell suspension by negative selection using Magnetic Activated Cell Sorting (MACS) with a $CD8a^+$ T cell isolation kit II (Miltenyi Biotec) according to the manufacturer's instructions. Briefly, unneeded cells were magnetically labelled and depleted using a cocktail of biotin-conjugated antibodies (against CD4, CD11b, CD11c, CD19, CD45R, CD49b, CD105, MHC class II, Ter-119 and TCRγδ) and magnetic microbeads. The purity of isolated CD8 T cells ($CD3^+CD8^+CD90.1^+$) exceeded 96% based on flow cytometry analysis.

2.7 CD8 T cell stimulation in vitro

aAPCs or membrane vesicles from aAPCs or BMDCs were first pulsed with the indicated peptide for 2 hours (37°C, 5% CO_2) before co-culture with 2C or OT-1 CD8 T cells (5 x 10^4 cells/well, 96 well flat-bottom plate, Corning). After co-culture for the indicated time, early activation of CD8 T cells was evaluated by cell surface staining for activation marker CD25 or CD69 along with CD8 and CD90.1 to gate for TCR-transgenic CD8 T cells during flow cytometry analysis. Proliferative responses of CD8 T cells in the co-cultures were evaluated by ^{3}H-thymidine incorporation assay (see below).

2.8 ^{3}H-thymidine incorporation assay

Co-cultures of CD8 T cells with the indicated stimuli were pulsed with 1 μCi ^{3}H-thymidine (American Radiolabeled Chemicals) for 8 hours before harvest at day 3 (if not specified). Cells were then disrupted with distilled water to release ^{3}H-thymidine incorporated DNA which was harvested onto Glass Fiber Filters

(PerkinElmer). The filters were rendered dry in a 37°C oven and then assembled into a 96 well base plate. Micorscint-20 scintillation cocktail solution (PerkinElmer, 25 μl/well) was added before counting radioactivity with TopCount (PerkinElmer) as counts per minute (c.p.m.). Each sample had triplicate cultures and mean and standard deviation (SD) of c.p.m. were shown.

2.9 ELISA

Culture supernatant was taken from co-cultures of 2C CD8 T cells, QL9 peptide and aAPCs. Mouse IL-2 or IFNγ ELISA Set (BD) was used to detect IL-2 or IFNγ in the supernatant, according to the manufacturer's instructions. Briefly, EIA plate microwells were coated with capture antibody in coating buffer and then incubated overnight at 4°C. The plate was washed with wash buffer and then blocked with assay diluent for 1 hour at room temperature (RT). After washing, the plate was incubated with standards and samples (culture supernatant) for 2 hours at RT. After another washing, detection antibody was added along with SAv-HRP reagent (BD) for 1 hour incubation at RT. After final washing, TMB substrate solution (BD) was added for 30 minutes incubation at RT, followed by addition of stop solution and absorbance reading at 450 nm.

2.10 Revised BMDC culture method

Femurs and tibias were surgically removed from 6 – 8 weeks old C57BL/6 mice. Muscles were then trimmed off from the bones and clean bones were immersed in 70% ethanol for 2 minutes, followed by washing with ice-cold RPMI-1640 medium. Ends of bones were cut off with clean scissors and bone marrow was obtained by flushing out with RPMI-1640 medium and a syringe. Clumps were broken up by pipetting and then transferred to a 50ml collection tube by passing through a 70μm Nylon cell strainer. After centrifugation, the cell pellet was resuspended with red blood cell (RBC) lysis buffer, followed by 2 minutes incubation on ice, then addition of complete media and centrifugation. After removing supernatant, bone marrow (BM) cells were resuspended for

BMDC culture as detailed in the Results section. Briefly, the density of BM cells was adjusted to 2 x 10^5 cells/ml with DC media containing 20 ng/ml murine GMCSF and seeded into 150 mm sterile petri dishes (BD; 23 ml/dish). After 3 days, fresh DC media was added to the culture (23 ml/dish). At day 6, the cultures were supplemented with fresh DC media by removing and centrifuging the upper 50% volume of the cultures; the cells in the pellet were added back to the cultures together with fresh media. At day 8 and 9, media was changed as at day 6. At day 9, LPS was added at a final concentration of 20 ng/ml. At day 10, after overnight LPS stimulation, both non-adherent and adherent cells were harvested by scraping and pipetting. Frequent monitoring of BMDC culture was found to be essential to prevent the cultures from turning yellow. Cells were not exposed to LPS stimulation for longer than 18 hours to prevent the cells from dying following LPS-induced activation. If the viability was lower than 90% (by trypan blue exclusion), dead cells were removed before use (see below).

2.11 Dead cell removal

Dead cells in final BMDC culture were removed by using OptiPrep density gradient medium (Axis-shield, Norway) according to the manufacturer's instructions with some modifications. Briefly, cells were resuspended with 3x volumes of PBS (Gibco) and then mixed well with 1x volume of OptiPrep density gradient medium. The mixture was carefully overlaid with 1x volume of PBS to form a fine density gradient, followed by centrifugation at 450 x g for 30 minutes without using the brake. Floating cells were viable cells (dead cells were in the pellet) which were collected and mixed with a large volume of PBS to reduce density. Viable cells were then pelleted with centrifugation at 450 x g for 10 minutes, followed by resuspension with homogenization buffer for membrane vesicle preparation (see below).

2.12 Revised membrane vesicle preparation method

Membrane vesicles from aAPCs and BMDCs were prepared by modifying the protocol of Kovar et al (Kovar et al., 2006). The modifications made to this protocol are described in detail in the Results section. In brief, APCs were first resuspended in PBS and a 15 mL sample tube. After centrifugation (500 x g, 10 minutes), the pellet was resuspended in homogenization buffer (10x, relative to cell pellet volume) containing a cocktail of protease inhibitors (Roche). After resuspending by brief vortexing, cells were gently homogenized with a loose-fitting Dounce homogenizer (Kontes Glass Co.) to achieve > 90% cell breakage which was constantly monitored by taking a few microliters of homogenates for phase contrast microscopy analysis. Tonicity buffer (1x) was then added, followed by low speed centrifugation (800 x g, 10 – 20 minutes, without brake) to remove nuclei and large dead cells and debris. Supernatants were carefully taken without disturbing the solid pellet and samples could then be frozen for later processing or directly subjected to 3 cycles of freezing and thawing. After that, samples were sonicated until they changed from cloudy to clear. To avoid overheating, sample tubes were dipped in ice slurry and sonicated with automatic "ON" and "OFF" cycles. Sonicated samples were then centrifuged at 3,000 x g for 20 – 30 minutes without using the brake. Supernatants were taken for pelleting membrane vesicles by ultracentrifugation (100,000 x g, 1 – 2 hours). The pellet was then resuspended with a tight-fitting Dounce homogenizer and used as vesicle-aggregates (V-hom) or further sonicated to generate nano-vesicles (V-hom-son).

2.13 DC protein assay

The protein content of membrane vesicle was measured by *DC* protein assay (Bio-Rad), according to the manufacturer's instructions with some modifications. 7 dilutions of a BSA protein standard (Bio-Rad) containing from 0.072 mg/ml to 1.287 mg/ml protein were prepared and mixed with 10% SDS to a final concentration of 1% SDS. In the same way, 27 μl of membrane vesicle samples were mixed with 3 μl of 10% SDS. Both standards and samples were incubated at 95°C for 10 minutes and then loaded onto a flat-bottom 96

well EIA plate (Nunc); 5 μl/well in triplicate. Mixture of Reagent S and A (1:50, Bio-Rad) were then added (25 μl/well), followed by addition of Reagent B (Bio-Rad, 200 μl/well) and absorbance measurement at 630 nm.

2.14 Phase contrast microscopy

Membrane vesicles or cells were 1:1 diluted with 0.4% trypan blue solution (Sigma) and loaded onto a phase haemocytometer (Hausser Scientific, USA) and then covered with a coverglass (ProSciTech, Australia). Samples were then observed by phase contrast microscopy (Leica) at 20x magnification.

2.15 Zetasizer Nano analysis

The size of membrane vesicle was measured in triplicate using a Zetasizer Nano ZSP (Malvern) with a 633 nm He-Ne laser. Each measurement consisted of 15 runs, each run lasting for 10 seconds. Measurements were carried out at room temperature using a scattering detection angle of 173°.

2.16 Vesicle surface staining and flow cytometry

Membrane vesicles containing aggregates (e.g. V-hom or V-hom-son-FT) were diluted with FACS buffer to a final concentration of 0.3 – 0.5 mg/ml and then transferred to a 1.5 mL sample tube (100 μl/tube). Mouse BD Fc Block (anti-CD16/32; 1 μg/sample) was added for 10 minutes incubation, followed by addition of pre-titrated fluorochrome-conjugated antibodies against vesicle surface molecules. After 30 minutes incubation, FACS buffer was added (200 μl/tube) and whole sample was transferred to 5 ml round-bottom tubes (BD) by filtering through 35 μm cell-strainer cap. Stained vesicles were then directly analysed by flow cytometry (FACSCanto II with Diva software, BD). Vesicles plus isotype control antibodies, fluorochrome-conjugated antibodies alone (without vesicles), and vesicles without antibodies were used as controls. The size detection limit of FACSCanto II is about 0.5 μm, therefore, free antibodies are not detectable. All procedures were performed at 4°C or on ice. Acquired

data were later analysed with FlowJo software (Tree Star).

2.17 PKH26 labelling of membrane vesicles

Membrane vesicles were labelled with PKH26 Red Fluorescent Cell Linker Kits (Sigma) according to the manufacturer's instructions with some modifications. Briefly, membrane vesicles in PBS were pelleted by ultracentrifugation (100,000 x g, 2 hours, 4°C) in order to resuspend in Diluent C by tight-fitting homogenization. After dispersing vesicle-aggregates by sonication, nano-vesicles in Diluent C were 1:1 mixed with 2x PKH26 Dye Solution. The mixture was then pelleted by ultracentrifugation. After discarding supernatant, PKH26 labelled membrane vesicles were resuspended in PBS and then pelleted by another ultracentrifugation to remove residual dye solution. Finally, pelleted membrane vesicles were resuspended in PBS for subsequent uses.

2.18 Immunoblotting of membrane vesicles

Membrane vesicles (total 5 μg protein contents) were mixed with RIPA lysis buffer (Sigma) and NuPAGE LDS Sample Buffer and Reducing Agent (InVitrogen), followed by incubation at 70°C for 10 minutes. Samples were then loaded in NuPAGE Novex 4 – 12% Bis-TrisGel (InVitrogen). Gels were then electroblotted on polyvinylidene difluoride membranes (Millipore), followed by labelling with indicated primary antibodies and HRP conjugated secondary antibodies. Blots were visualised using SuperSignal West Pico Chemiluminescent Substrate (Thermo Scientific).

2.19 Irradiated splenocytes preparation

Single cell suspensions were prepared from spleens of C57BL/6 mice. Cells were then treated with RBC lysis buffer, followed by washing and resuspension in complete media. Splenocytes were then irradiated with X-RAD 320 X-ray irradiator (Precision X-Ray, USA; 2000 rads) and used for *in vitro* co-culture.

2.20 Intra-cellular staining

To detect intra-cellular molecules (e.g. perforin, granzyme-B and IFNγ), single cell suspensions were first stained for surface molecules (e.g. CD8 and CD90.1) as described above. Cells were then incubated with Cytofix/Cytoperm (BD, 100 μl/sample). After 20 minutes, cells were washed twice with 1x Perm/Wash solution and centrifugation. Permeabilised cells were then resuspended in 1x Perm/Wash solution (50 μl/sample) containing fluorochrome-conjugated antibodies against intra-cellular molecules. 30 minutes later, stained cells were resuspended in FACS buffer after removing un-bound antibodies by repeated FACS buffer washing and centrifugation. All procedures were performed at 4°C or on ice.

For single cell suspension containing donor OT-1 CD8 T cells from immunised mice (see below), cells were first re-stimulated *in vitro* with 10 μM SIINFEKL peptide in the presence of GolgiPlug (BD, 1μl/sample) for 4 hours (37°C, 5% CO_2) before intra-cellular staining.

2.21 Adoptive transfer and in vivo stimulation

For stimulation of TCR transgenic donor CD8 T cells *in vivo*, 2C or OT-1 CD8 T cells were resuspended in PBS and transferred I.V. to normal C57BL/6 mice (1 x 10^6 cells/mouse if not specified). The next day (if not specified), the mice were injected I.V. with peptide-pulsed membrane vesicles. At various time points after adoptive transfer, spleen and LN cells were analysed for donor cell recovery and expression of surface molecules by flow cytometry. To detect intra-cellular effector molecule (e.g. granzyme-B and IFNγ) production from donor cells, *in vitro* peptide re-stimulation was performed before flow cytometry analysis as described above.

2.22 CFSE proliferation assay

2C or OT-1 CD8 T cells were washed twice in PBS and resuspended at 5 x

10^7 cells/ml for staining with Carboxyfluorescein succinimidyl ester (CFSE) buffer containing 5 μM CFSE. Cells were incubated at 37°C for 10 minutes then washed twice with ice-cold complete media and centrifugation. Cells were then resuspended in PBS for adoptive transfer as described above. At various time points after adoptive transfer, spleen and lymph nodes cells were analysed by flow cytometry for donor cell CFSE dilution as an indication of proliferation.

2.23 In vitro CTL assay

To generate effector cytotoxic T lymphocytes (CTL), 2C CD8 T cells ($CD90.1^+$) were stimulated by culture (5 x 10^4 cells/well; 96 well flat-bottom plate) with membrane vesicles containing aggregates (V-hom; 10 μg/ml) in the presence of 0.3 μM SIYR peptide for 3 days at 37°C, 5% CO_2.

To prepare target cells, EL4 cells (ATCC) were pulsed with 10 μM SIYR peptide at 37°C for 1 hour before washing and labelling with 6 μM CFSE ($CFSE^{Hi}$). Peptide un-pulsed EL4 cells were labelled with 0.3 μM CFSE ($CFSE^{Lo}$).

Different numbers of 2C effector CD8 T cells were loaded on to a V-shaped 96 well plate, followed by addition of 1:1 mixture of $CFSE^{Hi}$ and $CFSE^{Lo}$ target cells. Cells were then mixed well by pipetting and briefly centrifuged to facilitate the rapid contact between the CTL and target cells. After 4 hours incubation (37°C, 5% CO_2), the cultures were examined for viable $CD90.1^-CFSE^+$ cells ($CFSE^{Hi}$ and $CFSE^{Lo}$) by flow cytometry.

2.24 In vivo CTL assay

Normal C57BL/6 mice ($CD45.2^+$) were adoptively transferred with 1 x 10^6 OT-1 CD8 T cells. For the next 4 days, the mice were immunised daily with peptide-pulsed membrane vesicles using the conditions specified.

To prepare antigen-presenting target cells, splenocytes from $CD45.1^+$ C57BL/6 mice were pulsed with 2 μM SIINFEKL peptide and labelled with 2 μM CFSE ($CFSE^{Hi}$). Some CD45.1+ splenocytes were labelled with 0.2 μM CFSE ($CFSE^{Lo}$) without peptide pulsing as control target cells. Target cells with or

without peptide antigen were 1:1 mixed and injected I.V. (total 5 x 10^6 cells) to immunised and control naïve C57BL/6 mice, 6 days after 1st immunisation.

1 day after target cell injection, spleens were removed and cell suspensions were analysed by flow cytometry to detect $CFSE^{Hi}$ versus $CFSE^{Lo}$ $CD45.1^+$ target cells. Specific killing (%) of antigen presenting $CFSE^{Hi}$ target cells was determined by (1-%$CFSE^{Hi}$/%$CFSE^{Lo}$) x 100.

2.25 Immunofluorescence microscopy

C57BL/6 mice were injected I.V. with PKH26-labelled membrane vesicles (V-hom-son; 100 μg/mouse). 5 minutes later, spleens were removed from the mice and frozen in OCT compound (Tissue-Tek). Later, 6 – 7 μm sections were prepared with Leica Cryostat CM3050S, fixed in acetone and blocked with 10% horse serum. The sections were then incubated with Alexa Fluor 647-conjugated antibodies against mouse FcγRII/III and F4/80. Finally, the sections were analysed by a Leica DM 5500 microscope.

2.26 Tumour challenge and immunisations

To vaccinate against tumour growth, C57BL/6 mice were first injected I.V. with peptide-pulsed membrane vesicles as indicated. 6 days later, the mice were subcutaneously injected with the indicated mouse tumour cell lines (2 x 10^5 cells/50μl/mouse) on the back.

To induce rejection of established tumours, C57BL/6 mice were first injected with the indicated tumour cell lines as above. When tumours were palpable, the mice were injected I.V. or I.T. (Intra-Tumour) with peptide-pulsed membrane vesicles as indicated. For I.T. injection, the syringe needle was inserted subcutaneously ~ 8 mm away from the tumour and then injected directly into the tumour.

2.27 Data analysis and statistics

Data are reported as the mean ± standard deviation (SD), along with the

calculated *P* values. Unpaired 2-tailed Student's t-Test was used to calculate *P* values and determine statistically significant differences. *P* values of < 0.05 were considered statistically significant.

3 Experimental Data

3.1 Preparation of bulk populations of mature dendritic cells from mouse bone marrow

3.1.1 Introduction

As outlined in the Introduction, cancer immunotherapy by injection of tumour antigen-loaded DCs can be beneficial but is hampered by a number of problems, including poor localisation of injected DCs in the lymphoid tissues and the difficulty of preparing large numbers of mature DCs for injection. This thesis aims to overcome the limitations of current DC-based therapy by using membrane vesicles prepared from APCs as a subcellular antigen presentation system to stimulate CD8 T cells. To prepare membrane vesicles, large numbers of APCs are required. In initial studies, I describe the use of a transfected cell line as a source of artificial APCs (aAPCs). I then describe the development of a new method for preparing large numbers of murine bone marrow-derived DCs (BMDCs) expressing a high density of co-stimulatory molecules. Generation of membrane vesicles from these APCs is described in Section 3.2.

3.1.2 Results

3.1.2.1 Artificial APCs: both TCR and co-stimulatory signals are required for full CD8 T cell activation

Our group has previously generated transfected *Drosophila* S2 cells as aAPCs and used them to study various aspects of T cell activation (Cai et al., 1996; Cai et al., 1997b; Huang et al., 1999; Hwang et al., 2000). S2 cells derived from *Drosophila melanogaster* embryos were transfected with cDNA encoding murine L^d MHC class I and β_2-microglobulin ($a.L^d$). In addition to L^d and β_2-microglobulin, some S2 cells were co-transfected with cDNA encoding murine B7-1 and ICAM-1 co-stimulatory molecules ($a.L^d$.B7-1.ICAM-1) (Cai et al., 1996). Transfected gene expression can be induced by treating cells with 1mM

copper sulfate for 24 hours and the expression is confirmed with mAbs staining and flow cytometry (Figure 3).

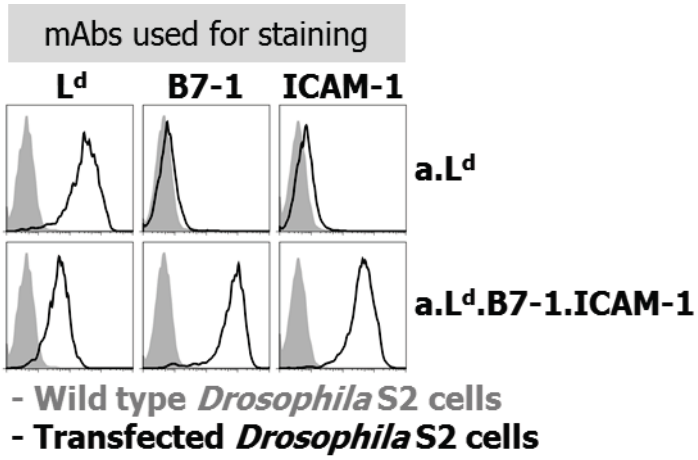

Figure 3. Artificial APCs (aAPCs).
Drosophila S2 cells transfected with murine MHC class I L^d alone ($a.L^d$) or along with murine B7-1 and ICAM-1 ($a.L^d$.B7-1.ICAM-1) were stimulated with 1mM copper sulfate for 24 hours to induce the expression of transfected genes. Cells were stained with mAbs against each molecule and then analysed with flow cytometry. Wild type *Drosophila* S2 cells without transfected genes were used as a control and are shown in grey. The data are representative of more than ten independent experiments.

To evaluate the signals required for CD8 T cell activation, naïve 2C CD8 T cells were prepared from lymph nodes of 2C TCR transgenic mice with a $CD8a^+$ T Cell Isolation Kit II (Miltenyi Biotec). 2C TCR transgenic mice are on a C57BL/6 background, and thus 2C CD8 T cells express K^b MHC class I and react to SIYR peptide (SIYRYYGL) bound to K^b. 2C CD8 T cells also show strong allo-reactivity to QL9 peptide (QLSPFPFDL) presented on L^d, and QL9 peptide cannot be presented on K^b. Therefore, when QL9 peptide and L^d-expressing aAPCs are used, 2C CD8 T cells can only receive antigenic signals from aAPCs and not from T cells themselves, thus avoiding the problem of co-stimulation via T cell to T cell interaction. Consistent with the previous report by Cai et al (Cai et al., 1997a), in the presence of 10μM QL9 peptide, $a.L^d$ APCs were totally non-stimulatory and failed to upregulate the expression of the early T cell activation marker, CD69, on 2C CD8 T cells, but did induce a marked reduction

of surface TCR (Figure 4 A). By contrast, a.L^d.B7-1.ICAM-1 APCs not only down-regulated surface TCR, but also strongly upregulated CD69 on 2C CD8 T cells and induced strong proliferation on day 2 and day 3 in *in vitro* cultures (Figure 4 B). 2C CD8 T cells co-cultured with a.L^d.B7-1.ICAM-1 plus QL9 peptide for 3 days also secreted both IL-2 and IFNγ (Figure 4 C), indicating differentiation of 2C CD8 T cells into effector cells. These studies confirm that, at least with aAPCs, naïve CD8 T cells are unresponsive to Signal 1 alone (MHC I plus peptide) but are fully responsive to APCs expressing Signal 1 plus Signal 2 (B7-1 plus ICAM-1). As discussed below, the results can be different with other forms of antigen presentation.

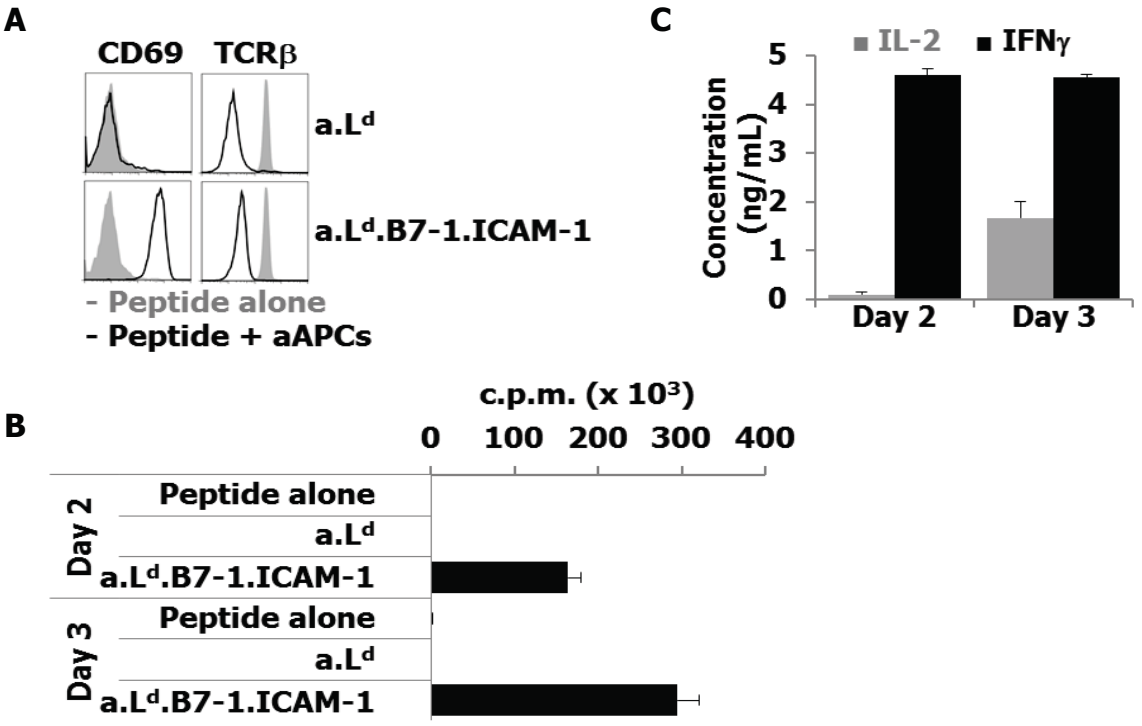

Figure 4. Co-stimulatory molecules are essential for full CD8 T cell activation. 2C CD8 T cells (5 x 10^4 cells) were cultured with QL9 peptide alone (10 μM) or peptide plus the indicated aAPCs (5 x 10^4 cells): (A) for 16 hours followed by staining with anti-CD69 or anti-TCRβ mAbs, then flow cytometry analysis (staining for 2C CD8 T cells cultured with peptide alone are shown in grey), (B) for 2 or 3 days for measurement of proliferation by ^{3}H-thymidine incorporation assay (mean and SD, triplicate cultures), or (C) for 2 or 3 days to measure synthesis of the indicated cytokines by ELISA (mean and SD, triplicate cultures). The data are representative of more than three independent experiments.

3.1.2.2 Immunogenicity of aAPCs is maintained after fixation with paraformaldehyde

A feature of *Drosophila* S2 cells is that, unlike natural APCs such as DCs, they do not secrete cytokines that may facilitate CD8 T cell activation. However, as a.L^d.B7-1.ICAM-1 APCs were able to fully activate 2C CD8 T cells, APC presentation of a dense array of peptide-MHC class I (pMHC) and co-stimulatory molecules may bypass the need for cytokine production by APCs. Indeed, T cells can be activated by pMHC and co-stimulatory molecules presented on different structures such as 2D-supported lipid bilayers, liposomes and latex microbeads (Irvine and Doh, 2007; Oelke et al., 2003; Prakken et al., 2000). Moreover, previous studies showed that 2C CD8 T cells could be stimulated by glutaraldehyde-fixed mouse erythrocytes loaded with L^d plus QL9 peptide (Luxembourg et al., 1998). In support of this finding, a.L^d.B7-1.ICAM-1 APCs were immunogenic for 2C CD8 T cells after fixation with 1% paraformaldehyde. Thus, these fixed APCs were able to activate 2C CD8 T cells to proliferate in the presence of QL9 peptide as evidenced by up-regulation of the early activation marker CD25 after 16 hours of *in vitro* culture and by ^{3}H-thymidine incorporation on day 2 and day 3 of culture (Figure 5 A and B). Fixed a.L^d.B7-1.ICAM-1 APC were equally as potent as non-fixed APC at inducing CD25 expression but were slightly less potent at inducing proliferation, perhaps reflecting that optimal formation of immunological synapses (IS) during T/APC interaction requires membrane fluidity to organise pMHC, co-stimulatory and adhesion molecules into ring-like supramolecular activation clusters (SMACs) (Hsu et al., 2012). Nevertheless, the data are in agreement with the view that the immunogenicity of APCs, including peptide-loaded DCs (Fujii et al., 2004; Fujii et al., 2003), is preserved after cell-fixation.

Another feature of *Drosophila* S2 cells is that they grow optimally at 26 – 28°C and die rapidly at 37°C, which is the temperature used for all *in vitro* culture studies related to this thesis. Consistent with the above fixation studies, when a.L^d.B7-1.ICAM-1 APCs were first cultured at 37°C overnight (to allow them to die) and then cultured with 2C CD8 T cells in the presence of QL9

peptide, the cells were still able to up-regulate the expression of CD25 on 2C CD8 T cell surface after 12 hours of co-culture (data not shown).

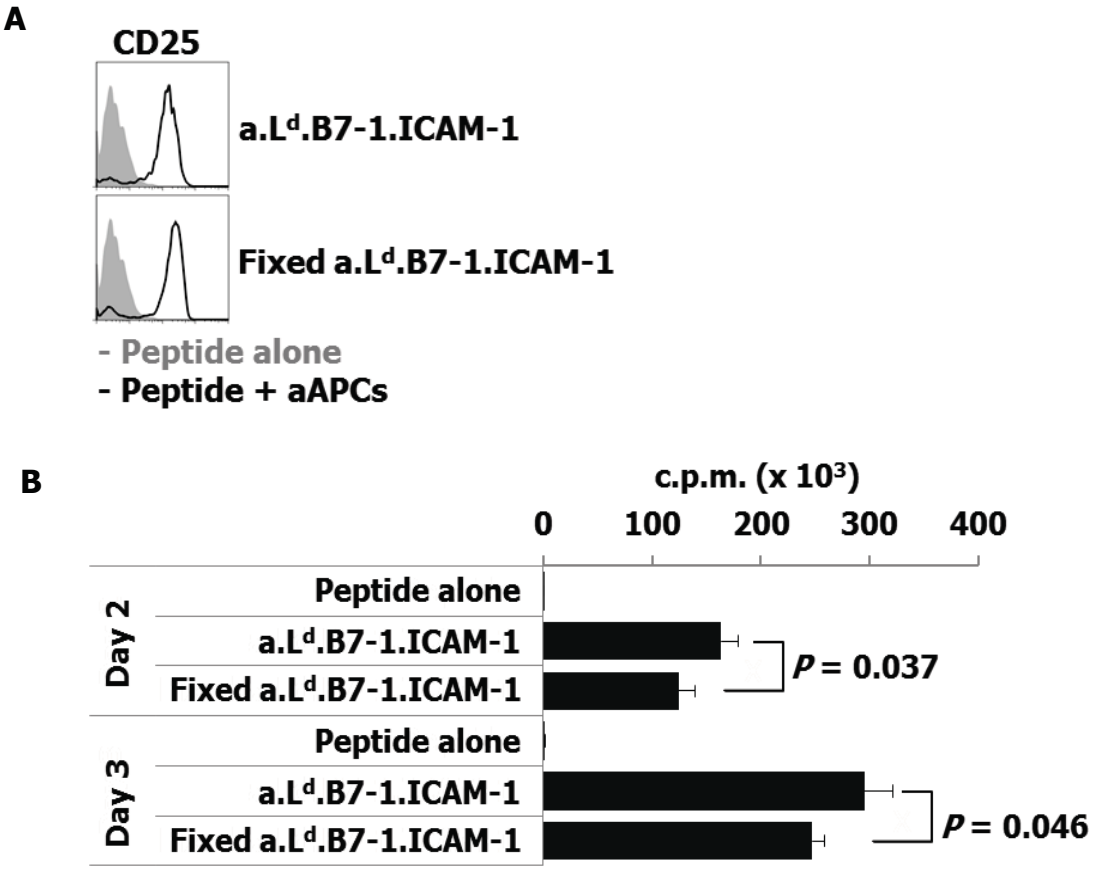

Figure 5. Fixed aAPCs effectively stimulate CD8 T cells. 2C CD8 T cells were cultured with QL9 peptide alone (10 μM) or along with a.L^d.B7-1.ICAM-1 with or without fixation of APC with 1% paraformaldehyde. Cells were cultured for 16 hours followed by staining with anti-CD25 mAb and flow cytometry analysis to measure CD25 expression (A), or for 2 or 3 days to measure ^{3}H-thymidine incorporation (B) (mean and SD, using 5 x 10^4 cells/well). The data are representative of three independent experiments.

The main conclusion from the above studies is that APCs do not have to be viable to be immunogenic, with the proviso that APCs express a high density of pMHC and co-stimulatory molecules on the cell surface before fixation. The original report that fixation abolishes APC function (Jenkins et al., 1987) can be attributed to the fact that the APC used in this study (immature DC from spleen) were fixed before overnight culture, thereby preventing the cells from upregulating co-stimulatory molecules. This finding applies with limiting

amounts of pMHC: however, at a high concentration, pMHC on fixed APC can be directly immunogenic in the absence of co-stimulation (Luxembourg et al., 1998). Likewise, co-stimulation is not essential when T cells are stimulated via mAb cross linking of TCR/CD3. With viable APCs and a limiting concentration of pMHC, however, lateral movement of pMHC in the lipid bilayer prevents crosslinking, resulting in a crucial need for co-stimulation to induce T cell stimulation.

In the next chapter, evidence will be presented that membrane vesicles from a.L^d.B7-1.ICAM-1 APCs are directly immunogenic for 2C CD8 T cells *in vitro*. This finding together with information from the above studies suggest that generation of immunogenic membrane vesicles from normal APCs would depend on preparing vesicles from fully-mature DCs expressing a high density of MHC I and costimulatory molecules. It was therefore crucial to devise a method for generating fully-mature DCs in large numbers.

3.1.2.3 A new method for producing large numbers of mature BMDCs

Since their first discovery (Steinman and Cohn, 1973), DCs have attracted widespread attention because of their unique capacity to stimulate immune responses by naïve T cells. However, studies on DCs have been hampered by the scarcity of these cells in normal lymphoid tissues (Inaba et al., 2009; Williams et al., 1994). This problem can be partly overcome by generating DCs from mouse bone marrow progenitors. The method was originally developed by Inaba et al from Ralph Steinman's group (shown as Inaba method in Figure 6), and it has already become the standard method to prepare bone marrow derived DCs (BMDCs) (Inaba et al., 1992; Inaba et al., 2009), although it has since been modified by many groups, including Lutz et al. (Lutz et al., 1999). In the Inaba method, mouse bone marrow (BM) progenitors (prepared from mouse femurs and tibias) are seeded at 1 x 10^6 cells/ml in complete RPMI media supplemented with 20 ng/ml of granulocyte macrophage colony-stimulating factor (GMCSF). As DC precursors tend to be adherent to plastic surfaces at early stages of culture, non-adherent cells are rinsed off on days 2

and 4 of culture to remove granulocytes and lymphocytes. After 8 days of culture and changing media every 2 days, non-adherent cells are harvested as mature DCs after overnight LPS stimulation (Figure 6).

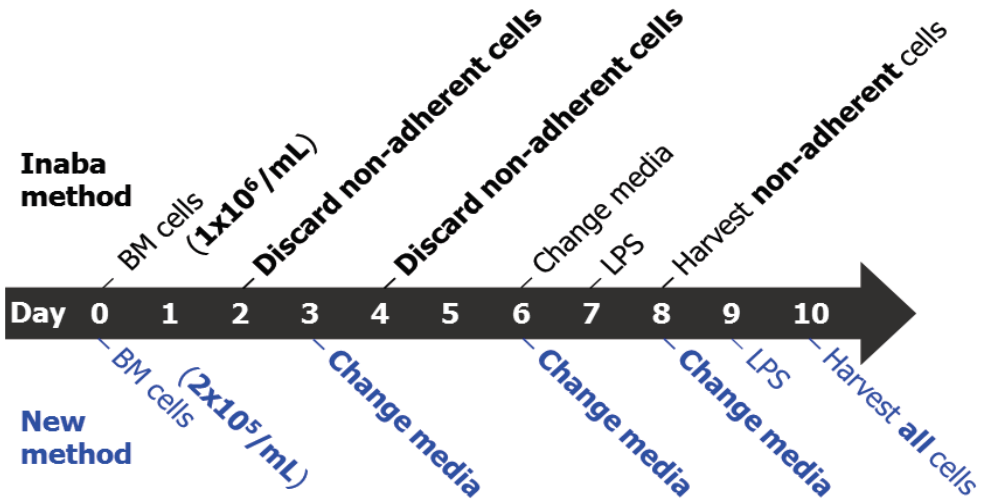

Figure 6. Modification of Inaba method for preparing BMDCs. Using unseparated BM cells from young C57BL/6 mice, Inaba et al (2009) cultured BM cells at high density (1 x 10^6 cells/ml) in GMCSF (20 ng/ml) supplemented medium at 37^o C, then washed the cultures to remove non-adherent cells at day 2 and again at day 4 of culture; LPS was added on day 7 and non-adherent cells were harvested 1 day later for use as APCs. The new method described in this thesis involved culturing BM cells at a lower density (2 x 10^5 cells/ml) in GMCSF (20 ng/ml) supplemented medium and adding new medium (containing the same concentration of GMCSF) to the cells every 2 or 3 days without discarding cells. After overnight addition of LPS on day 9, both non-adherent and adherent cells were harvested at day 10. For both culture methods, cells were cultured in sterile 150mm petri dishes.

With this method, consistent with the report by Inaba et al, I was able to prepare highly-purified BMDCs (~ 5 x 10^6 cells/mouse), of which >95% were $CD11c^+$ MHC class I $(K^b)^+$ $ICAM\text{-}1^+$ and >60% highly expressed co-stimulatory molecule B7-1 (Figure 7); CD11c is a DC-specific marker in the mouse, although it is also expressed on monocytes and activated B cells in humans (Inaba et al., 2009). Generation of DC from BM precursors is certainly an improvement over enrichment of DC from mouse spleen by magnetic selection or by other methods where usually only about 1 x 10^6 DCs/mouse can be obtained (Inaba et al., 2009). However, with the Inaba method, BM progenitors from dozens of

mice are needed in order to prepare sufficient amounts of membrane vesicles from mature BMDCs (discussed in chapter 3.2), which diminishes its potential for clinical application.

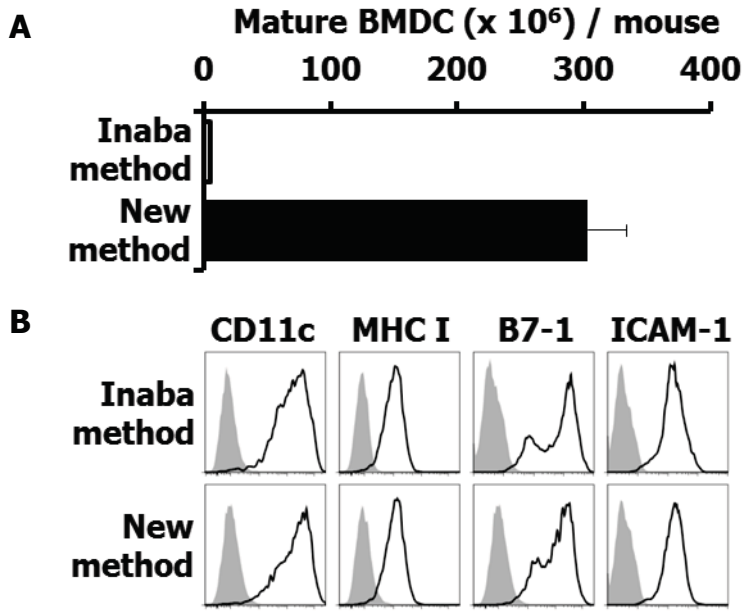

Figure 7. New method for preparing BMDCs generates large numbers of mature DC. BMDCs generated by the standard method of Inaba et al (2009) versus the new method described in Figure 6 were compared for cell yield/mouse (mean and SD) after culture (A) and expression of various cell-surface markers (B). Mature BMDC refers to $CD11c^{+}$ $B7\text{-}1^{Hi}$ cells present in total adherent plus non-adherent cells for the new method and only for non-adherent cells for the Inaba method. Cells were stained with antibodies against the indicated molecules and analysed with flow cytometry. The data are representative of at least three independent experiments.

Therefore, I sought to modify the Inaba method to prepare large yields of mature BMDCs (Figure 6 and 7). As described below, I have made a number of major modifications of the Inaba method, namely: 1) BM progenitors are initially cultured at a low density (2 x 10^5 cells/ml), 2) non-adherent cells are not discarded on days 2 and 4 of culture, 3) the culture period is extended to 10 days, 4) at the end of culture, both non-adherent and adherent cells are harvested (using a cell scraper) after overnight LPS stimulation. With these modifications, cell viability is generally high (70 - 90%); dead cells are removed with OptiPrep gradient if the cell viability is lower than 90%.

With the new method, the yield of mature DCs has been improved dramatically, i.e. from 5 x 10^6/mouse to 3 x 10^8/mouse of mature BMDCs, which express a high density of CD11c, MHC I (K^b), B7-1, B7-2, and ICAM-1 (Figure 7, 8). Prior overnight stimulation with TLR ligands (e.g. CpG or LPS) is critical to increase B7 (B7-1, B7-2) expression as without such stimulation the cells show only low B7 expression and thereby resemble immature DCs (Figure 8).

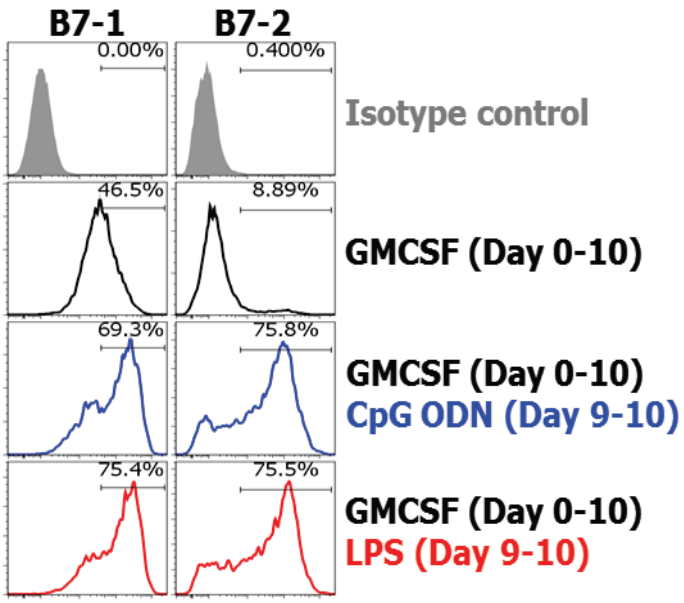

Figure 8. TLR signalling is required for full BMDC maturation.
BMDCs prepared by the new protocol were stimulated overnight on day 9 with 20 ng/ml LPS or 0.5 μg/ml CpG ODN 1668 or left untreated in GMCSF supplemented medium alone. Cells were then stained for antibodies against B7-1 and B7-2 and analysed by flow cytometry. The data are representative of at least two independent experiments.

The marked increase in mature BMDC yields found with the new method is due in part to the inclusion of adherent cells, in addition to non-adherent cells, in the final step of cell harvest (Figure 9 A). Adherent cells in GMCSF supplemented BM cell culture are generally considered to be macrophages and are therefore usually discarded during DC preparation (Inaba et al., 2009; Lutz et al., 1999). However, recent studies have challenged this notion by showing that adherent cells and non-adherent cells have no significant difference in their expression of an array of DC markers and in their ability to stimulate T cell proliferation (Li and Lu, 2010; Yi and Lu, 2012). In support of this finding, non-adherent cells and adherent cells prepared with the new method expressed similar levels of CD11c and surface molecules involved in antigen presentation (K^b MHC class I) and co-stimulation (B7-1 and ICAM-1) (Figure 9 B).

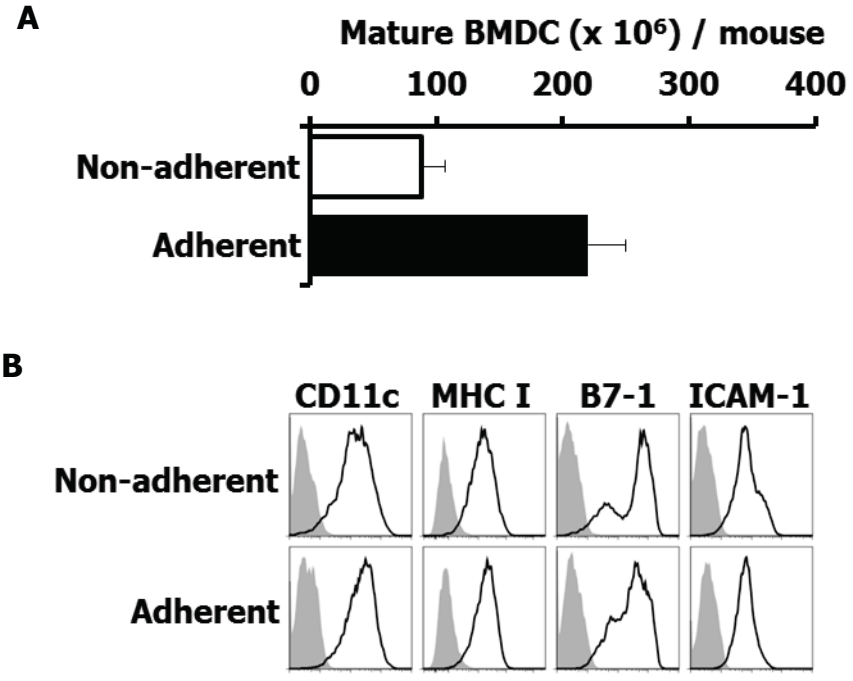

Figure 9. Both adherent and non-adherent cells harvested at the end of the culture period show the surface markers of mature DCs. Non-adherent and adherent BMDCs prepared by the new protocol after overnight LPS stimulation were counted separately (A; mean and SD) and analysed by flow cytometry (B) as in Figure 7. Adherent cells were dislodged with a cell scraper. The data are representative of more than seven independent experiments.

Of note, non-adherent and adherent cells both do not express F4/80 which is a macrophage marker (data not shown). Importantly, the yield of adherent mature BMDCs is about twice that of non-adherent mature BMDCs, so including adherent cells significantly improves final yields. One interesting observation during BMDCs culture is that many cells are only semi-adherent or non-adherent on day 9 of culture, and large numbers of cells become detached after gently tapping and shaking the culture dishes. However, the majority of the floating cells become adherent on day 10 of culture after overnight LPS stimulation, suggesting that at least some of the adherent cells on day 10 are derived from non-adherent populations.

As also reported by Lutz et al. (Lutz et al., 1999), seeding BM cells at a low density is an especially important contributing factor for the increase in cell yields. Thus, when BM cells were initially cultured at a high density (1×10^6 cells/ml) as used in the Inaba method, the yield of mature BMDCs after 10 days of culture was dramatically decreased, though cell yields on day 7 were the same (Figure 10). Why culture at a high density causes cell yields to decrease sharply between days 7 – 10 is unclear. However, it is of interest that culturing splenic DCs in a high concentration (5×10^6/ml) has been found to induce spontaneous activation of DCs and result in the cells expressing a much higher level of co-stimulatory molecules, compared to cells cultured in a low concentration (2×10^5/ml) (Vremec et al., 2011). It is also known that activation of immature DCs leads not only to up-regulation of costimulatory molecules but also to down-regulation of Bcl-2, thereby causing mature DCs to die, thus regulating the intensity of the immune response (Hou and Van Parijs, 2004; Kushwah and Hu, 2010). Therefore, it is tempting to speculate that culturing cells at a high cell density (1×10^6/ml) promotes activation of BMDCs at an early stage of culture, causing spontaneously-matured BMDCs to start to die after around 7 days of culture, thereby resulting in a marked reduction in yields on day 10 compared to day 7. By contrast, low density culture allows BMDCs to remain relatively immature, enabling their survival and proliferation for at least 10 days of culture (Figure 10).

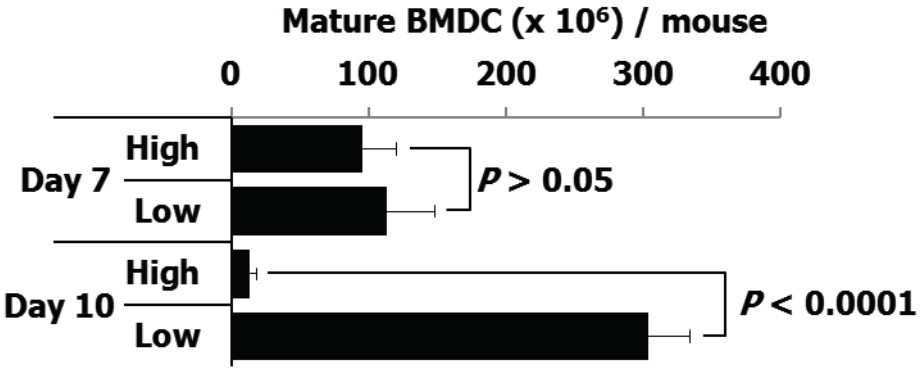

Figure 10. Higher cell density during culture reduces yield of mature BMDC. Using the new protocol, BM cells were cultured on day 0 either at the low density used above (2 x 10^5 cells/ml) or at a high density (1 x 10^6 cells/ml) and then harvested at the indicated time points after overnight stimulation with LPS. Cells were then counted and analysed by flow cytometry. As in preceding Figures, mature BMDC refers to $CD11c^+$ $B7\text{-}1^{Hi}$ cells (mean and SD). The data are representative of more than three independent experiments.

Finally, 10 days of prolonged culture is critical to prepare highly-pure $CD11c^+$ $B7^{Hi}$ DCs. Thus, the proportion of these cells generated after overnight culture with LPS in the new method is clearly higher on day 10 than on day 8 (used by Inaba) (Figure 11). Moreover, in contrast to the Inaba method there is no need to discard non-adherent cells on day 2 and day 4 of culture. Also, the problem of B cell generation in the Inaba cultures (Inaba et al., 2009) is avoided. On this point, Inaba et al found that, even after discarding non-adherent cells on day 2 and day 4, some B cells could still be found after 8 days of culture, often necessitating the use of anti-CD11c magnetic microbeads to enrich for $CD11c^+$ DCs (Hou and Van Parijs, 2004). As shown here, this problem can be avoided simply by prolonging the culture until day 10, at which stage nearly all cells are $CD11c^+$ (Figure 11). As mentioned above, however, this approach depends critically on culturing cells at a low density.

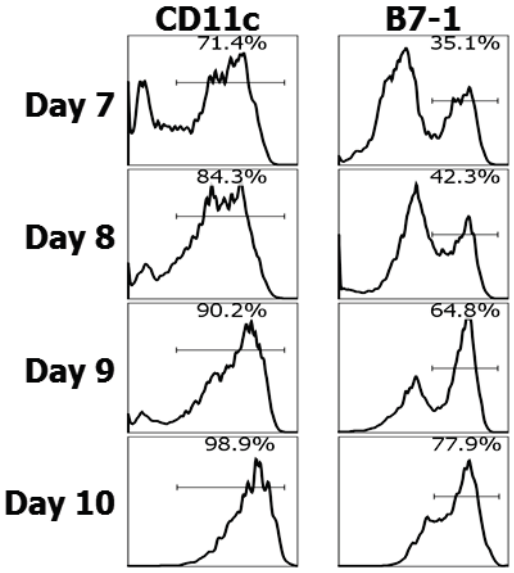

Figure 11. Prolonged culture improves both purity and maturation of BMDCs. BMDCs were prepared by the new protocol and harvested at the indicated time points after overnight stimulation with LPS. Cells were then stained with antibodies against CD11c and B7-1, followed by flow cytometry analysis. The data are representative of more than three independent experiments.

3.1.2.4 Effects of supplementing BMDC cultures with IL-4

In addition to GMCSF, many other growth factors and cytokines have been tested in BMDC cultures, including interleukin-4 (IL-4), FMS-related tyrosine kinase 3 ligand (Flt3L) and IL-3. Changing the combination and concentrations of these factors were found to result in major differences in BMDC phenotype (Lutz and Rossner, 2007; Menges et al., 2005; Xu et al., 2007). Among them, GMCSF plus IL-4 is probably the most widely used combination, and IL-4 is known to promote BMDC maturation (Labeur et al., 1999; Lutz et al., 2002; Lutz et al., 2000). Also in humans, GMCSF plus IL-4 are routinely used for the generation of dendritic cells from peripheral blood monocytes (Nair et al., 2012; Sallusto and Lanzavecchia, 1994). For these reasons, I investigated whether the efficiency of the new method for preparing murine BMDCs could be further improved by the addition of a mixture of GMCSF (20 ng/ml) plus IL-4 (40 ng/ml) starting on day 0; control cultures contained GMCSF alone.

Examination of the cultures on day 7 showed that, relative to GMCSF alone, the combination of GMCSF plus IL-4 led to poor overall cell recoveries and cell death as revealed by subcellular debris (black arrows) and the presence of cells with pyknotic nuclei (white arrows) as assessed by phase contrast microscopy (Fig 12 A, B). Moreover, the GMCSF plus IL-4 cultures contained significant numbers of $B220^{+}$ and $Ly6G^{+}$ cells, indicating the presence of B cells and granulocytes, respectively (Figure 12 C); many of these cells were small (FSC^{lo}) and were probably in early stages of cell death (Fig 12 D). Consistent with previous reports, GMCSF plus IL-4 culture promoted spontaneous maturation of BMDCs without LPS stimulation as indicated by significant proportions of cells expressing MHC II (IA^{b}), B7-1 and B7-2 (Figure 12 E). By contrast, these cells were rare in cultures with GMCSF alone. With addition of LPS overnight, both types of cultures were equally enriched for mature DCs, i.e. cells expressing a high density of MHC II, B7-1 and B7-2 (Figure 12 E).

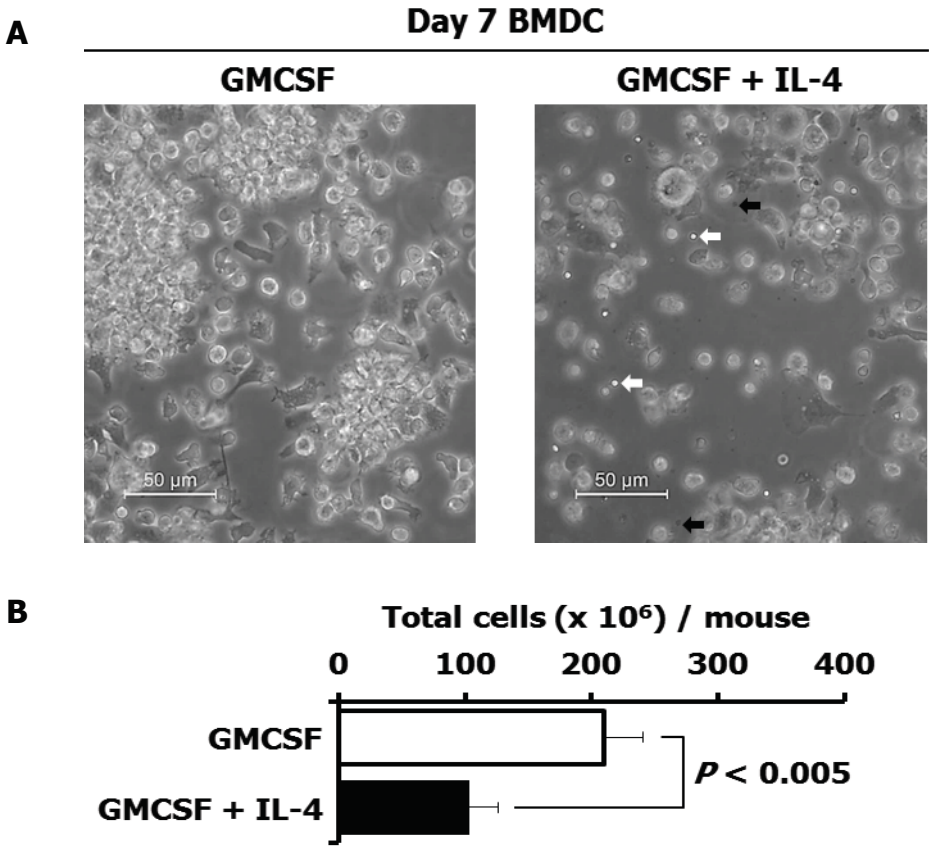

Figure 12. (Continued below)

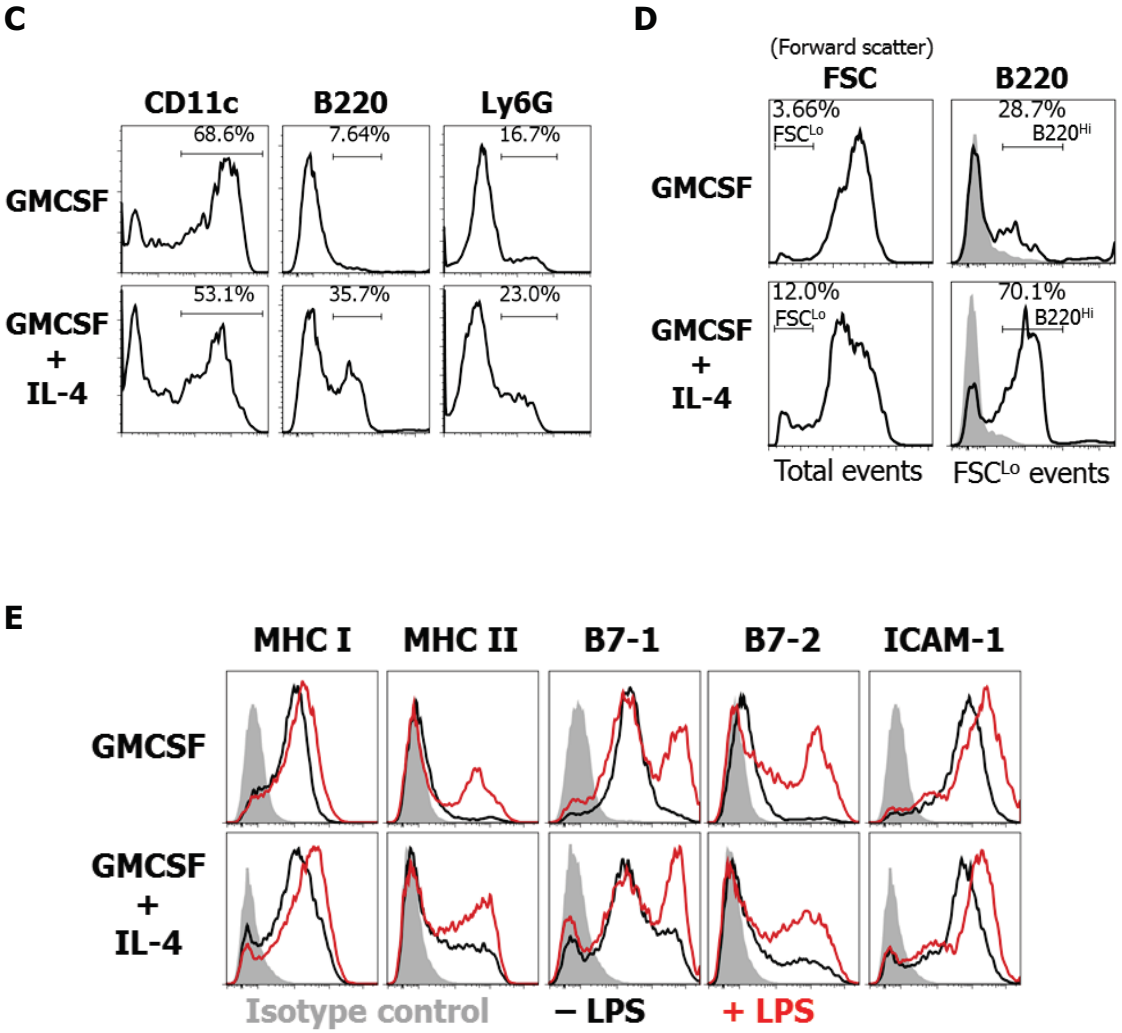

Figure 12. IL-4 induces spontaneous BMDC maturation and decreases purity of DCs after 7 days of culture. BMDCs were cultured with the new method in the presence of 20 ng/ml GMCSF only or 20 ng/ml GMCSF plus 40 ng/ml IL-4 for 7 days without (A, B, C, D and E) or with overnight LPS stimulation (E). Cells were first analysed by phase contrast microscopy (A) and then harvested and placed in a haemocytometer in the presence of 0.4% trypan blue solution to count total live cell yields per mouse (B). Finally, cells were stained with antibodies against the indicated molecules and analysed by flow cytometry (C, D and E). Relative cell size as measured by forward scatter (FSC) is shown (D). Subcellular debris and cells with pyknotic nuclei are indicated with black and white arrows, respectively (A). The data are representative of at least five independent experiments.

When cultures were examined on day 10, cell numbers in GMCSF plus IL-4 cultures were no higher than on day 7 (data not shown) and dying cells were prominent (Figure 13 A). Of the viable cells, many of the cells showed the markers of mature DCs, especially MHC II and B7-2, even without LPS addition (Figure 13 B). These findings were in marked contrast to culture with GMCSF without IL-4. Here, cell yields increased markedly between day 7 and day 10 (data not shown) and differentiation into mature DCs depended on prior overnight culture with LPS (Figure 13 B, C). Hence, adding IL-4 to the cultures had an overall negative effect: like culture at high concentrations, adding IL-4 to the cultures caused terminal differentiation into mature DCs and thereby led to only low BMDC yields and cell viability on day 10.

The capacity of IL-4 to cause BMDC maturation raised the question whether adding IL-4 at a late stage of culture would promote cell maturation without lowering cell yields. This was indeed found to be the case. Thus, for cells cultured in GMCSF from day 0 and harvested on day 10 after overnight LPS addition, supplementing the cultures with IL-4 on day 8 caused the proportion of B7-1^{hi} cells to rise from 75% to 90% (Figure 13 D); there were also increases in the expression of ICAM-1 and MHC I. Of note, there was no reduction in total cell yields (data not shown).

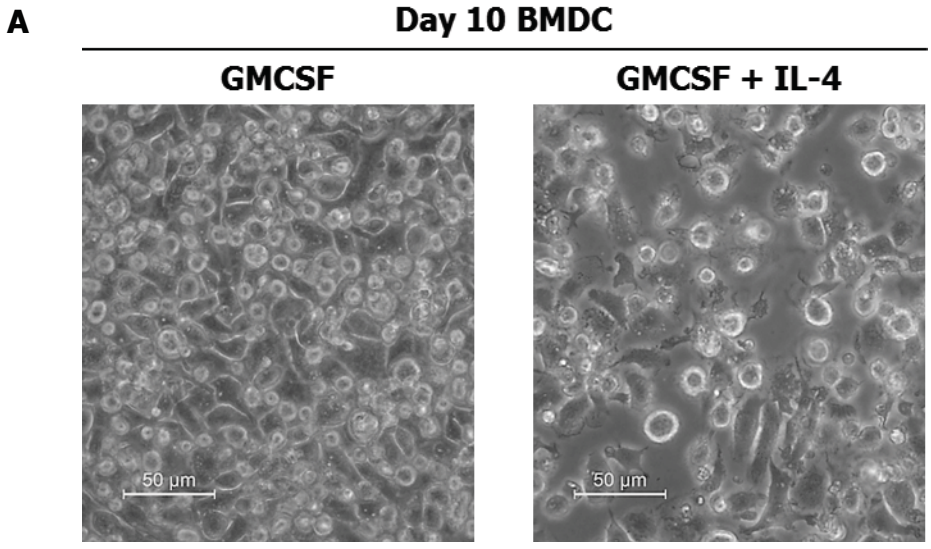

Figure 13. (Continued below)

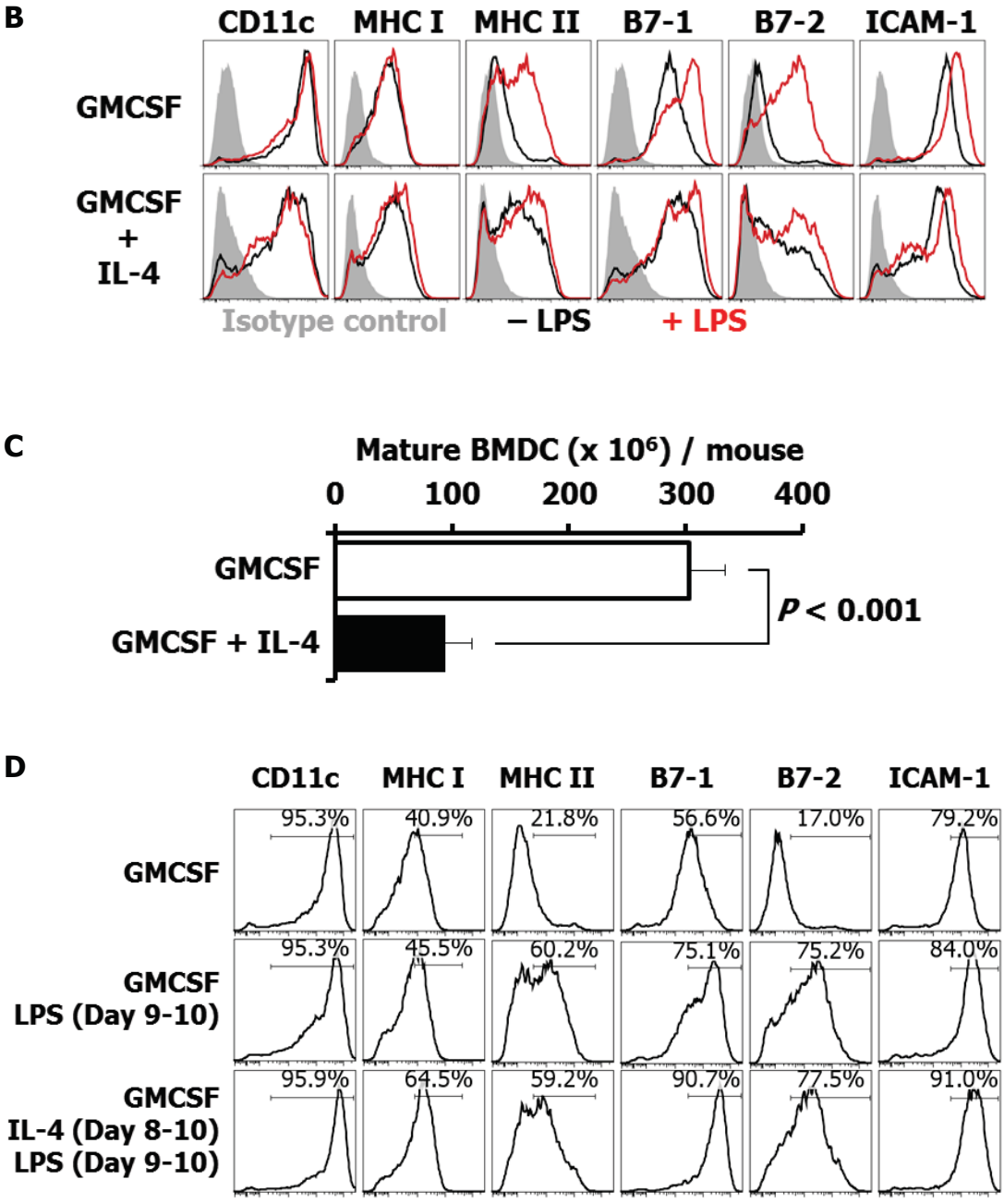

Figure 13. Continuous exposure to IL-4 markedly decreases the yield of mature BMDCs after 10 days of culture. BMDCs were cultured and analysed as in Figure 12 but after 10 days of culture (A and B). Mature BMDC yields refers to $CD11c^{+}$ $B7\text{-}1^{Hi}$ cells from day 10 cultures after overnight LPS stimulation (C; mean and SD). In some cultures, addition of IL-4 was delayed until day 8 followed by harvest on day 10 after overnight LPS stimulation (D). In controls, cells were cultured with GMCSF alone or GMCSF plus overnight LPS. In all cultures, GMCSF was added from day 0 to day 10. The data are representative of at least five (A – C) or two (D) independent experiments.

3.1.3 Summary and conclusion

Initial studies with transfected insect cells as aAPCs confirmed that stimulation of naïve CD8 T cells requires contact with pMHC and a high density of at least two co-stimulatory molecules, B7-1 and ICAM-1. An important finding was that immunogenicity was retained by non-viable aAPCs, i.e. by paraformaldehyde-fixed aAPCs and also by heat-killed aAPCs. These findings supported the idea that immunogenic membrane vesicles could be prepared from normal APCs, provided that these cells could be prepared in large numbers and express a high density of costimulatory molecules. I therefore sought to devise a new method for generating bulk populations of mature DCs from mouse bone marrow by modifying the standard BMDC culture method developed by Inaba et al. Modifying this method was necessary because the yield of mature BMDCs at the end of culture in the Inaba protocol was relatively low. This finding probably reflected that culture at high cell density with GMCSF in the Inaba method induced terminal differentiation of precursor cells into mature DC early in culture. Similar findings applied when cells were cultured with a mixture of GMCSF and IL-4. However, I found that the problem of early DC maturation could be avoided simply by culturing cells at low density in GMCSF alone. Thus, the combination of low cell density culture, inclusion of non-adherent cells at early stages of culture, inclusion of adherent cells as DCs after prolonged culture worked together to dramatically increase overall mature BMDC yields on day 10. With this new method of BMDC culture, the maturation of DCs can be tightly controlled by overnight stimulation with TLR ligands such as LPS before the cells are harvested.

And at the end of 10 days culture, 3 x 10^8 live mature BMDCs can be prepared from a single mouse. This yield is ~ 60 fold higher than in the Inaba method (culture period 7 – 8 days) and 2 – 3 fold higher than in the modification of the Inaba method described by Lutz et al (1999) (culture period 10 – 12 days). Also, in the new method described here, the proportion of recovered BMDCs with a mature B7-2^{hi} phenotype is higher (~75%) than in the method of Lutz et al. (~50%). With late addition of IL-4 to the cultures, there

was no change in the proportion of B7-2^{hi} cells but the proportion of B7-1^{hi} cells rose to 90%.

Development of the improved method for preparing bulk populations of mature DCs made it possible to prepare immunogenic vesicles from normal APCs, as described in the next chapter.

3.2 Preparation of immunogenic membrane vesicles from APCs

3.2.1 Introduction

Previous studies of our group on the immunogenicity of APC-derived vesicles were restricted to experiments with exosomes shed by *Drosophila* aAPCs (Hwang et al., 2003) and membrane vesicles prepared from disrupted DC2.4 cells, a dendritic cell line (Kovar et al., 2006). For the latter study, DC2.4 cells were pretreated with IFNγ to induce strong expression of MHC I, B7-1, B7-2, and ICAM-1. When loaded with specific peptide, the vesicles from these IFNγ-treated cells were strongly immunogenic for naïve 2C CD8 T cells both *in vitro* and *in vivo*. Notably, vesicles from the DC line were more immunogenic than exosomes from this line. Therefore, to assess clinical relevance, it is important to know whether immunogenic membrane vesicles can be prepared from normal APCs. This chapter describes the preparation of immunogenic membrane vesicles in large quantities, using the above BMDC culture system. For these experiments, if not specifically indicated vesicles were prepared from BMDCs cultured in GMCSF plus overnight LPS but without IL-4.

3.2.2 Results

The original membrane vesicle preparation protocol devised by Kovar et al for DC 2.4 cells involves 7 key steps: 1) resuspend cells in homogenization buffer, 2) homogenize cells for lysis (and then restore tonicity to 0.15 M NaCl), 3) low-speed centrifuge (500 x g) to remove nuclei, 4) sonicate supernatant, 5) high-speed centrifuge (10,000 x g) to remove mitochondria and larger cell debris, 6) ultra-speed centrifuge (100,000 x g) supernatant to pellet the vesicles, 7) resuspend the pellet with PBS as membrane vesicles (Figure 14) (Kovar et al., 2006). In extending this protocol to normal APCs, I have re-evaluated each step of the original protocol (highlighted in red, Figure 15 – Figure 24) with the aim of further improving both yields and immunogenicity.

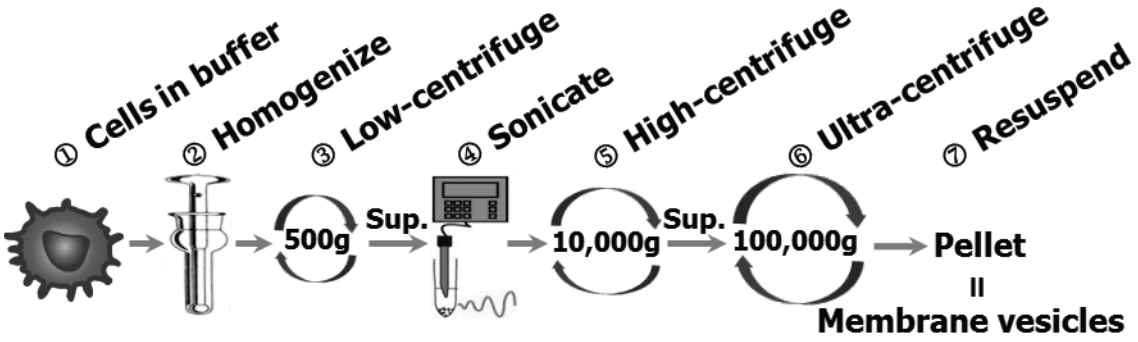

Figure 14. Original procedure for preparing membrane vesicles. The diagram shows 7 key steps of the original protocol devised by Kovar et al. (2006) for preparing membrane vesicles from cell suspensions using homogenization, sonication and ultracentrifugation.

3.2.2.1 Co-stimulatory molecules determine vesicle immunogenicity

To confirm the importance of co-stimulation in vesicle immunogenicity, I initially tested vesicles from aAPCs and then examined vesicles from immature versus mature BMDCs. For aAPCs, using the original protocol, I prepared membrane vesicles from *Drosophila* aAPCs a.L^d or a.L^d.B7-1.ICAM-1; the vesicles are referred to as v.L^d or v.L^d.B7-1.ICAM-1, respectively (Figure 15 A). When the two sources of vesicles were pulsed with QL9 peptide and used to stimulate 2C CD8 T cells, consistent with the findings with intact aAPCs (Figure 4), v.L^d.B7-1.ICAM-1 stimulated strong CD69 up-regulation and proliferative responses as measured by ^{3}thymidine incorporation (Figure 15 B and C). Like intact a.L^d (Figure 4), v.L^d failed to induce proliferation of 2C cells (Figure 15 C). However, unlike aAPCs, v.L^d did cause low but significant CD69 up-regulation (Figure 15B), probably reflecting transfer of pMHC (QL9-L^d) from vesicles to T cells by "cross-dressing" (Thery et al., 2002; Wakim and Bevan, 2011), thus allowing low-level TCR signalling via T-T interaction; note that T cells express ICAM-1 (Figure 15 D) and also B7-2 (Taylor et al., 2004).

The importance of co-stimulation in vesicle immunogenicity was confirmed with membrane vesicles prepared from BMDCs left untreated or pretreated with CpG or LPS (Figure 8); these will be referred to as vDC, vDC-CpG and vDC-LPS, respectively. Membrane vesicles were also prepared from dead cells isolated from LPS-pretreated BMDCs, referred to as vDC-Dead. Interestingly, yields of

vDC-CpG and vDC-LPS were significantly higher than vDC (Figure 15 E), which correlates with the fact that, upon activation, DCs not only up-regulate co-stimulatory molecules (Figure 8), but also increase in size (Pearce and Everts, 2015). The important finding, however, was that, like vesicles from *Drosophila* aAPCs, vDC-CpG and vDC-LPS were both strongly immunogenic. Thus, in the presence of SIINFEKL peptide, both types of vesicles stimulated strong proliferative responses by OT-1 CD8 T cells (Figure 15 F); this finding applied with a relatively low concentration of vesicles (1 μg/ml) and occurred in the absence of APCs. Responses were significantly lower with vDCs, which correlated with the lower density of costimulatory molecules on these immature DCs. By contrast, vDC-Dead were totally non-immunogenic (Figure 15 F), probably reflecting degradation of MHC and costimulatory molecules on dead cells. This finding contrasted with the retention of immunogenicity by heat-killed or fixed aAPCs (Figure 5), presumably because cell-surface proteins may remain intact and functional after rapid killing of cells by heat or fixation. Overall, the above data indicate that immunogenic vesicles can indeed be prepared from both normal APCs as well as from *Drosophila* aAPCs; in both cases, immunogenicity depends on high expression of co-stimulatory molecules.

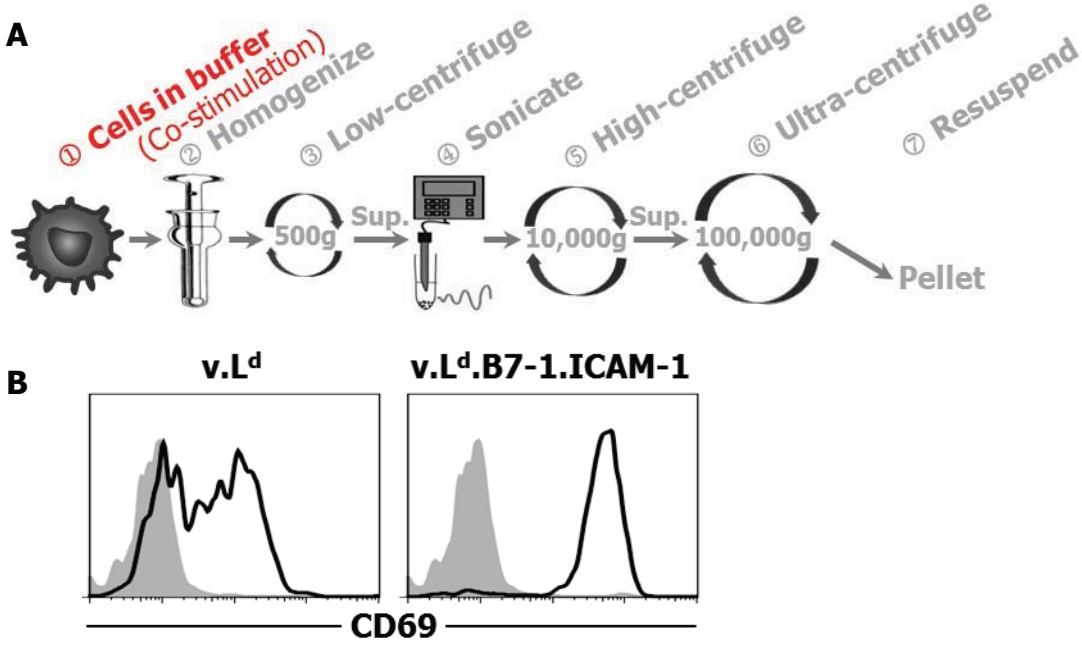

Figure 15 (Continued below)

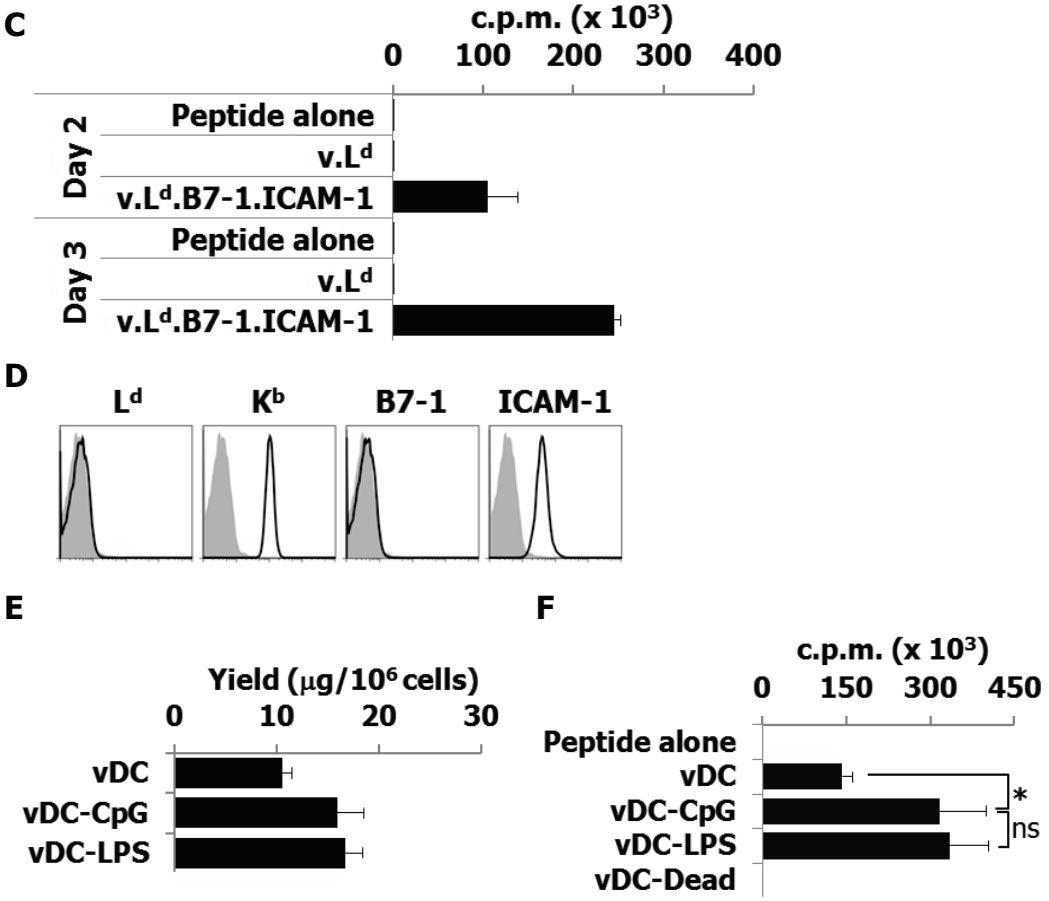

Figure 15. Co-stimulatory molecules are required for membrane vesicles to induce CD8 T cell stimulation. To examine the need for expression of costimulation molecules (marked in red in the diagram A)**,** membrane vesicles were prepared from a.L^d or a.L^d.B7-1.ICAM-1 and co-cultured at 10 μg/ml with 5 x 10^4 2C CD8 T cells in the presence of 1 μM QL9 peptide for 16 hours to measure CD69 expression by flow cytometry (B) or for 2 and 3 days to measure proliferation using a ^{3}H-thymidine incorporation assay (C, mean and SD of triplicate cultures). Flow cytometry was used to measure expression of cell-surface markers on naïve 2C CD8 T cells (D). In other experiments, membrane vesicles were prepared from live BMDCs by the new protocol without (vDC) or with overnight CpG or LPS stimulation (vDC-CpG, vDC-LPS), or from dead cells isolated from LPS stimulated BMDCs (vDC-Dead). The yield is calculated by the total protein content of membrane vesicles from one million live BMDCs (E; mean and SD). OT-1 CD8 T cells (5 x 10^4 cells/well) were cultured with indicated membrane vesicles (1 μg/ml) in the presence of 0.3 nM SIINFEKL peptide and analysed by ^{3}H-thymidine incorporation assay after 3 days of culture (F; mean and SD). The data are representative of at least three independent experiments. *P < 0.01; ns, not significant.

3.2.2.2 Mild homogenization improves both yields and immunogenicity of vesicles

In optimising the yield of membrane vesicles, I evaluated the effect of cell density in the homogenization buffer and strength of homogenization. To measure the effect of cell density, day 10 BMDCs pretreated with LPS were resuspended with 3.5 x or 10 x volume of homogenization buffer (relative to cell pellet volume) and then subjected to loose-fitting homogenization and the other steps of membrane vesicle preparation as depicted in Figure 16 A. The important finding was that lower cell density was beneficial for both yields and immunogenicity of vesicles (Figure 16 B and C).

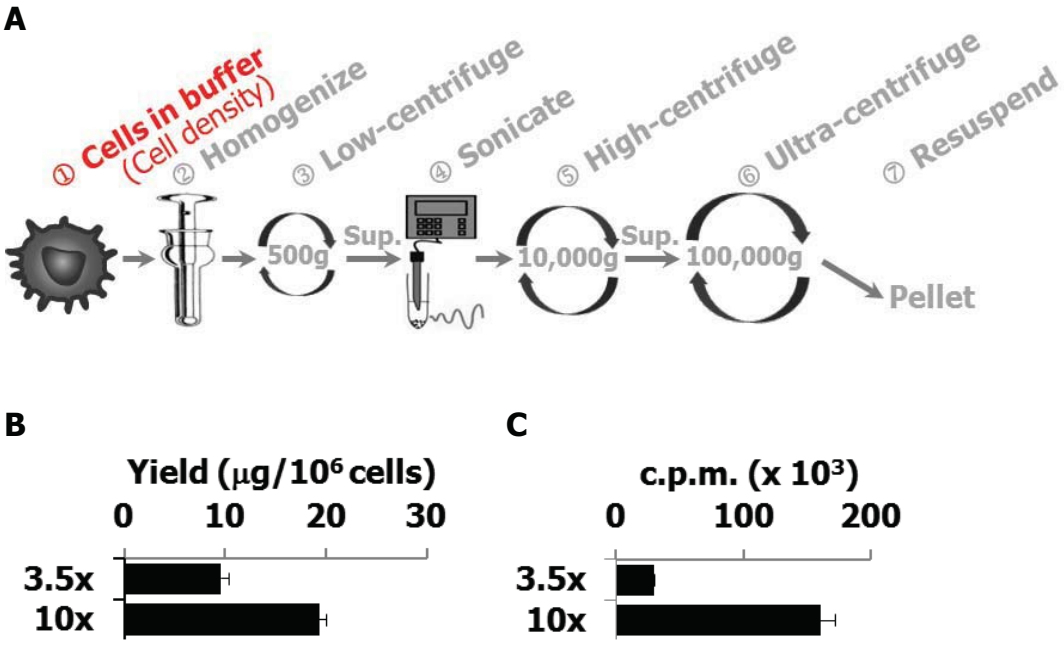

Figure 16. Low cell density in buffer used for homogenization is critical for both the yield and immunogenicity of membrane vesicles. To assess the effect of cell density during homogenization (A), membrane vesicles were prepared from LPS-stimulated BMDCs suspended in 3.5x or 10x volumes of homogenization buffer (relative to the cell pellet volume). (B) The yield of membrane vesicles in the pellet (step 7) was calculated in terms of the total protein content obtained from 1 x 10^6 BMDCs (mean and SD). (C) Immunogenicity of the vesicles was assessed by culturing 5 x 10^4 2C CD8 T cells with the indicated membrane vesicles (1 μg/ml) in the presence of 300 nM SIYR peptide and measuring proliferation by ^{3}H-thymidine incorporation after 3 days of culture (C; mean and SD). The data are representative of more than five independent experiments.

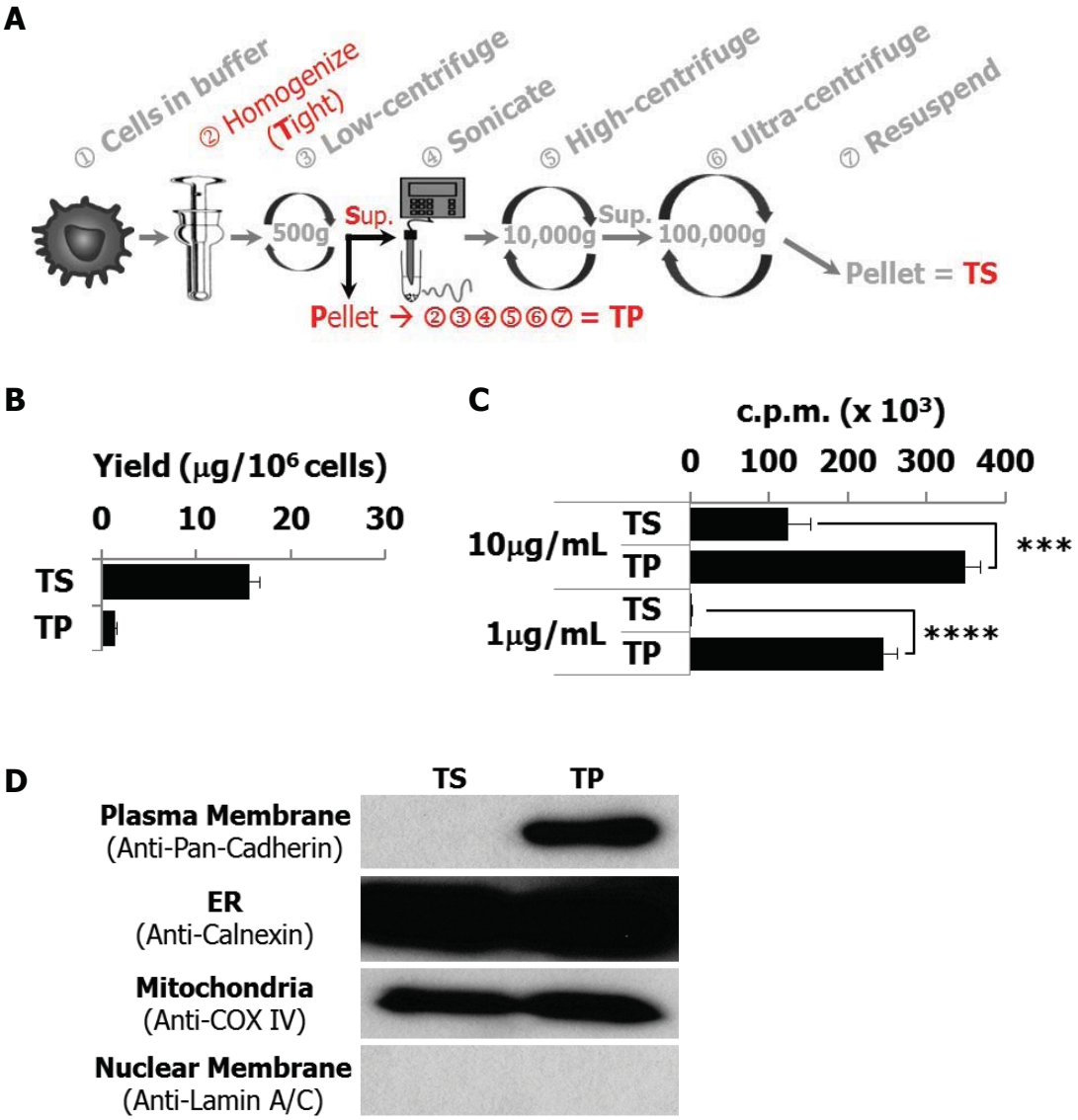

Figure 17. Tight homogenization gives high yields of vesicles but with poor immunogenicity. (A) To assess the influence of pestle clearance during homogenization, membrane vesicles were prepared from LPS-stimulated BMDCs after tight (T) homogenization (pestle clearance = 25 – 76 μm). (B) Yields of vesicles after ultracentrifugation of material prepared from the supernatant (TS) versus the pellet (TP) following homogenization and low centrifugation; yields (mean and SD) were calculated as total protein content/1 x 10^6 BMDCs as for Figure 15. (C) Immunogenicity of TS versus TP vesicles as defined by capacity to stimulate ^{3}H-thymidine incorporation by 2C CD8 T cells (5 x 10^4 cells/well) in the presence of 300 nM SIYR peptide; proliferation was measured on day 3 of culture at the indicated concentration of vesicles (mean and SD). (D) Immunoblotting of TS versus TP vesicles with antibodies against organelle-specific proteins as indicated. The data are representative of four independent experiments. ***$P < 0.0005$; ****$P < 0.00005$.

However, with low cell density and loose-fitting homogenization, less than 80% cell breakage was achieved after 30 strokes of homogenization (data not shown), suggesting that the yield of membrane vesicles could be further increased with tight-fitting homogenization (Graham, 2002). However, when the vesicles were prepared by homogenization using a tight-fitting pestle (Figure 17 A), the yield of vesicles in the resuspended pellet (TS) was high but the immunogenicity of the vesicles was poor and apparent only with a high concentration of vesicles (Figure 17 B, C); for these experiments, proliferative responses of 2C CD8 T cells to SIYR peptide were examined. Intriguingly, when vesicles (TP) were recovered not from the supernatant but from the pellet after 500 x g low-speed centrifugation (Figure 17 A), these vesicles were strongly stimulatory, although their yield was low (Figure 17 B and C). The immunogenicity of the two types of vesicles correlated directly with the much higher density of plasma membrane components in the stimulatory vesicles (TP) than in the non-stimulatory vesicles (TS) (Figure 17 D).

The above findings applied with tight homogenization. When vesicles were prepared with a combination of low cell density and loose-fitting homogenization (with > 100 strokes to achieve > 90% cell breakage) as in Figure 18 A, vesicles prepared either from the supernatant (LS) or the pellet after low-speed centrifugation (LP) were both strongly immunogenic, although the LS yield was far higher than the LP yield (Figure 18 B, C). Again, the strong immunogenicity of these vesicles (LS) correlated with the presence of plasma membrane and also β-2-microglobulin, a component of MHC I (Figure 18 D).

These findings indicate that rapid disruption of cells (which is often recommended for effective cell lysis) with high-density and tight-fitting homogenization is detrimental to vesicle immunogenicity. By contrast, mild homogenization gives high yields of strongly immunogenic vesicles.

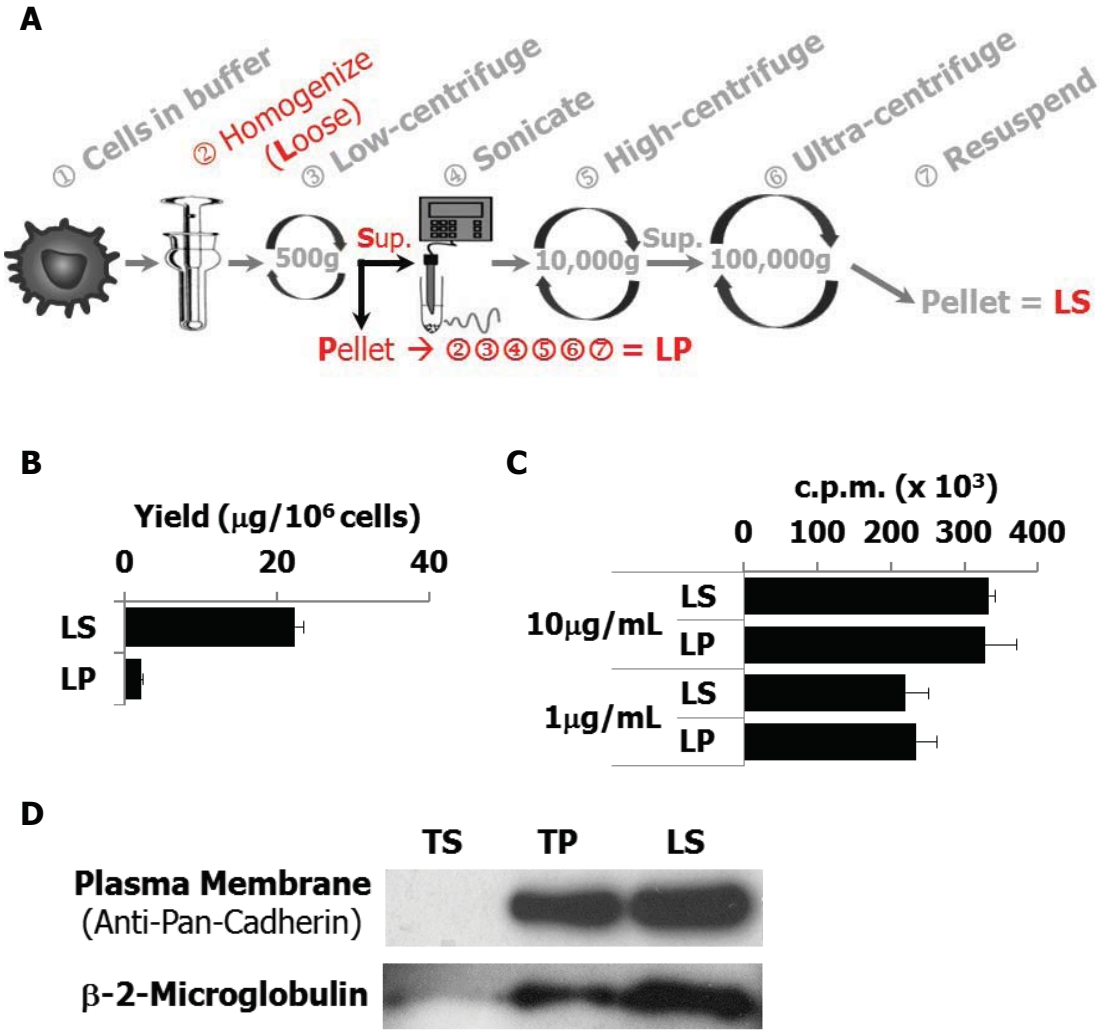

Figure 18. Loose homogenization improves both the yield and immunogenicity of membrane vesicles. Membrane vesicles were prepared as outlined (A) from LPS-stimulated BMDCs after loose homogenization (pestle clearance = 89 – 165 μm) and analysed as in Figure 17. Yields (B) and immunogenicity (C) of LS versus LP vesicles and immunoblotting (D) of LS vesicles are shown; for immunoblotting, TS and TP vesicles (Figure 17) were used as controls. The data are representative of more than three independent experiments.

3.2.2.3 Immunogenic material is enriched in supernatant after 3,000 x g centrifugation

To further improve the yield and immunogenicity of the vesicles, I used serial centrifugation to find out what speed is optimal for removing non-immunogenic material (Figure 19 A).

Using LPS-pretreated BMDCs, initial studies showed that, after low-speed 800 x g centrifugation of homogenized cells, the protein yield of the material in the pellet (p800) was high but immunogenicity was low, as defined by proliferative responses of OT-1 CD8 T cells to 0.3 nM SIINFEKL peptide and 1 μg/ml of the pelleted material (Figure 19 B, C). Therefore, to remove cell debris and nuclei before serial centrifugation, cells were first homogenized, then centrifuged at 800 x g centrifugation, followed by sonication of the supernatant. Then at each centrifugation step the pellet (p) was tested for protein yield and immunogenicity while the supernatant (s) was subjected to higher centrifugation (Figure 19 A).

The results of this approach showed that, after 3,000 x g, the protein yield and immunogenicity of pelleted material (p3,000) were both relatively low. By contrast, protein yield and immunogenicity were both high for p10,000, and also p100,000. However, the p200,000 material was nonimmunogenic, presumably reflecting a lack of cell-membrane material (Figure 19 B, C).

The significant yield and strong immunogenicity of p10,000 is important because, in the original protocol (Figure 14), p10,000 was discarded before ultracentrifugation, which presumably led to substantial loss of immunogenic material. For this reason, I have now modified the original protocol by reducing the speed of high-speed centrifugation before ultracentrifugation from 10,000 x g to 3,000 x g, thereby achieving better yields and immunogenicity.

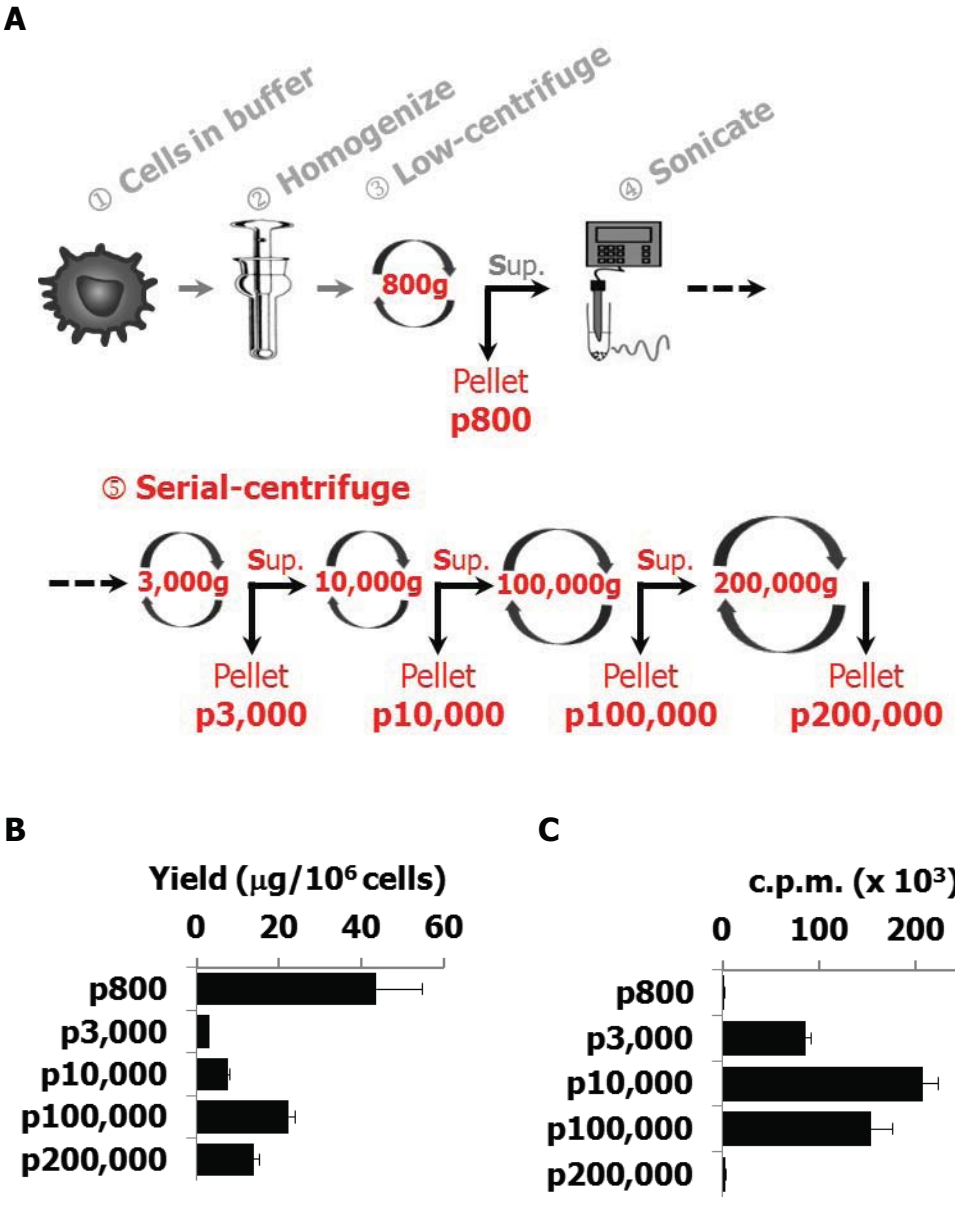

Figure 19. Strongly immunogenic material is in supernatants obtained after centrifugation of cell homogenates at 3000 x g. LPS-stimulated BMDCs were first subjected to homogenization, followed by low-speed centrifugation (800 x g) to remove nuclei and large cell debris (A). The supernatant was sonicated and then subjected to serial centrifugation to measure yields (B) and immunogenicity (C) of material in the pellets. To measure immunogenicity, OT-1 CD8 T cells were cultured at 5 x 10^4 cells/well with the pelleted material (1 μg/ml) in the presence of 0.3 nM SIINFEKL peptide; ^{3}H-thymidine incorporation (mean and SD) was measured on day 3 of culture. The data are representative of more than five independent experiments.

3.2.2.4 Effects of sonication and freezing-thawing on vesicle yields and immunogenicity

I next examined the efficiency of sonication, which is widely used for biological studies for various purposes, including cell and fragment disruption, plasma membrane vesiculation and nanoparticle dispersion. The strong cavitation energy generated by sonication delivers not only strong shear force, but also a considerable amount of heat which can denature proteins.

To investigate the effects of sonication, vesicles were prepared from LPS-stimulated BMDCs with sonication at three different power settings (3, 5 or 7) (Figure 20 A). Notably, despite a high yield of protein, the vesicles generated with the high power setting (S7) almost completely failed to stimulate the proliferation of OT-1 CD8 T cells in the presence of SIINFEKL peptide (Figure 20 B, C).

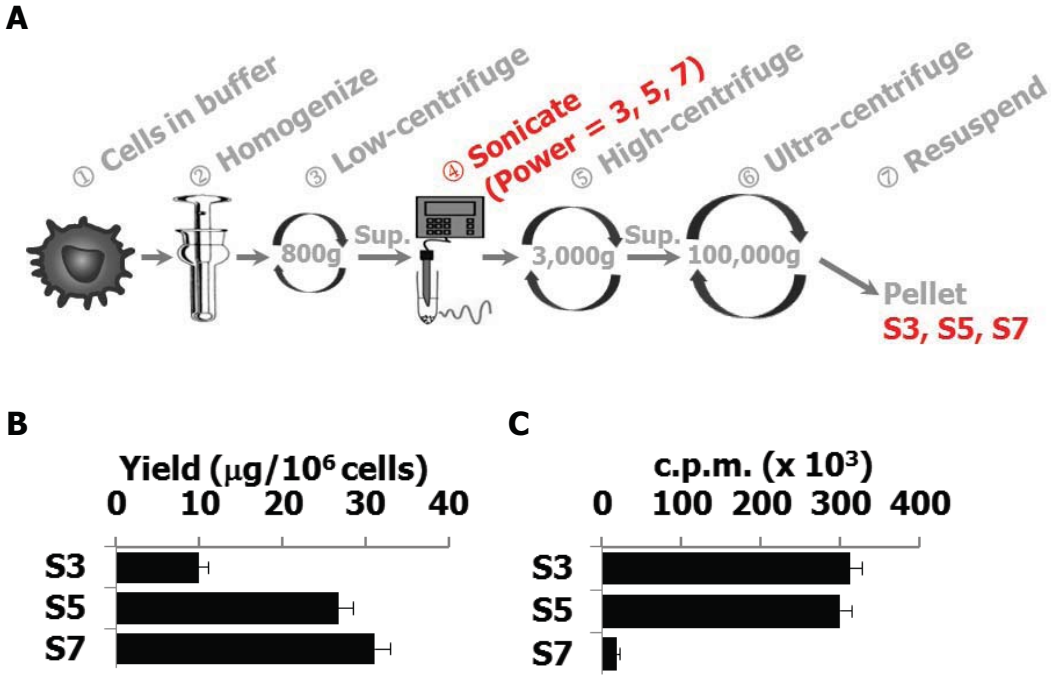

Figure 20. Strength of sonication is critical for both the yield and immunogenicity of membrane vesicles. Membrane vesicles were prepared from LPS-stimulated BMDCs using sonication at different power strengths followed by centrifugation at 3,000 x g, then 100,000 x g (A). Yields (B) and immunogenicity (C) of material in the pellets were then measured as in Figure 19. The data are representative of at least three independent experiments.

The vesicles generated with lower sonication power (S3 and S5) showed similar strong immmunogenicity (Figure 20 C), although vesicles prepared with the lowest sonication power (S3) had a poor yield (Figure 20 B). These findings emphasise the importance of sonication settings for optimal vesicle generation and, in partiular, indicate that, when used at excessive strength, sonication can ablate immunogenicity.

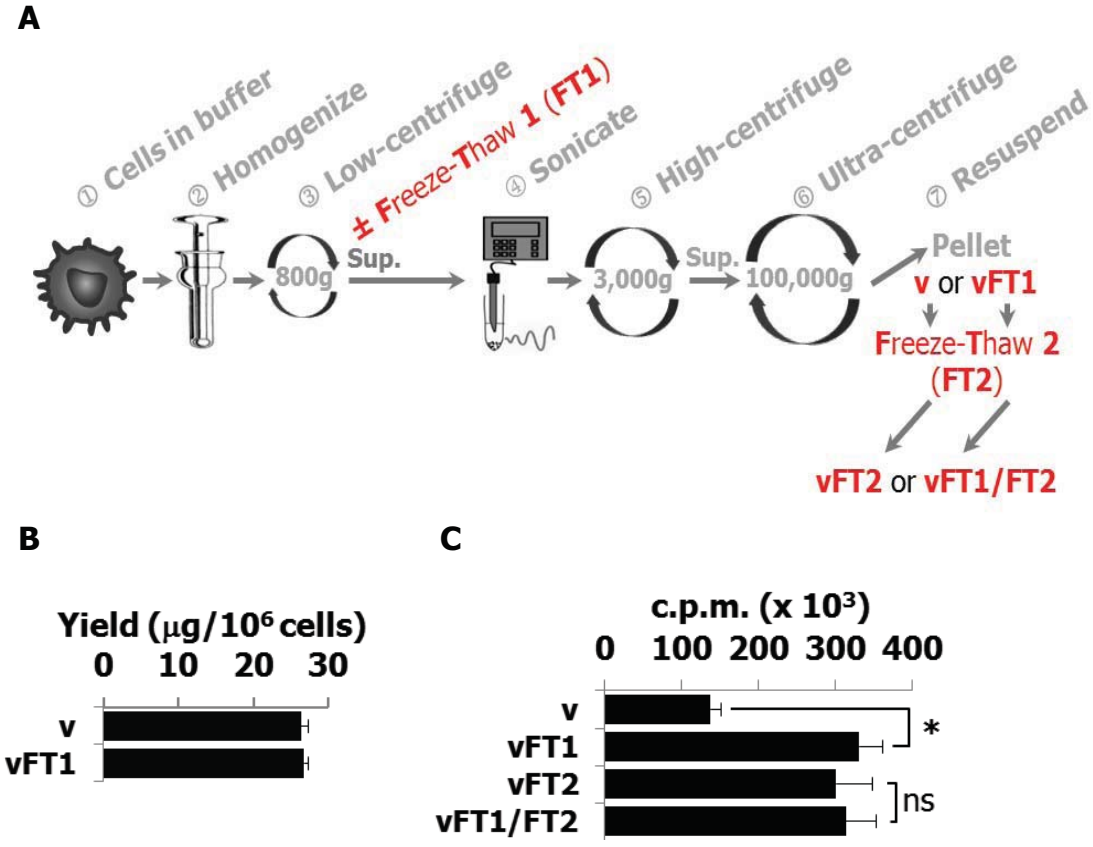

Figure 21. Freezing and thawing improves immunogenicity of membrane vesicles. Following homogenization and low-speed centrifugation of LPS-stimulated BMDCs, supernatants were subjected to freezing/thawing (vFT1) or not (v) followed by sonication (power = 5), 3,000 x g and 100,000 x g centrifugation. The pelleted material was then tested for yields (B) and immunogenicity (C), either directly (v, vFT1) or after a further freeze/thaw step (vFT2, vFT1/FT2). Yields in the pellets and immunogenicity were assessed as in Figure 19. The data are representative of at least three independent experiments. $*P < 0.05$; ns, not significant.

As discussed earlier, one of the advantages of DC-derived exosomes is that, unlike intact DCs, exosomes can be frozen for prolonged periods with preservation of their phenotype and function (Viaud et al., 2010). To test if this advantage also applies to membrane vesicles from BMDCs, I examined the effects of freezing and thawing on membrane vesicles prepared from LPS-stimulated BMDCs. As shown in Figure 21 A, a freeze-thaw step was applied either before sonication (vFT1), or after vesicle preparation from the pellet (vFT2), or at both of these stages (vFT1/FT2); vesicles that were not freeze thawed (v) were used as a control. Unexpectedly, though there was no change in protein yield (Figure 21 B), the immunogenicity of membrane vesicles was actually improved by the freezing-thawing process (Figure 21 C). Thus, proliferation of OT-1 CD8 T cells in the presence of SIINFEKL peptide was significantly better with vFT1, vFT2 and vFT1/FT2 vesicles than with control v vesicles. Why freezing-thawing improves vesicle immunogenicity is not clear, although it is possible that this process increases expression of stimulatory ligands. Thus, it may be relevant that membrane vesicles contain calnexin, an endoplasmic reticulum (ER) marker (Figure 17), and that freezing-thawing augments inside-out exposure of ER MHC and co-stimulatory molecules (Sofra et al., 2009).

3.2.2.5 Generation of nano-vesicles from vesicle-aggregates

Membrane vesicles prepared from DC2.4 cell lines by the original protocol contained a heterogenous mixture of exosome-sized nano-vesicles and small and large fragments (Kovar et al., 2006). The heterogenous nature of membrane vesicles also applies to v and vFT1 vesicles prepared from LPS-stimulated BMDCs (Figure 21). Therefore, when the 100,000 x g ultracentrifugation pellets are resuspended in PBS using a syringe with a 29 gauge needle, fragments and vesicles of different sizes are prominent under phase contrast microscope in both v vesicles (prepared without freezing and thawing) and vFT1 vesicles (prepared with freezing and thawing before sonication), reflecting that the freeze-thaw step before sonication does not have

a major effect on membrane vesicle morphology (Figure 22 lower). Of note, the supernatants used for ultracentrifugation are free from any large particles detectable by phase contrast microscopy (Figure 22 upper). Hence, it is the ultracentrifugation pelleting process that causes the aggregation of small vesicles; moreover, the aggregates in the pellet are stable and are not dispersed by syringe/small-needle passage. However, this latter finding is not surprising given that the diameter of the syringe needle used for the resuspension is far larger (330 μm) than the micrometre-sized aggregates (mostly < 10μm).

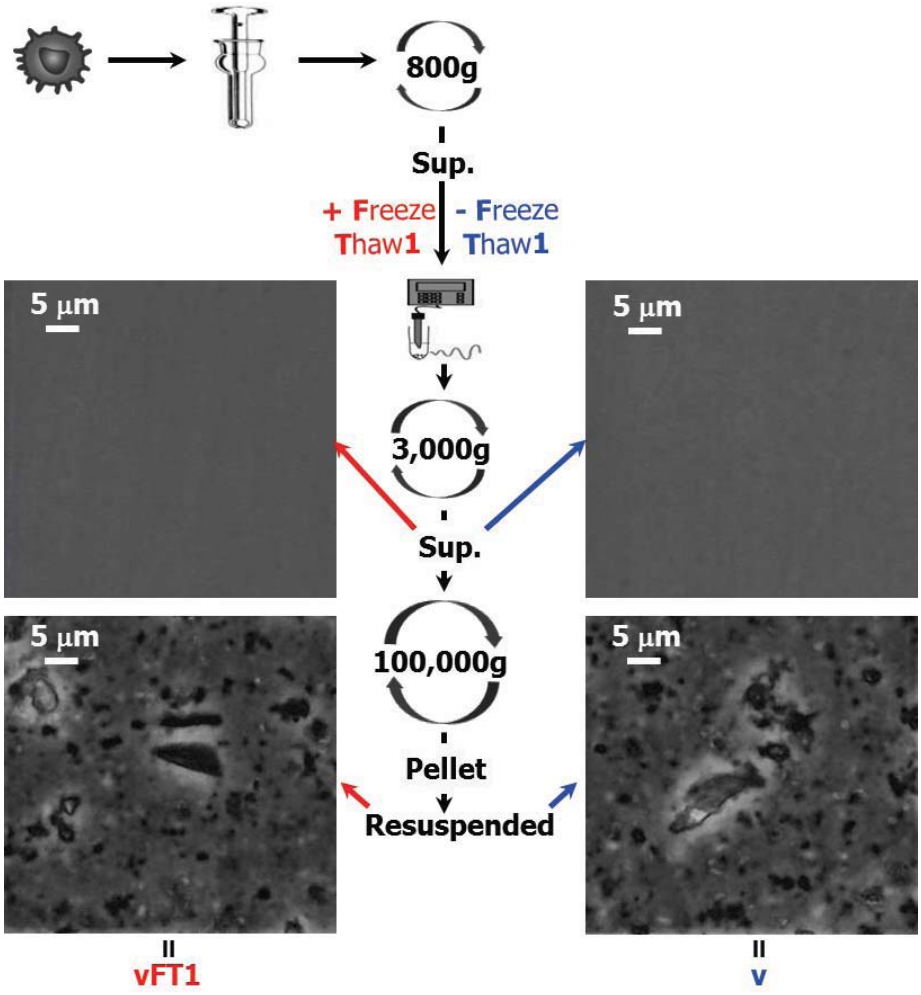

Figure 22. Morphology of membrane vesicles. Membrane vesicles were prepared from LPS-stimulated BMDCs (as v or vFT1 in Figure 21). The final pellet was resuspended using a syringe with a 29 gauge needle and viewed by phase contrast microscopy in a haemocytometer at 20x magnification. For both v and vFT1, small and large fragments are visible (lower figure), whereas supernatant taken after 3,000 x g centrifugation showed no aggregates (upper figures). Similar findings were seen in > 10 independent experiments.

In a search to find an effective method of de-aggregation, treating the ultracentrifugation pellet to the combination of tight-homogenization and sonication was found to be extremely efficient at dispersing the aggregates. Thus, when the vFT1 were prepared and resuspended as in Figure 22, and then subjected to tight-homogenization and sonication, the presence of aggregates was dramatically reduced, both as visualised by phase contrast microscope and by the Zetasizer Nano ZSP particle characterisation system (Figure 23 A and B). Combining homogenization and sonication was found to be critical for successful de-aggregation: the initial tight-homogenization step (20 – 55 μm pestle clearance) effectively turns large fragments into small fragments (V-hom), and the subsequent sonication step efficiently disrupts the small fragments into a relatively homogeneous mixture of nano-vesicles (V-hom-son), which are all smaller than 600 nm and with a mean size of 180 nm (Figure 23 B). With some (but not all) vesicle preparations, sonicated nano-vesicles (V-hom-son) re-aggregate after an additional freeze-thaw step (V-hom-son-FT; Figure 23 A and B). Therefore, when vesicle preparations are frozen for storage, nano-vesicles can be quickly prepared by subjecting the thawed preparations to homogenization and sonication just before use.

A

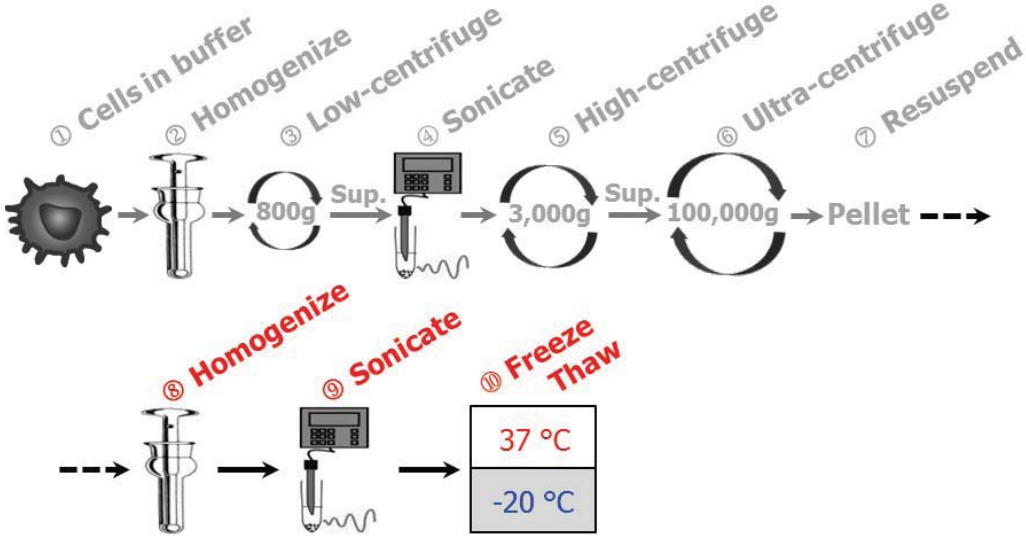

Figure 23 (Continued below)

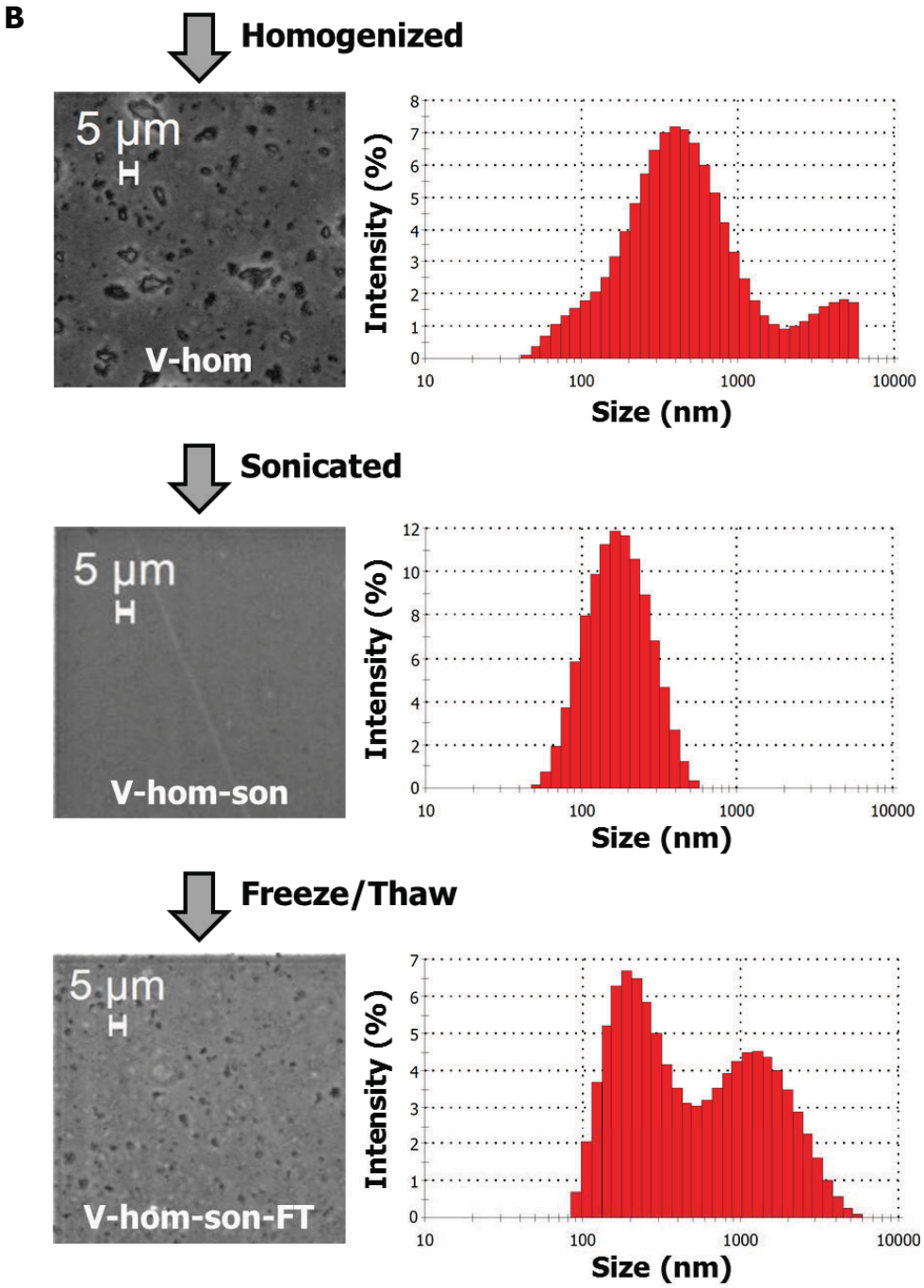

Figure 23. Aggregates in membrane vesicle preparations are effectively removed by treating pellets by homogenization plus sonication. After ultracentrifugation, the pellet of membrane vesicles prepared from LPS-stimulated BMDCs (vFT1, as in Figure 22) was subjected to extra steps of tight homogenization (V-hom) and then sonication (V-hom-son), and finally freezing/thawing (V-hom-son-FT) (A). The size of the resultant material was measured with light microscopy (as in Figure 22) and Zetasizer Nano ZSP (size distribution by intensity is shown) (B). The data are representative of at least three independent experiments.

The V-hom-son-FT vesicles prepared as in Figure 23 can be directly analysed by flow cytometry after staining with antibodies, thereby enabling detection of cell-membrane markers. The size of particles in V-hom-son-FT varies from small (low in FSC-A) to large (high in FSC-A) (Figure 24 A). Importantly, V-hom-son-FT vesicles stain positive for all the molecules (CD11c, MHC I, MHC II, B7-1, B7-2 and ICAM-1) which can be found on the surface of the LPS-stimulated BMDCs (Figure 13) used for vesicle preparation; staining is specific because there is no staining for CD3, a T cell marker. As expected, B7-1 expression proved to be higher in V-hom-son-FT (vesicles prepared from LPS-stimulated mature BMDCs) than in iV-hom-son-FT (vesicles prepared from immature BMDCs that were not treated with LPS) (Figure 24 B).

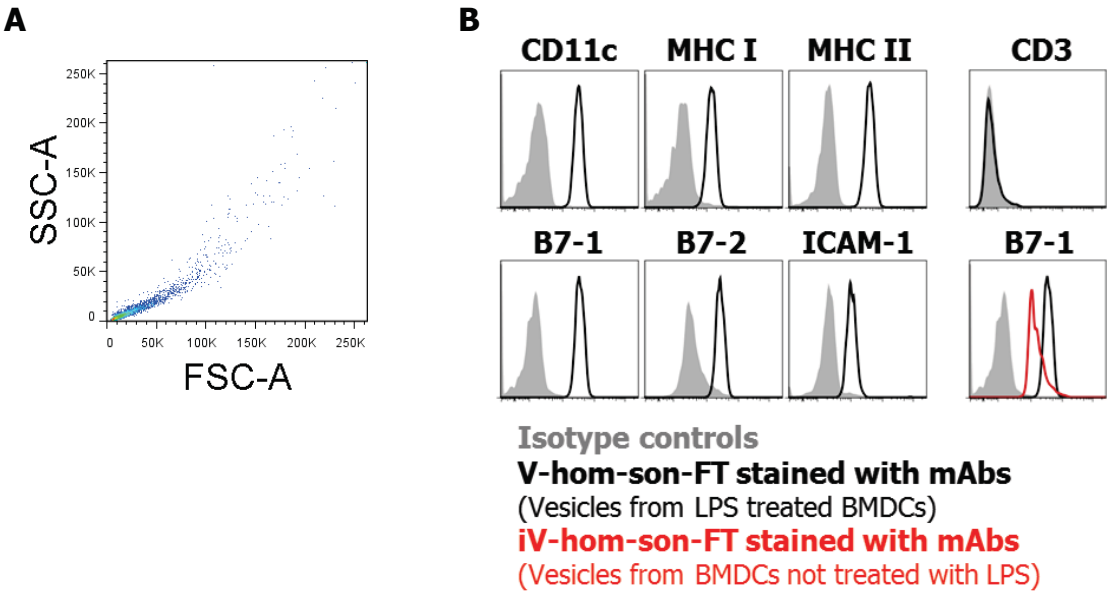

Figure 24. Analysis of surface markers on membrane vesicles. Membrane vesicles (V-hom-son-FT from LPS-stimulated BMDCs) were prepared as in Figure 23 and were analysed by BD FACSCanto II flow cytometry to examine: A) vesicle size by forward (FSC-A) and side (SSC-A) scatter, and B) expression of various markers found on mature DCs after staining with the indicated mAbs (CD3 staining was used as a negative control). B7-1 expression on V-hom-son-FT prepared from immature BMDCs that were not treated with LPS (iV-hom-son-FT) is shown as a control. The data are representative of at least four independent experiments.

The important conclusion, therefore, is that the cell-surface molecules involved in antigen presentation and co-stimulation by mature BMDCs are preserved at a comparable density on the surface of small membrane vesicles. It should be mentioned that similar data apply to staining of V-hom, though V-hom contain larger aggregates than V-hom-son-FT.

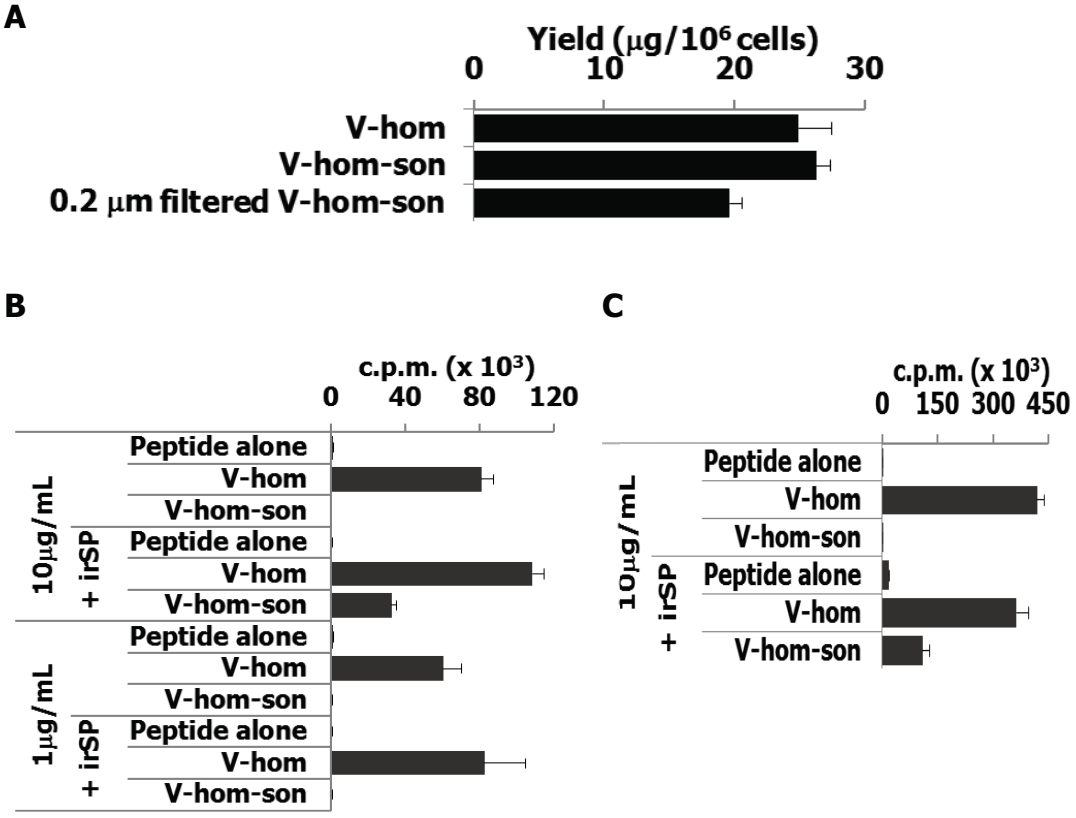

Figure 25. Nano-vesicles are not directly immunogenic for CD8 T cells *in vitro* unless supplemented with APC. Membrane vesicles (V-hom and V-hom-son) were prepared as in Figure 23 and then tested for yield/10^6 BMDC (A) and immunogenicity (B and C). For measuring yields, some of the material (V-hom-son) was passed through a 0.2 μm filter before protein measurement (shown as 0.2 μm filtered V-hom-son). Immunogenicity was assessed by culturing 5 x 10^4 2C CD8 T cells (B) or OT-1 CD8 T cells (C) with the vesicle preparations (1 or 10 μg/ml as indicated) plus 30 nM SIYR peptide (B) or 0.3nM SIINFEKL peptide (C) with or without addition of 2 x 10^5 irradiated C57BL/6 splenocytes (irSP) as a source of APC; ^{3}H-thymidine incorporation was measured on day 3 of culture (mean and SD). The data are representative of more than three independent experiments.

3.2.2.6 Immunogenicity of vesicle-aggregates and nano-vesicles

In support of their small size, the V-hom-son vesicles prepared from V-hom (Figure 23) readily passed through a 0.2 μm pore sized filter. The recovery after filtration was about 75% (Figure 25 A), suggesting that the majority of the vesicles in V-hom-son are smaller than 200 nm. Notably, in marked contrast to V-hom (aggregated vesicles), V-hom-son (nano-vesicles) totally failed to stimulate proliferation of 2C CD8 T cells in the presence of 30nM SIYR peptide Figure 25 B. However, V-hom-son did display immunogenicity with addition of APCs (irradiated C57BL/6 splenocytes), though responses were clearly less than with V-hom, with or without APCs. (Figure 25 B). Similar findings were also observed with OT-1 CD8 T cells and SIINFEKL peptide (Figure 25 C).

Unlike V-hom-son, V-hom vesicles could not be passaged through a 0.4μm or 0.2μm filter (Figure 26 A), indicating that V-hom consist almost entirely of large aggregates with minimal presence of small nano-vesicles. The small amount of material that did pass through the 0.2μm filter appeared to be nano-particles because this material failed to cause either T cell activation (CD25 upregulation) or proliferation (Figure 26 B, C); low but significant T cell responses were seen after 0.4μm filtration, but these responses were far lower than with unfiltered V-hom.

The strong activation and proliferation of CD8 T cells induced by peptide pulsed V-hom was also associated with differentiation into effector CD8 T cells. Thus, when 2C CD8 T cells were co-cultured with 10 μg/ml of V-hom in the presence of 300 nM SIYR peptide for 3 days, they expressed both Perforin and Granzyme B, which are cytolytic enzymes important in target cell lysis (Figure 27 A). To measure cytotoxicity, the effector 2C CD8 T cells were co-cultured at different ratios with a 1:1 mix of two types of EL4 target cells: 1) antigen (SIYR peptide)-loaded target cells labelled with a high concentration of CFSE, 2) control (no antigen) target cells labelled with a low concentration of CFSE. Indeed, significant antigen-specific target cell lysis (as shown by a decrease in the $CFSE^{Hi}$ population) was observed at all effector to target cell ratios, relative to control cultures that lacked effector cells (Figure 27 B). These findings

indicate that 2C CD8 T cells cultured with peptide-pulsed V-hom (without APCs) led to strong proliferation followed by efficient differentiation into cytotoxic effector cells.

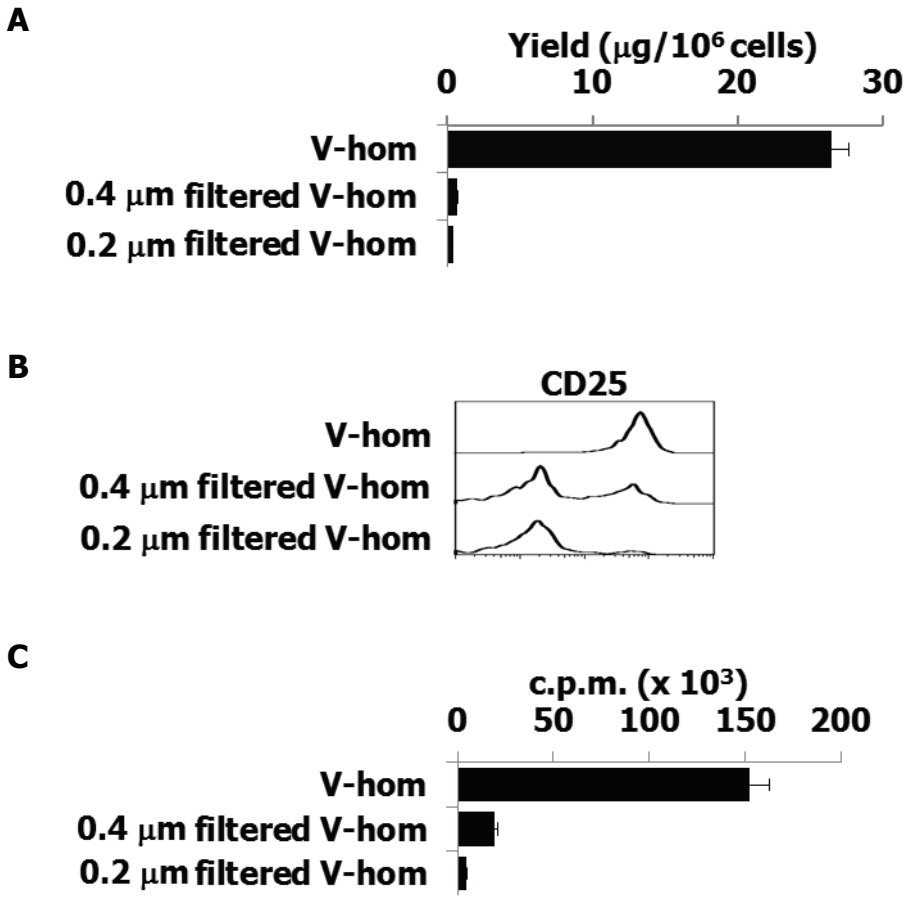

Figure 26. Filtration of vesicles prepared with homogenization without sonication removes immunogenic material. Membrane vesicles (V-hom) were prepared as in Figure 24 and then tested for yield/10^6 BMDC (A) and immunogenicity (B and C). For measuring yields, some of the material (V-hom) was passed through a 0.4 μm or 0.2 μm filter before protein measurement (as in Figure 24). Immunogenicity was measured by culturing 5 x 10^4 2C CD8 T cells with the vesicle preparations plus 300 nM SIYR peptide followed by staining for CD25 expression at 16 hours of culture using flow cytometry (B) and measurement of ^{3}H-thymidine incorporation on day 3 of culture (C; mean and SD). The data are representative of more than three independent experiments.

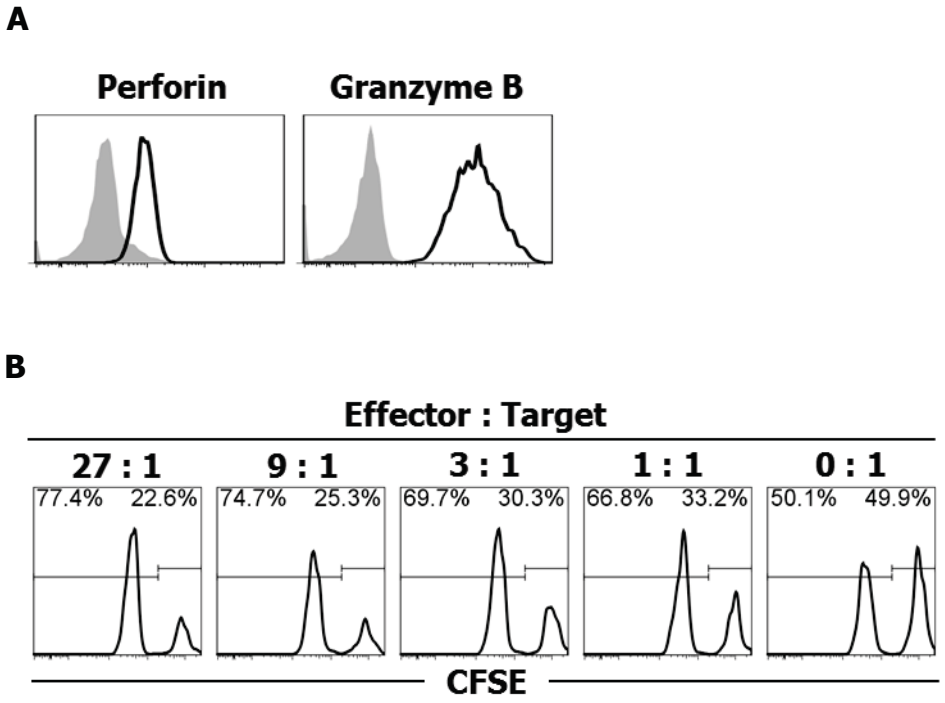

Figure 27. Vesicles containing aggregates induce effector function of CD8 T cells *in vitro*. Membrane vesicles (V-hom) were prepared as in Figure 23 and then were co-cultured at 10 μg/ml with 5 x 10^4 2C CD8 T cells in the presence of 300 nM SIYR peptide for 3 days (without APCs). To measure expression of effector molecules, the T cells were analysed by flow cytometry after intracellular staining against the indicated proteins (A; isotype antibody controls are shown in grey). In parallel, the cells were tested for effector function in an *in vitro* CTL assay (B). For the latter assay, 2C CD8 T cells were incubated with a 1:1 mix of a) SIYR-peptide-loaded EL-4 (H-2^b) cells labelled with a high concentration of CFSE ($CFSE^{Hi}$), together with b) control $CFSE^{Lo}$ EL4 cells not loaded with peptide; different ratios of effector to target cells were used as indicated. 4 hours later, the cultures were examined for viable cells by flow cytometry. The data are representative of two independent experiments.

3.2.3 Summary and conclusion

As demonstrated in this chapter, yields and immunogenicity of membrane vesicles are both affected by many factors, including the density of co-stimulatory molecules on the cells used to prepare vesicles, the cell density used in the homogenization buffer, the strength of homogenization and sonication, centrifugation speeds, and the influence of freezing and thawing. Highly immunogenic membrane vesicles can only be prepared when all these factors are optimised. For this reason, much of my time has been devoted to optimisation of membrane vesicle preparation. With the current protocol, I can now prepare highly immunogenic membrane vesicles from mature BMDCs in large quantities (~ 30 $\mu g/10^6$ cells) which is a significant improvement over the original protocol devised by Kovar et al for DC2.4 cells (~ 5 $\mu g/10^6$ cells).

With regard to immunogenicity, the size of the vesicles proved to be crucial. When presented as aggregates (V-hom), the vesicles are strongly immunogenic *in vitro* and lead to proliferation and effector cell differentiation in the absence of APCs. By contrast, dispersal of the aggregates into nano-vesicles abolishes immunogenicity unless these small vesicles are supplemented with APCs. As discussed below, the results are quite different when the vesicles are tested *in vivo*.

3.3 Immunogenicity of membrane vesicles in vivo

3.3.1 Introduction

The finding that large vesicle aggregates are far more immunogenic than small vesicles for CD8 T cells *in vitro* is in agreement with previous findings that stimulation of CD8 T cell proliferation and CTL responses to antigen on latex beads is much more effective with large beads than with small beads (Luxembourg et al., 1998; Mescher, 1992). However, the observation that the failure of nano-vesicles to stimulate CD8 T cells could be overcome by addition of APCs *in vitro* implies that the results could be different under *in vivo* conditions. Indeed, many reports support the advantage of nanoparticles as vaccine carriers which can easily reach lymphoid organs due to their small size, allowing local uptake and cross-presentation by APCs and the induction of CD8 T cell responses (Bachmann and Jennings, 2010; Manolova et al., 2008). This chapter demonstrates that nano-vesicles prepared from mature BMDCs display strong immunogenicity *in vivo* and lead to intense proliferative responses and differentiation of CD8 T cells into effector cells, especially when co-delivered with anti-CD9 mAb and CpG ODN in multiple injections.

3.3.2 Results

3.3.2.1 Nano-vesicles prepared from mature BMDCs efficiently stimulate CD8 T cells to proliferate *in vivo*

Immunogenicity of BMDC vesicles *in vivo* was assessed by injecting CFSE-labelled OT-1 CD8 T cells (1 x 10^6/mouse) intravenously (I.V.) into C57BL/6 mice, followed 1 day later by I.V. injection of SIINFEKL peptide-pulsed V-hom or V-hom-son vesicles (30 μg/mouse); proliferative responses were measured by CSFE dilution. The results for the two types of vesicles were surprisingly different. For V-hom, in contrast to the strong immunogenicity of these vesicle-aggregates *in vitro*, V-hom were poorly immunogenic *in vivo.* Thus, proliferative responses on day 3 were relatively weak in spleen and lymph nodes (LNs) as

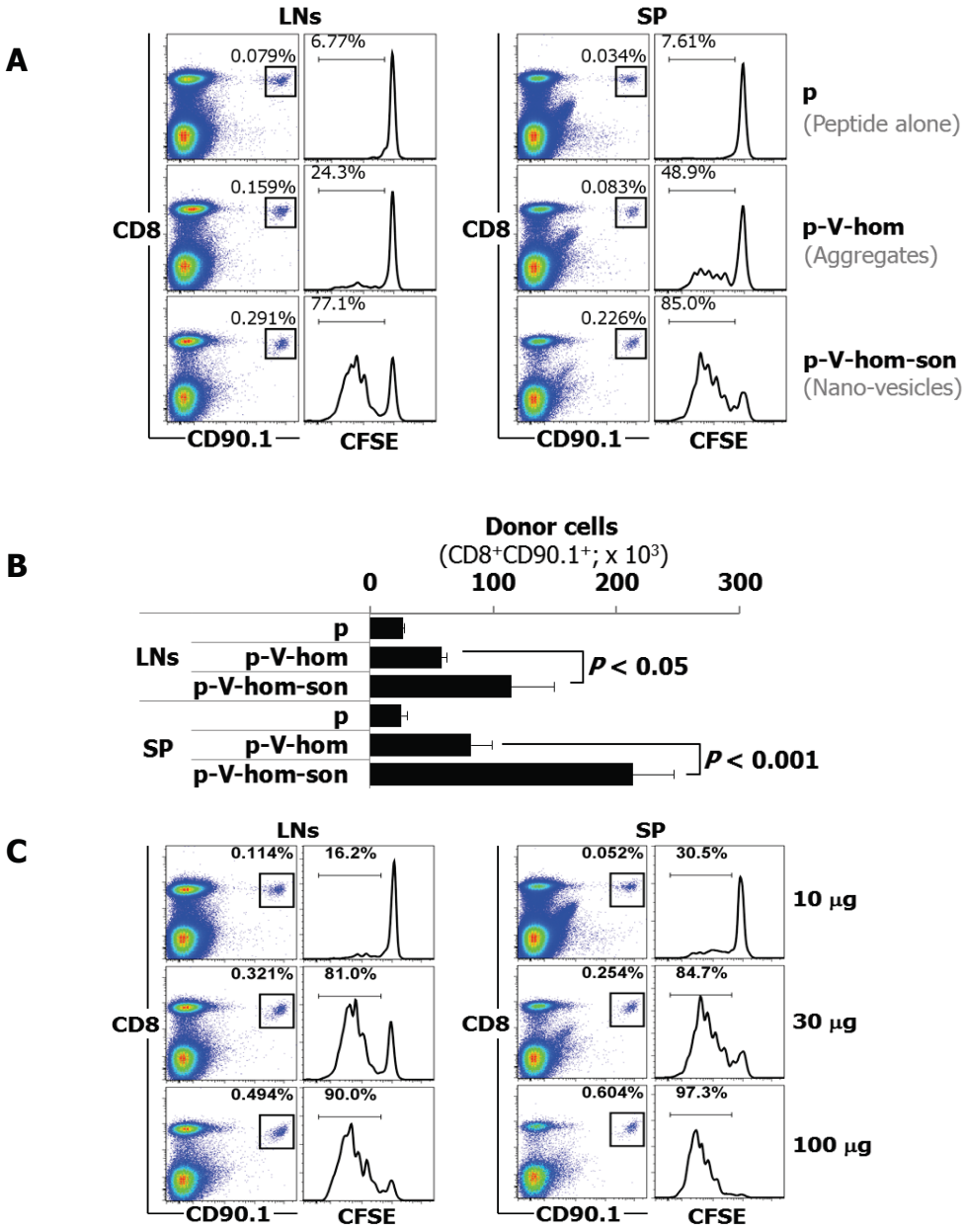

Figure 28. Nano-vesicles stimulate CD8 T cells to proliferate *in vivo*. C57BL/6 mice were adoptively transferred I.V. with 1 x 10^6 CFSE-labelled OT-1 CD8 T cells ($CD90.1^+$). 1 day later, the mice were injected I.V. either with SIINFEKL peptide (p) alone (0.03 nmol/mouse) or with a mixture of peptide and LPS-stimulated BMDC-derived V-hom or V-hom-son, given as a single dose of 30 μg/mouse (A), or in doses of 10, 30, or 100 μg/mouse, for V-hom-son only, (C). At 3 days after injection, suspensions of pooled lymph node (LNs) and spleen (SP) cells were analysed for surface markers and CFSE expression by flow cytometry. The data show the percentages of donor OT-1 CD8 T cells ($CD8^+CD90.1^+$) in lymphocytes and CFSE expression in donor OT-1 CD8 T cells (A). Total number of donor cells from LNs or SP was calculated based on the percentages in total cells and total cell counts (B; mean and SD).

indicated by both CFSE dilution and the recovery of donor cells, relative to controls injected with peptide alone (Figure 28 A, B). In marked contrast, injection of V-hom-son led to strong proliferation and high recovery (expansion) of donor CD8 T cells. For V-hom-son, injection of vesicles in graded doses led to a progressive increase in the extent of T cell expansion, total recoveries of donor CD8 T cells in spleen being about 10-fold higher with 100 μg vesicles than with 10 μg (Figure 28 C).

The poor immunogenicity of V-hom vesicles *in vivo* presumably reflects that after IV injection these large vesicles become trapped in the capillary network of non-lymphoid tissues, notably lung and liver, resulting in only a small proportion of the vesicles reaching lymphoid tissues. By contrast, the small size of V-hom-son enables these nano-vesicles to evade trapping and readily reach the lymphoid tissues. In these sites, the strong immunogenicity of the vesicles may reflect binding and direct presentation to T cells in the T cell zones. If so, an important question is whether the co-stimulation required for T cell activation is provided by the vesicles themselves or by the APCs that bind the vesicles. The latter possibility seems unlikely because no adjuvant was used, hence host APCs would presumably be in a resting state and express only a low density of costimulatory molecules.

To seek direct support for co-stimulation provided by the vesicles themselves, I tested the effects of injecting V-hom-son prepared from LPS-treated mature BMDCs compared with V-hom-son from immature (non-LPS treated) BMDCs (iV-hom-son) (prepared as in Figure 15 F). The striking finding in this experiment was that V-hom-son were clearly more immunogenic than iV-hom-son, both in terms of CFSE dilution and donor T cell yields (Figure 29 A, B); this finding correlated directly with the higher density of costimulatory molecules on V-hom-son than iV-hom-son (Figure 24 B). Though not excluding low-level co-stimulation from host APCs, this experiment clearly suggests that, as *in vitro*, the immunogenicity of membrane vesicles *in vivo* requires that the vesicles express a high density of costimulatory molecules.

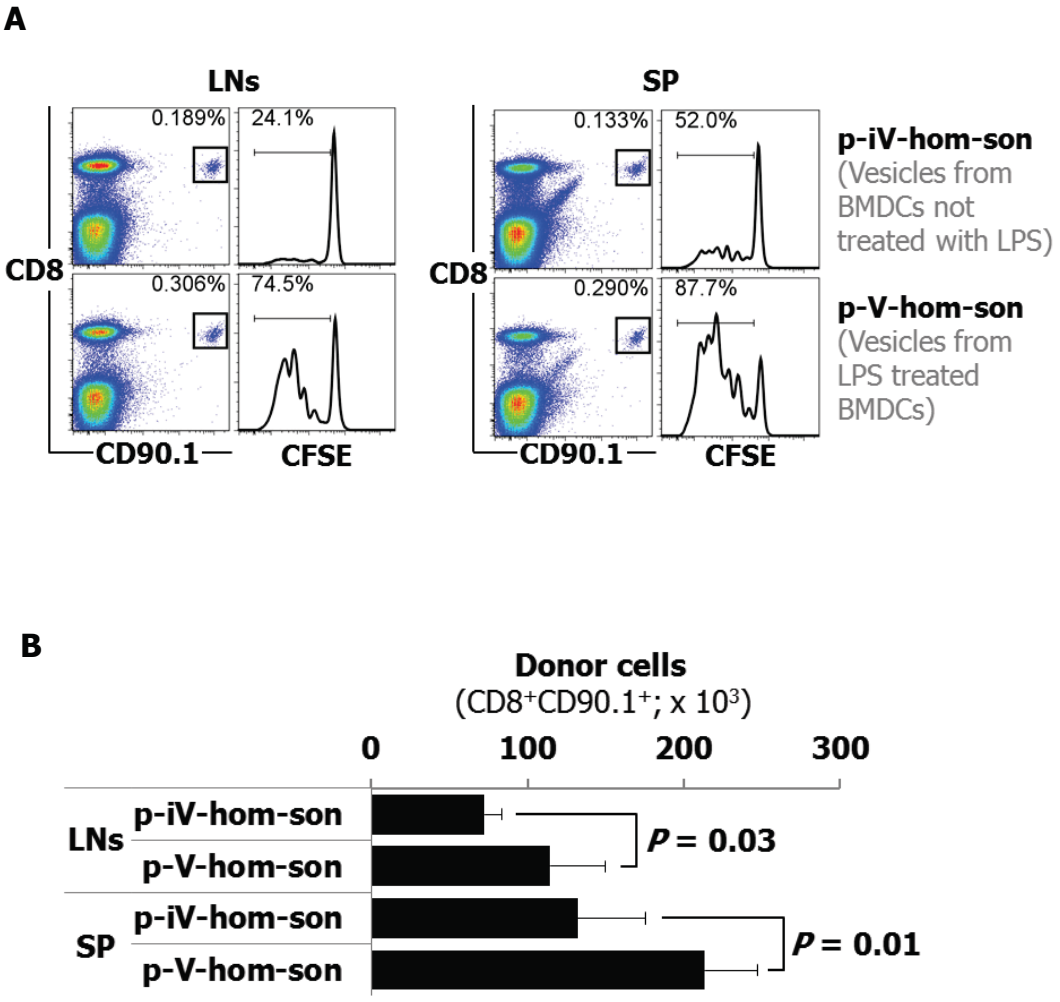

Figure 29. Co-stimulatory molecules improve immunogenicity of membrane vesicles *in vivo*.

Using the same immunization protocol as in in Figure 28, the immunogenicity of V-hom-son prepared from LPS-treated BMDCs was compared with the immunogenicity of control V-hom-son prepared from non-LPS-treated (immature) BMDCs (iV-hom-son). The data are representative of more than two independent experiments with at least three mice in each group.

3.3.2.2 Localisation of injected membrane vesicles in the lymphoid tissues

To determine the localisation of nano-vesicles after I.V. injection, V-hom prepared from LPS-treated BMDCs were first labelled with PKH26 fluorescent general membrane dye to generate V-hom-PKH26. Specific labelling was verified by flow cytometry analysis, relative to unlabelled vesicles (Figure 30 A). V-hom-PKH26 were then subjected to sonication to generate V-hom-son-PKH26 and used for I.V. injection into C57BL/6 mice (Figure 30 A). When spleens were collected 5 minutes after the injection, examination of spleen sections by fluorescent microscopy revealed PKH26 staining largely in the marginal zone associated with co-localisation (white spots in the merged photos) with FcγR II/III and F4/80 (Figure 30 B). FcγR II/III staining was relatively restricted to the ring-like structure of the marginal zone, implying distribution on marginal zone macrophages or DCs. Although other markers and time points were not examined, these findings indicate that the membrane vesicles entering the spleen from the blood localised initially in the marginal zone. Since CD8 T cell responses to antigen occur primarily in the T cell zone (peri-arteriolar lymphoid sheaths of the white pulp, PALS), the implication is that the response to the vesicles depended on prior transport of the vesicles from the marginal zone to the T cell zones. Since transport of bacterial antigens by this route is controlled by $CD11c^+$ DC (Aoshi et al., 2008), I tested whether cell uptake of the injected vesicles included $CD11c^+$ cells. Cell suspensions from the injected mice were used for these studies.

To seek direct evidence of cell uptake of V-hom-son-PKH26 after injection, suspensions of splenocytes and LNs were prepared at 3 or 24 hours after injection and examined by flow cytometry. At 3 hours after vesicle injection, a significant proportion of $CD11c^+$ cells (which are mainly dendritic cells) were positive for PKH26, relative to no staining of these cells in recipients of unlabelled vesicles (Figure 30 C); staining of $CD11c^-$ cells was minimal. $CD11c^+PKH26^+$ cells could also be detected at 24 hours after V-hom-son-PKH26 injection, but to a lesser extent than at 3 hours (Figure 30 D). These data

indicate that, by 3 hours after injection, the vesicles were bound largely by $CD11c^+$ DCs, presumably in the T cell zones though this point was not proved directly. Notably, despite the donor T cell proliferation seen in LNs (Figure 28), the injected vesicles were undetectable in LN suspensions (Figure 30 D). This paradox will be discussed later.

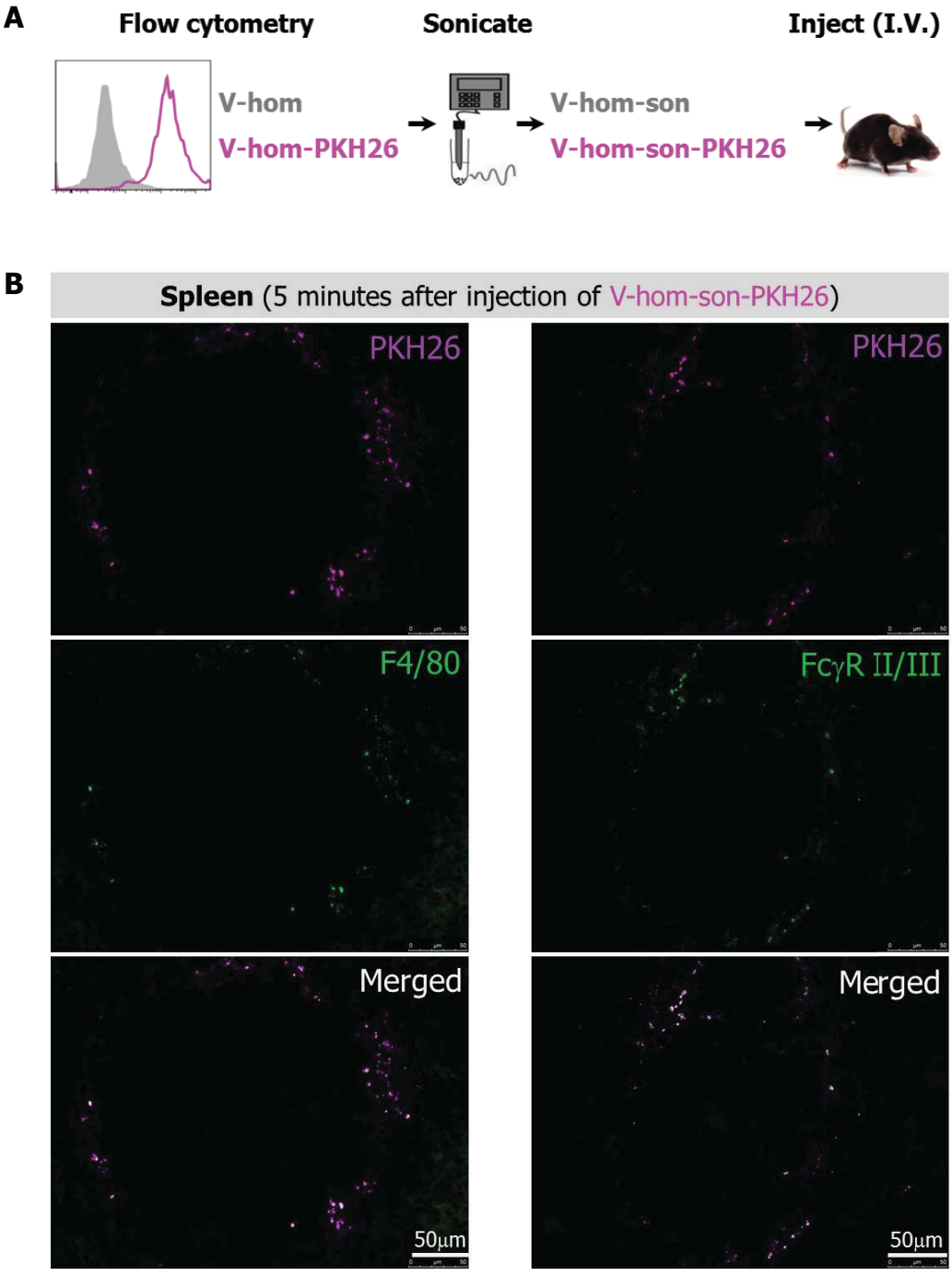

Figure 30 (Continued below)

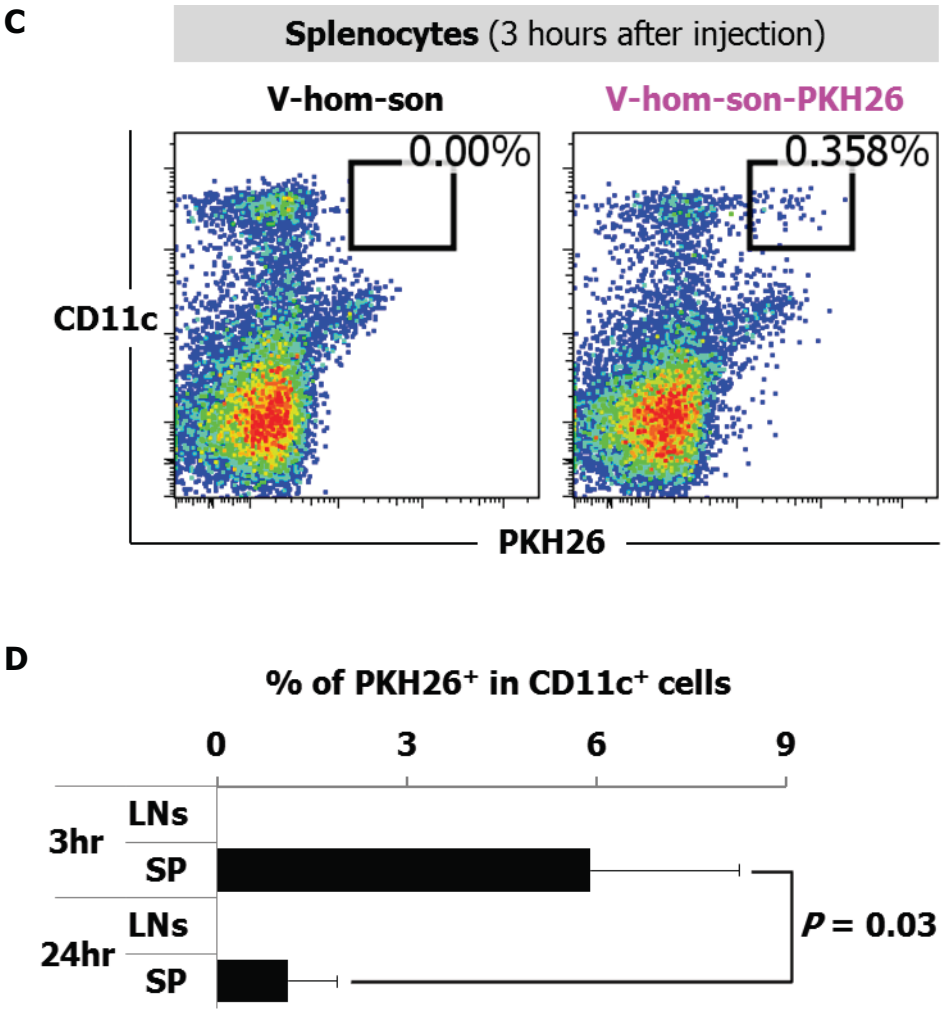

Figure 30. Localization of nano-vesicles in the lymphoid tissues after I.V. injection. V-hom from LPS-stimulated BMDCs were labelled with a membrane dye, PKH26, and then analysed by flow cytometry or subjected to sonication to prepare V-hom-son (A). The latter were then injected I.V. into C57BL/6 mice (100 μg/mouse). B) Distribution of PKH26-labelled vesicles in the spleen sections at 5 min after injection showing co-distribution of PKH26 fluorescence with staining for FcγRII/III and F4/80, detected with Alexa Fluor 647-conjugated mAbs. C) Spleen cell suspensions prepared at 3 hr after vesicle injection show that a significant proportion of $CD11c^+$ cells show PKH26 fluorescence. D) Comparison of spleen and LNs suspensions after vesicle injection shows that PKH26 fluorescence is apparent in $CD11c^+$ cells at both 3 and 24 hr in spleen but is undetectable in LNs. The data show pooled % staining of $CD11c^+$ cells from two independent experiments (mean and SD, three mice per group).

3.3.2.3 Longevity of injected membrane vesicles in the lymphoid tissues

The finding that vesicle PKH26 staining declined between 3 hr and 24 hr after injection raised the question of how long the peptide-pulsed nano-vesicles survive in immunogenic form *in vivo*. To answer this question, C57BL/6 mice were I.V. injected with SIINFEKL peptide-pulsed V-hom-son 9, 3, or 1 day before the adoptive transfer of CFSE-labelled OT-1 CD8 T cells ($CD90.1^+$); LNs and SP were collected 3 days after T cell transfer and $CD8^+$ $CD90.1^+$ donor T cell proliferation was analysed for CFSE dilution by flow cytometry. The results showed that donor T cell proliferation in spleen and LNs was high in mice injected with vesicles 1 day before and was still apparent, though low at 3 days but undetectable at 9 days. Hence the vesicles survived in immunogenic form for at least 3 days after IV injection (Figure 31).

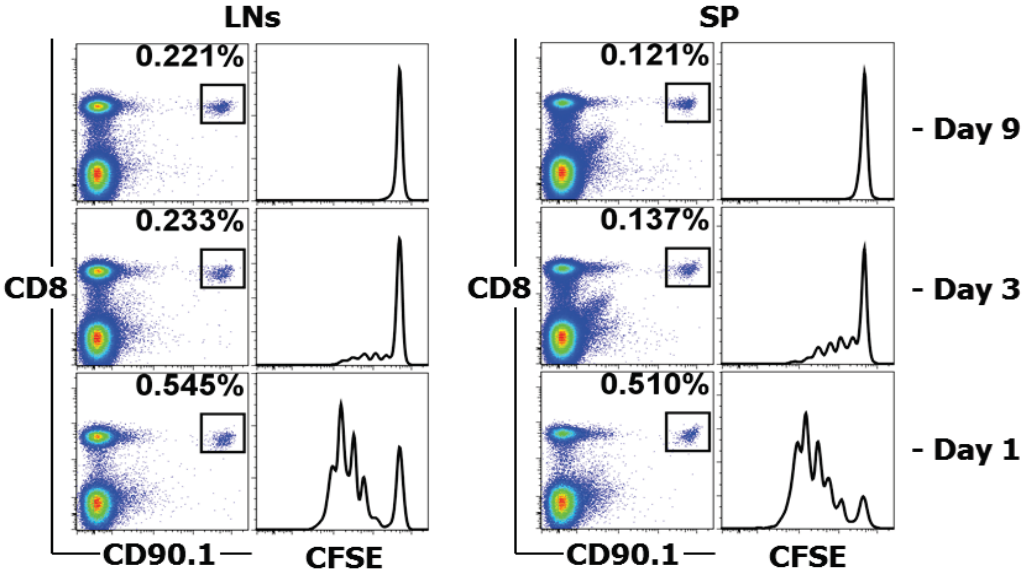

Figure 31. Slow decline in immunogenicity of nano-vesicles after injection. V-hom-son from LPS-stimulated BMDCs were injected I.V. into C57BL/6 mice (100 μg/mouse) together with SIINFEKL peptide (0.03 nmol/mouse). At 9, 3, or 1 day later, the vesicle-injected mice were injected I.V. with CFSE-labelled OT-1 CD8 T cells ($CD90.1^+$). Lymph nodes (LNs) and spleens (SP) were collected 3 days after T cell transfer and $CD8^+$ $CD90.1^+$ lymphocytes were analysed for CFSE dilution by flow cytometry to measure proliferation. The data are representative of two independent experiments with three mice in each group.

3.3.2.4 Kinetics of T cell proliferation after vesicle injection

To elucidate the kinetics of CD8 T cell proliferation after I.V. injection of nano-vesicles, CD8 T cell activation and proliferation were examined at various times after injection. For this experiment, C57BL/6 mice were injected with CFSE-labelled OT-1 CD8 T cells ($CD90.1^+$) and then, 1 day later, the host mice were injected I.V. with SIINFEKL peptide-pulsed V-hom-son. When the donor T cells were examined 1 – 3 days later, CD69 up-regulation (a sign of early activation) was apparent on T cells in SP at day 1 but was undetectable thereafter (Figure 32 A). In LNs, by contrast, CD69 up-regulation was not detectable at any stage, including day 1. For proliferation, CFSE dilution was not seen on day 1 but was prominent in SP on day 2 and day 3. Interestingly, CFSE dilution in LNs was very low on day 2 but as high as in spleen on day 3.

A

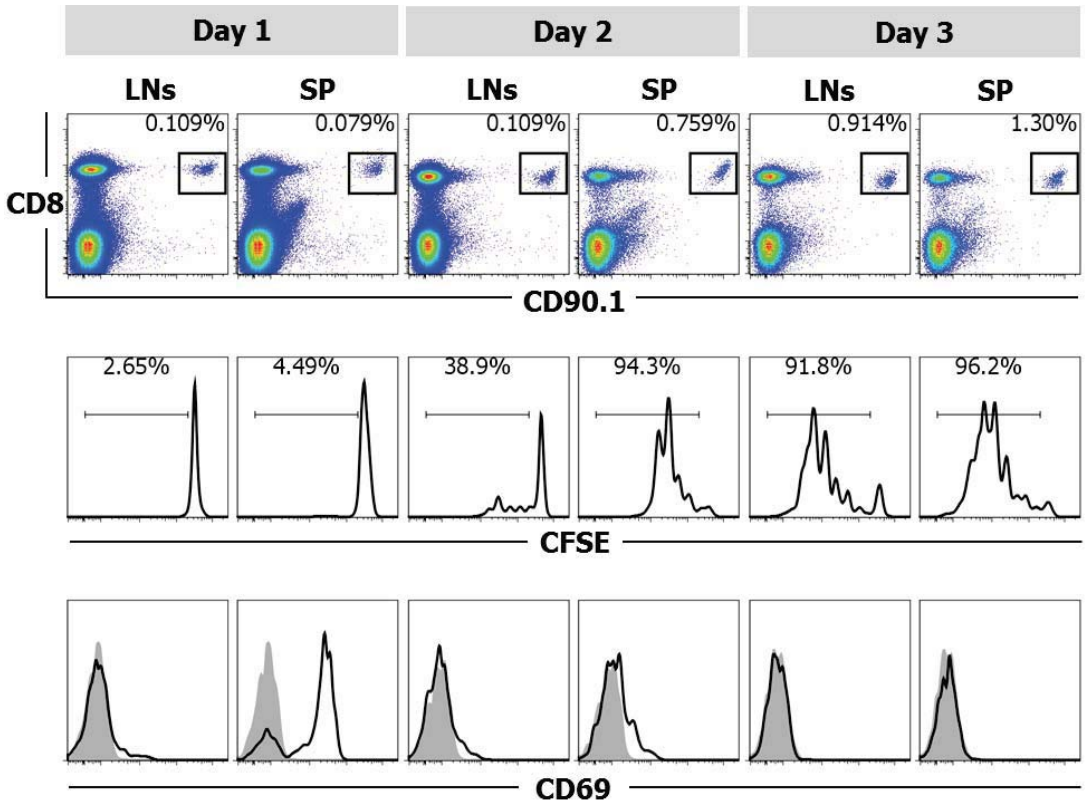

Figure 32 (Continued below)

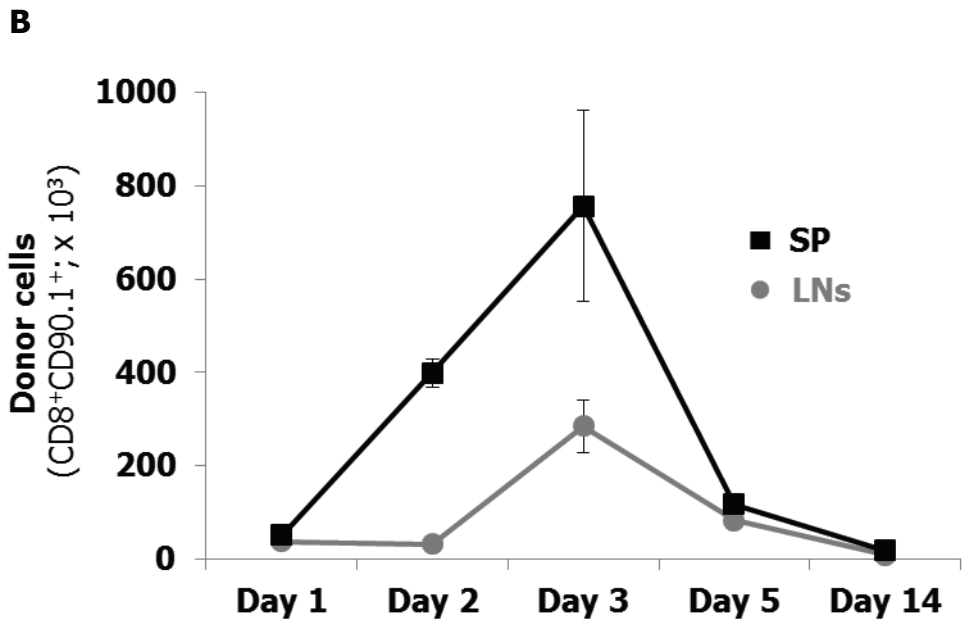

Figure 32. Kinetics of CD8 T cell proliferation in response to peptide-loaded nano-vesicles *in vivo*. Groups of C57BL/6 mice were injected I.V. with CFSE-labelled OT-1 CD8 T cells ($CD90.1^+$) at 1 x 10^6 cells/mouse. At 1 day later, V-hom-son nano-vesicles from LPS-stimulated BMDCs (100 μg vesicles/mouse) were injected I.V. along with SIINFEKL peptide (0.03nmol). At 1, 2, 3, 5, 14 days after vesicle injection, suspensions of lymph nodes (LNs) and spleens (SP) were stained and analysed by flow cytometry to measure total numbers of donor $CD8^+$ $CD90.1^+$ cells (A top, B), together with CFSE dilution (A middle) and CD69 expression (A bottom). Total number of donor CD8 T cells/mouse from SP or LNs was calculated based on the percentages in total cells and total cell counts (B). The data show representative data in A and mean ± SD values from two independent experiments (three mice in each time point) in B.

Likewise, total numbers of donor T cells increased rapidly between day 1 and day 3 in SP but more slowly in LNs (Figure 32 B).

The difference in kinetics between LNs and spleen suggested that the $CFSE^{Lo}$ CD8 T cells in LNs were not proliferating *in situ* but were derived from CD8 T cells activated by the vesicles in SP. This notion is in line with the finding that the vesicles failed to localise in LNs and that CD69 up-regulation at day 1 was seen only in SP and not LN. At time periods after day 3, numbers of donor cells in both SP and LNs declined abruptly to reach very low levels by day 14, presumably reflecting the disappearance of the injected vesicles after day 3.

3.3.2.5 Modulation of membrane vesicles to improve immunogenicity

The finding that uptake of membrane vesicles in the lymphoid tissues was largely restricted to $CD11c^+$ DCs raises the question of how such binding occurs. Although I have not addressed this issue directly, procedures designed to strengthen the binding of vesicles to DCs might be expected to further improve immunogenicity. Since DCs express high levels of Fc receptors (Guilliams et al., 2014), I tested whether coating membrane vesicles with specific mAbs would enhance their immunogenicity through Fc/FcR binding to APCs. Anti-CD9 mAb (αCD9) was chosen since CD9 is a cell-surface protein expressed by wide range of cells and is also found on the surface of exosomes (Segura et al., 2005).

The expression of CD9 on the vesicles (V-hom-son-FT) was confirmed by staining with Allophycocyanin-conjugated αCD9 (Figure 33 A). To test the effect of αCD9 binding on vesicle immunogenicity, I used 2C CD8 T cells since these cells generally give lower responses to vesicles than OT-1 CD8 T cells. C57BL/6 mice were first adoptively transferred with CFSE-labelled 2C CD8 T cells ($CD90.1^+$), followed 1 day later by I.V. injection of SIYR peptide-pulsed vesicles (V-hom-son) at 30 μg/mouse without (pV) or with αCD9 pre-incubation (pVαCD9). Some mice were injected with αCD9 at various times (0.5, 2, or 8 hours) before the injection of peptide-pulsed vesicles.

The results of this experimental approach were striking. Thus, in contrast to the relatively low proliferation (CFSE dilution) seen on day 3 with injection of vesicles alone (pV), marked proliferation occurred after injection of vesicles pre-incubated with αCD9 (pVαCD9) (Figure 33 B). In addition, total donor CD8 T cell yields were 2 - 3 fold higher with αCD9-coated vesicles, both on day 3 and day 7 (Figure 33 C, and data not shown). Importantly, at day 7 there was a prominent increase in donor cell effector function as defined by IFNγ synthesis. Thus, IFNγ synthesis by the donor cells in spleen on day 7 was minimal (<5%) with pV injection but conspicuous (~50%) with pVαCD9; in terms of total cells, $IFN\gamma^+$ cell numbers were about 10-fold higher with pVαCD9 than with pV (Figure 33 C). As controls for this experiment, no effect was seen with control mAb (pVconAb) or with injection of αCD9 without vesicles (pαCD9). The

enhancing action of αCD9 required pre-incubation with the vesicles because injection of αCD9 before vesicle injection was much less effective (Figure 33 B).

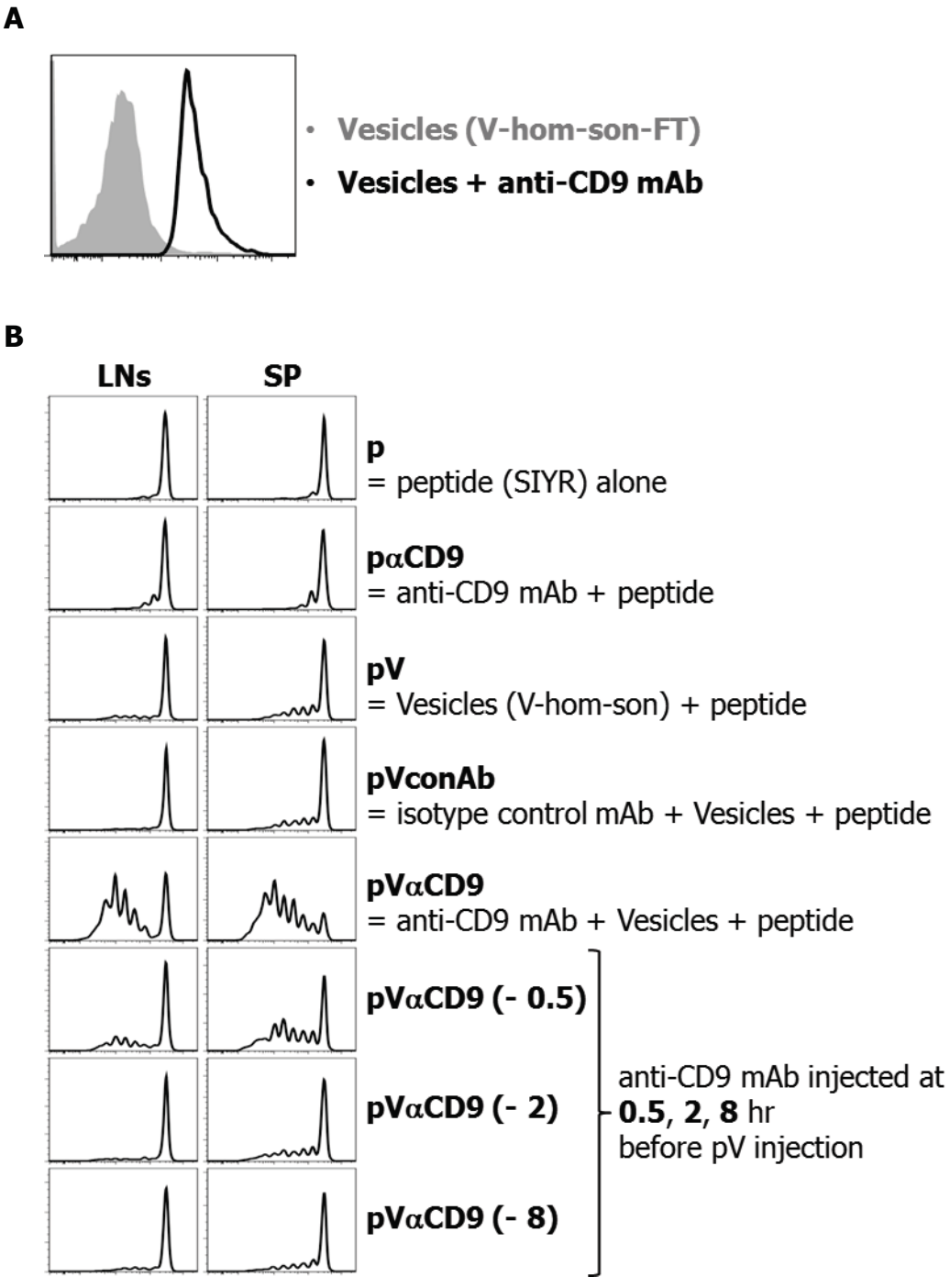

Figure 33 (Continued below)

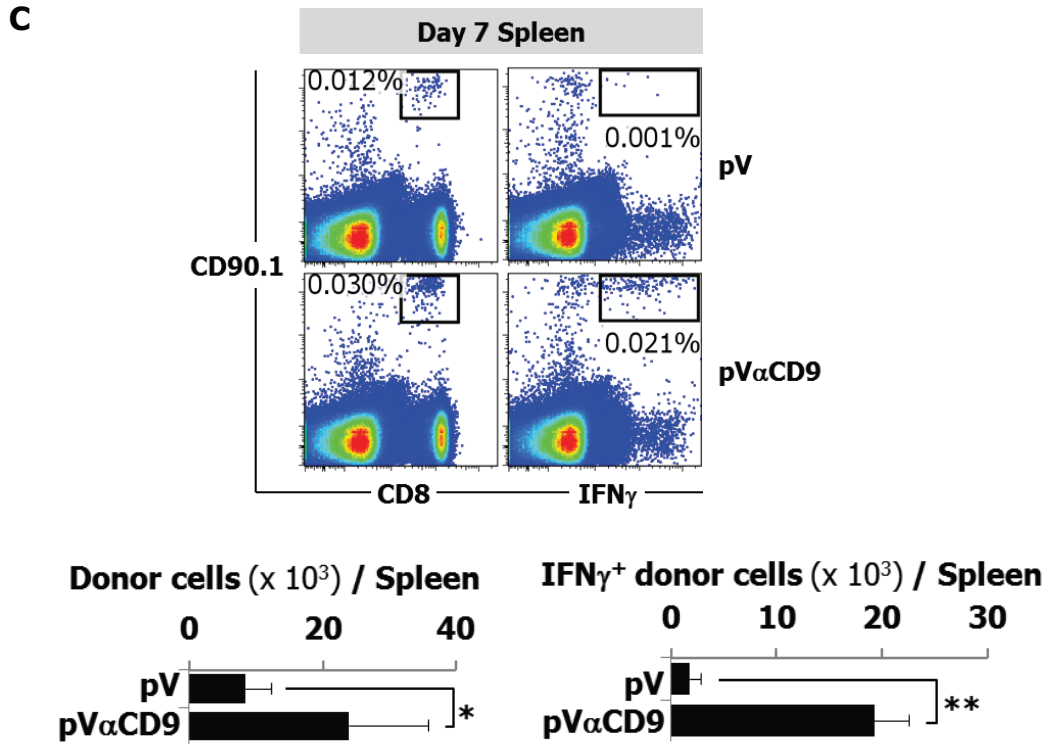

Figure 33. Immunogenicity of nano-vesicles *in vivo* is increased by coating with anti-CD9 mAb before injection. To investigate the capacity of anti-CD9 mAb to augment vesicle immunogenicity, C57BL/6 mice were first injected I.V. with 1 x 10^6 CFSE-labelled 2C CD8 T cells (CD90.1$^+$). Then, 1 day later, the mice were injected I.V. with nano-vesicles (V-hom-son) from LPS-stimulated BMDCs (30 μg vesicles/mouse). Before injection, these nano-vesicles were pre-incubated with SIYR peptide (0.2 nmol/mouse; 2 hours pre-incubation) plus either anti-CD9 or isotype control mAb (10 μg/mouse; 0.5 hour pre-incubation); some groups of mice were injected with anti-CD9 mAb at various times (0.5, 2, or 8 hours) before the injection of vesicles plus peptide. A) Flow cytometry data showing staining of vesicles after incubation with anti-CD9 mAb (Allophycocyanin conjugated); vesicles containing aggregates (V-hom-son-FT as in Figure 23) were used to measure mAb binding. B) Flow cytometry showing CFSE dilution (proliferation) of donor 2C cells in SP and LNs at 3 days after injection of vesicles, SIYR peptide (p) and either anti-CD9 or control mAb. C) Flow cytometry data showing effector function in SP at 7 days after vesicle injection as defined by expression of IFNγ in donor 2C CD8 T cells after 4hr re-stimulation with peptide *in vitro*. Total number of IFNγ$^+$ donor cells from each spleen was calculated based on the percentages in total splenocytes and total cell counts (mean and SD). The data are representative of two independent experiments with three mice in each group. *P = 0.02; **P < 0.005.

With regard to further improving vesicle immunogenicity, it should be emphasised that none of the above experiments involved the use of adjuvants. To study the effect of adding an adjuvant, I chose CpG ODNs which are known to activate APCs through interaction with endosomal TLR9 (Coffman et al., 2010). Recently, it has been reported that CpG ODNs specifically bind to cell-surface protein DEC-205 which allows uptake by and subsequent activation of DCs (Lahoud et al., 2012). The expression of DEC-205 on vesicles (V-hom-son-FT) was confirmed by staining with FITC-conjugated anti-DEC-205 mAb; incubation with CpG ODN 1668-FITC followed by flow cytometry confirmed that the vesicles bound CpG ODN, presumably via DEC-205 (Figure 34 A).

To test the effect of CpG ODN binding on vesicle immunogenicity, I reverted to OT-1 CD8 T cells and used a limiting dose of vesicles for injection (20 μg/mouse). C57BL/6 mice were first adoptively transferred with CFSE-labelled OT-1 CD8 T cells (CD90.1^{+}), followed 1 day later by I.V. injection of SIINFEKL peptide-pulsed vesicles (V-hom-son; 20 μg/mouse) without (pV) or with 1 μg CpG ODN 1668 pre-incubation (pV-CpG). The striking finding in this experiment is that addition of CpG to the vesicles caused a marked improvement of immunogenicity. Thus, at 3 days after transfer, proliferation (CFSE dilution) was much greater with pV-CpG than pV and led to a 2-fold higher recovery of donor CD8 T cells (Figure 34 B).

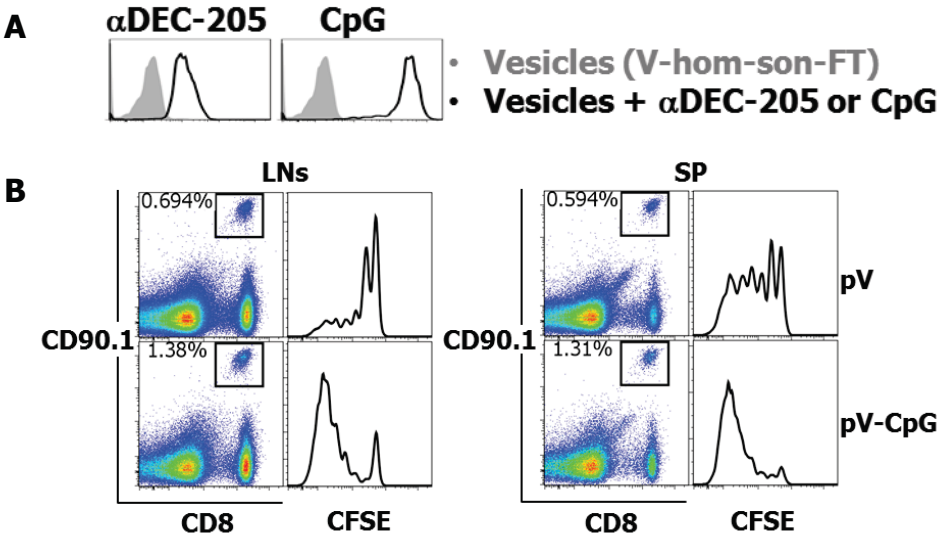

Figure 34 (Continued below)

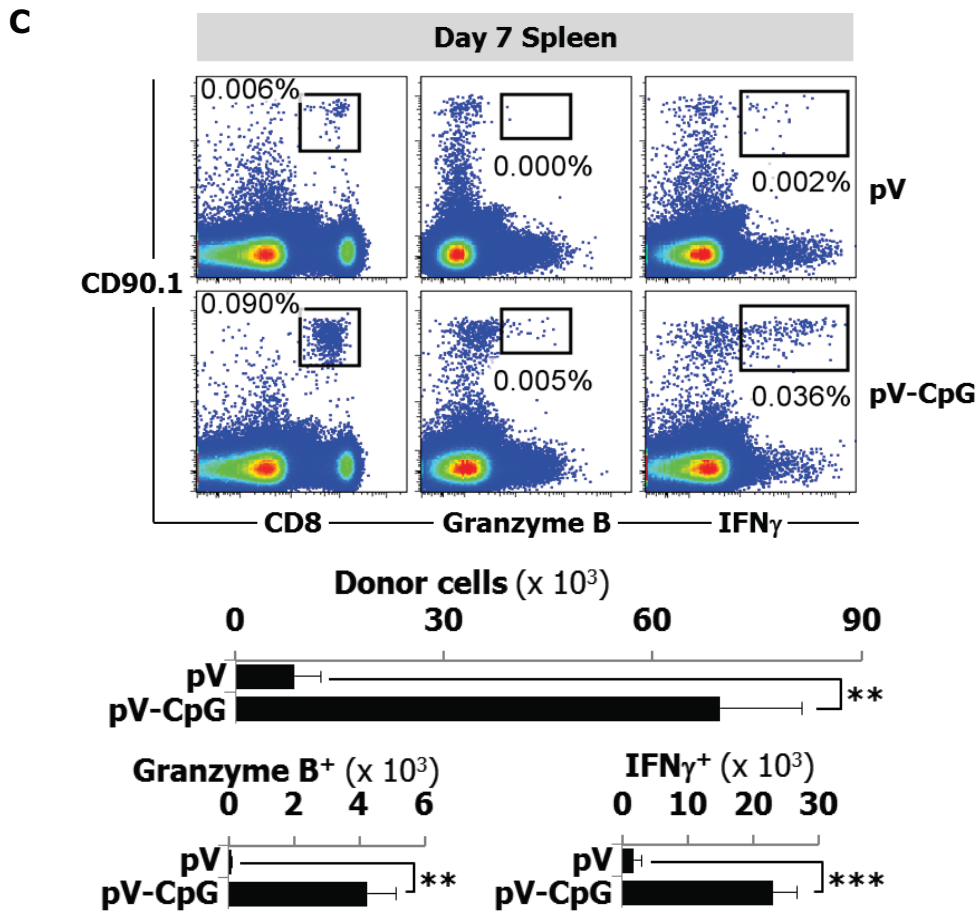

Figure 34. Immunogenicity of nano-vesicles *in vivo* is enhanced by loading with CpG ODN before injection. Nano-vesicles (V-hom-son) from LPS-stimulated BMDCs were mixed with SIINFEKL peptide with or without CpG ODN 1668 and injected I.V. into mice that had received 1 x 10^6 CFSE-labelled OT-1 CD8 T cells ($CD90.1^+$) 1 day previously; vesicles were injected at 20 μg/mouse, peptide at 0.03 nmol/mouse, and CpG ODN 1668 at 1 μg/mouse. A) Binding of CpG ODN to vesicles was analysed by flow cytometry after incubating aggregate-containing vesicles (v-hom-son-FT as in Figure 23) with CpG ODN 1668-FITC; vesicles were also stained with anti-DEC-205-FITC mAb to detect DEC-205, a known surface receptor for CpG ODN. B) Flow cytometry showing proliferation (CFSE dilution) of donor OT-1 cells in SP and pooled LNs at 3 days after injection of vesicles. C) Flow cytometry data showing effector function in SP at 7 days after vesicle injection as defined by expression of Granzyme B and IFNγ in OT-1 CD8 T cells after 4hr re-stimulation with peptide *in vitro*. Total number of donor cells ($CD8^+CD90.1^+$), Granzyme B^+ and $IFN\gamma^+$ donor cells from each spleen was calculated based on the percentages in total splenocytes and total cell counts (mean and SD). The data are representative of two independent experiments with three mice in each group. $^{**}P = 0.001$; $^{**}P = 0.0007$.

The results were more dramatic at day 7 (Figure 34 C). At this stage, donor CD8 T cell numbers were 8-fold higher with pV-CpG than pV. Also, unlike pV, pV-CpG led to strong induction of IFNγ synthesis. Thus, with pV-CpG, ~40% of the donor CD8 T cells in spleen showed IFNγ synthesis, compared with ~ 10% for pV. Granzyme B synthesis was much lower but was significant with pV-CpG (10%) and almost undetectable with pV (< 1%). In terms of total yields, numbers of IFNγ^+ and Granzyme B^+ donor cells were 10-fold higher with pV-CpG than with pV.

Collectively, these data indicate that coating the vesicles with αCD9 or CpG ODN before injection led to a marked increase in immunogenicity, both for proliferation and effector cell generation. Nevertheless, total recoveries of donor CD8 cells were low and no higher on day 7 than on day 3.

With regard to further improving vesicle immunogenicity, it should be emphasised that all of the above experiments involved injection of only a single dose of vesicles. Since the vesicles disappeared progressively over a period of several days (Figure 30 and 31) and donor T cell expansion ceased after day 3 (Figure 32), stimulation of T cells elicited by a single dose of vesicles was presumably quite brief. In contrast, in typical viral infections, the immune system is exposed to prolonged antigen presentation which increases exponentially as the virus replicates, until about one week when the virus is destroyed by effector cells and antigen has been cleared (Williams and Bevan, 2007). Therefore, I tested if multiple injections of vesicles can further improve effector CD8 T cell expansion, especially when given in exponential doses (Johansen et al., 2008).

3.3.2.6 Amplifying immunogenicity by multiple injection of vesicles

To test the effect of injecting vesicles in multiple doses, C57BL/6 mice were first adoptively transferred with OT-1 CD8 T cells on day -1. On the next day (day 0), groups of the mice were injected I.V. with peptide-pulsed vesicles under various conditions: each group received the same total dose of vesicles (0.03 nmol SIINFEKL peptide plus 156 μg V-hom-son/mouse) either as a single

dose or in multiple doses. There were 5 groups: 1) a control group given the peptide-loaded vesicles in unmodified form (pV) as a single injection on day 0 (shown as **One**); 2) pV injected daily in the same dose for 4 days starting on day 0 (shown as **4x**), 3) pV injected daily from day 0 in exponential doses, each dose being 5-fold higher than on the previous day (shown as **Ex**), 4) as for **Ex,** but with vesicles coated with αCD9 (shown as **ExA**), 5) as for **ExA,** but with vesicles also coated with CpG ODN 1668 (shown as **ExAC**).

When the immunised mice were sacrificed for analysis on day 6, their spleen and LNs were all of about the same size, with the exception of **ExAC** which had very large spleens and LNs (Figure 35 A, and data not shown). Data on the donor cells recovered from the lymphoid organs on day 6 can be summarised as follows:

For group **One,** it should be noted that the single dose of vesicles injected was substantially (5 – 8 fold) higher than in most previous experiments and led to much higher donor cell recoveries and prominent differentiation of the responding CD8 T cells into IFNγ$^+$ effector cells (compare Figure 35 B with Figure 34 C). For **4x**, injecting the vesicles in equal daily doses improved the total recovery of donor cells and IFNγ$^+$ cells by ~ 4-fold, relative to **One** (Figure 35 B, E). For **Ex**, injecting the vesicles daily in exponential doses caused a further 2-fold increase in donor cell recoveries and a 3-fold increase in IFNγ$^+$ cells, relative to **4x.** For **ExA,** injection of αCD9-coated vesicles in exponential doses induced an even more prominent increase in total recoveries of donor cells and IFNγ$^+$ cells; here, total numbers of these cells were ~ 40-fold higher than in the control group **One**, and the majority of the donor cells (~80%) synthesised IFNγ. For **ExAC,** exponential injection of vesicles coated with both αCD9 and CpG resulted in somewhat lower donor cell yields than in **ExA;** this reduction paralleled the large size of the lymphoid organs in **ExAC** and the presence in cell suspensions of many blast cells, a large proportion being dead as measured by trypan blue exclusion (see General Discussion).

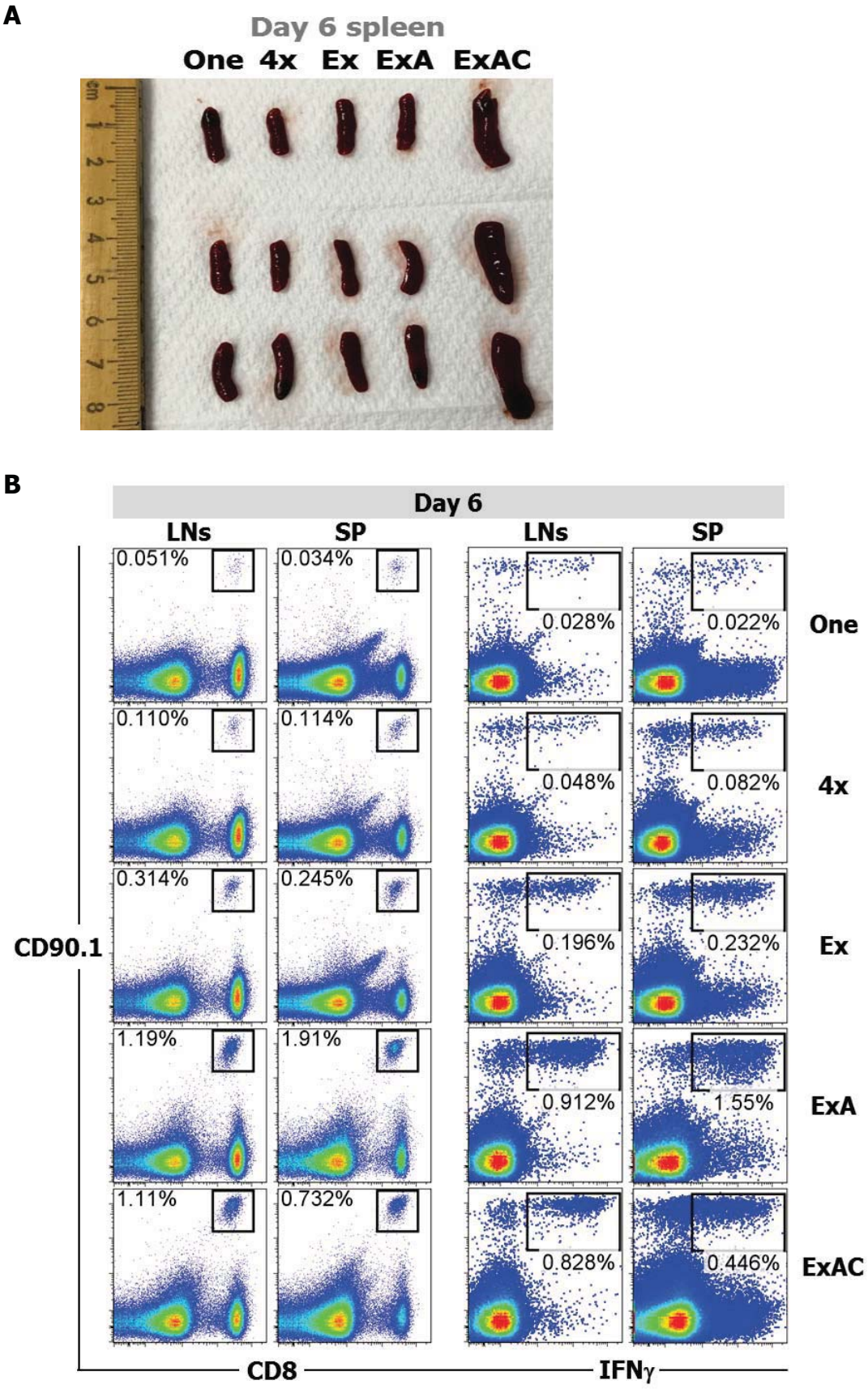

Figure 35 (Continued below)

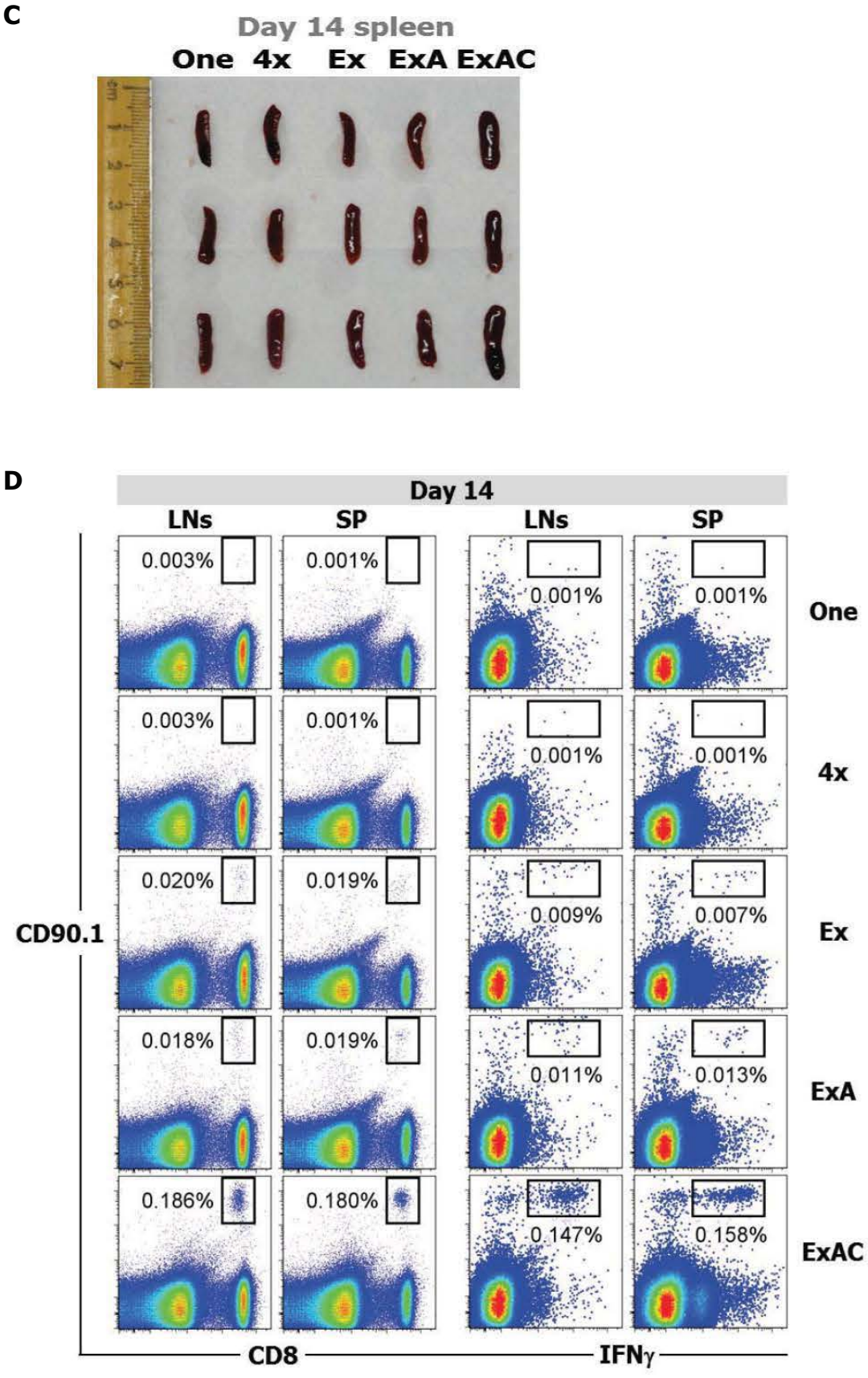

Figure 35 (Continued below)

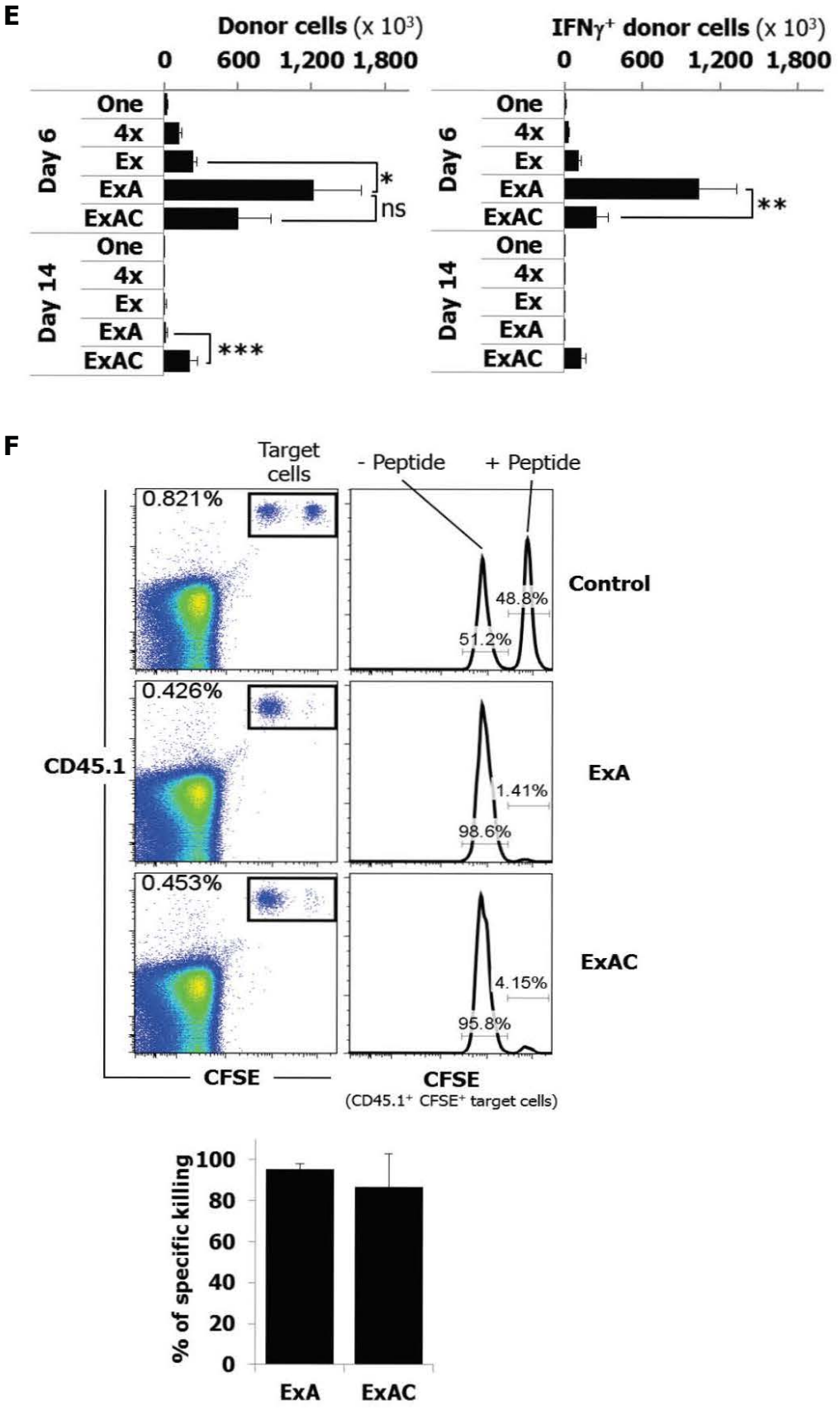

Figure 35 (Continued below)

Figure 35. Improved immunogenicity of nano-vesicles given daily in exponential doses. C57BL/6 mice were injected I.V. with 1 x 10^6 OT-1 CD8 T cells (CD90.1$^+$) on day -1 and then, 1 day later (day 0), groups of these mice were injected I.V. with nano-vesicles plus peptide under various conditions:

1) As one single dose of vesicles (156 μg/mouse) plus SIINFEKL peptide (0.03 nmol/mouse) injected on day 0 (shown as **One**),

2) As four equal doses of vesicles and peptide injected daily for 4 days starting on day 0 (39 μg/day of vesicles and 0.0075 nmol/day of peptide/injection) (shown as **4x**),

3) As exponential doses of a mixture of vesicles and peptide given in four daily injections starting on day 0, using a total dose of 156 μg vesicles and 0.03 nmol peptide/mouse (1x on day 1, 5x on day 2, 25x on day 3, 125x on day 4) (shown as **Ex**),

4) As exponential doses of a mixture of vesicles, peptide and anti-CD9 mAb given daily for 4 days as for **Ex,** using a total dose of 15.6 μg/mouse of anti-CD9 mAb (shown as **ExA**),

5) As exponential doses of a mixture of vesicles, peptide, anti-CD9 mAb and CpG ODN 1668 given daily for 4 days, using a total dose of 80 μg (12.5 nmol) CpG ODN/ mouse (shown as **ExAC**).

At 6 or 14 days after the first day of vesicle injection, SP and pooled LNs were removed to prepare cell suspensions to assess donor OT-1 CD8 T cells for expansion and effector function. A, C) Photograph of spleens removed at day 6 or day 14 after the first day of vesicle injection. B, D) Flow cytometry data showing percentages of donor (CD90.1$^+$) CD8 T cells and IFNγ$^+$ cells in total lymphocytes after 4hr re-stimulation with peptide *in vitro*. E) Total number of donor cells and IFNγ$^+$ donor cells from each spleen was calculated based on the percentages in total splenocytes and total cell counts (mean and SD). The data are representative of two independent experiments (three mice in each group).
F) Effector functions as defined by target cell lysis in an *in vivo* CTL assay at 6 days after the first day of vesicle injection. To measure CTL activity, mice from the **ExA** or **ExAC** groups (along with **Control** naïve C57BL/6 mice) were injected I.V. with 1:1 mix of CD45.1$^+$ C57BL/6 splenocytes labelled with either a high or low concentration of CFSE (CFSE^{Hi} cells, CFSE^{Lo} cells); CFSE^{Hi} cells were pulsed with 2 μM SIINFEKL peptide for 2 hours (followed by thorough washing) to act as antigen presenting target cells. Spleens were removed 1 day later and cell suspensions were analysed by flow cytometry to detect CFSE^{Hi} versus CFSE^{Lo} CD45.1$^+$ target cells. Specific killing (%) of antigen presenting CFSE^{Hi} target cells was determined by (1-%CFSE^{Hi}/%CFSE^{Lo}) x 100. The data are representative of two independent experiments (three mice in each group). $*P = 0.01$; $**P < 0.01$; $***P < 0.005$; ns, not significant.

The results on day 14 were different. At this stage, except for **ExAC,** total yields of donor cells were markedly lower than at day 7 for all groups (Figure 35 E). This dramatic decline in donor cell recoveries by day 14 was especially striking for ExA where the high recovery of donor cells on day 6 decreased by ~ 80-fold by day 14, indicating a near absence of early memory cell generation. For **ExAC,** by contrast, the results were surprisingly different. Here, spleen and LNs had returned to near-normal size by day 14 and the presence of activated cells in cell suspensions was much less prominent than at day 6, presumably reflecting clearance of CpG. The important finding for **ExAC** was that the decline in donor cell recoveries after day 6 was quite limited. Thus, in marked contrast to the near-complete disappearance of donor cells in the other groups, for **ExAC** the decrease in donor cells between day 6 and day 14 was only ~3-fold for total donor cells and ~2 fold for $IFN\gamma^+$ cells. The implications of this finding will be discussed later (see General Discussion).

In addition to measuring IFNγ synthesis, some of the mice in the above experiment were tested for donor CTL activity. For this experiment, 6 days after the first day of vesicle injection, groups of **ExA** and **ExAC mice** together with **Control** naïve C57BL/6 mice were injected with $CD45.1^+$ C57BL/6 splenocytes labelled with either a high or low concentration of CFSE ($CFSE^{Hi}$ cells, $CFSE^{Lo}$ cells) as 1:1 mixture; $CFSE^{Hi}$ cells were pulsed with SIINFEKL peptide to act as antigen-presenting target cells. 1 day later, splenocytes were analysed for the presence of $CD45.1^+CFSE^+$ target cells. As shown in Figure 35 F, CTLs generated by **ExA** and **ExAC** caused almost complete killing of the specific target cells ($CFSE^{Hi}$) while sparing target cells lacking antigen ($CFSE^{Lo}$). Hence, the responding CD8 T cells in the **ExA** and **ExAC** groups both displayed strong antigen-specific CTL activity.

3.3.2.7 Injection of vesicles leads to anti-tumour immunity

To examine whether the immunogenicity of membrane vesicles can be applied to elimination of tumours, three preliminary experiments were performed:

In the first experiment, C57BL/6 mice were injected subcutaneously (S.C.) with 2 x 10^5 OVA-expressing B16 melanoma tumour cells (B16-OVA). When tumours were palpable, mice were injected I.V. with a low dose of 1 x 10^3 OT-1 CD8 T cells; this low dose of OT-1 CD8 T cells was used to mimic the small precursor frequency of endogenous CD8 T cells responsive to specific tumour peptides in normal non-transgenic mice. Starting on the next day, mice were injected with SIINFEKL peptide-pulsed vesicles using the conditions **One**, **ExA** or **ExAC** as described in Figure 35; control mice received either tumour cells alone (**Control)** or tumour cells plus OT-1 cells without vesicles (**OT-1**). Tumour sizes were monitored every 3 days thereafter. As shown in Figure 36 A, compared to **Control**, tumour growth was not significantly reduced by injection of one single large dose of vesicles (**One**) or OT-1 cells without vesicles (**OT-1**). However, consistent with the prominent CTL killing of lymphoid cell targets demonstrated in Figure 35, groups **ExA** and **ExAC** did significantly retard tumour growth; suppression of tumour growth was especially effective with **ExAC.**

Though informative, the OT-1/B16-OVA model is not physiological because recognition of a strong foreign antigen by TCR transgenic T cells differs from the clinical setting where endogenous T cells respond to relatively weak tumour-associated antigens. For this reason, I tested whether injection of membrane vesicles could be used to induce endogenous CD8 T cells to respond to B16-F10 cells; these cells constitutively express melanoma peptide TRP-2 (Overwijk and Restifo, 2001). In an initial experiment, I examined whether injecting normal mice with TRP-2-loaded membrane vesicles could act as a vaccine and induce immunity against subsequent growth of B16-F10 cells. Here, normal C57BL/6 mice were injected with membrane vesicles pulsed with TRP-2, or with TRP-2 alone as a control, followed by S.C. injection of B16-F10

melanoma cells; as above, the vesicles were from LPS-activated BMDCs prepared from normal mice. For this experiment, mice were injected with a total dose of 156 μg vesicles incubated with 15.6 μg αCD9 plus 10 nmol TRP-2 peptide/mouse given exponentially over 4 days as in Figure 35 (**ExA**); controls received TRP-2 peptide alone, also given exponentially (**Peptide**). At 6 days after the first day of immunisation, the mice were injected S.C. with 2 x 10^5 B16-F10 melanoma tumour cells. As shown in Figure 36 B, tumours grew rapidly in the mice that received TRP-2 peptide alone (**peptide**) but much more slowly in the group primed with TRP-2-pulsed membrane vesicles (**ExA**).

These findings raised the question whether injection of TRP-2-loaded vesicles could inhibit the growth of established B16-F10 tumours. In considering how to design this experiment, I noted that other workers have shown that anti-tumour responses can be enhanced by injecting CpG directly into the tumour (Lou et al., 2011; Shirota et al., 2012; Zoglmeier et al., 2011). With this finding in mind, C57BL/6 mice were injected S.C. with 2 x 10^5 B16-F10 on both the right and left side of the back (Figure 36 C). When tumours were palpable 7 days after tumour inoculation, the mice were injected I.V. exponentially over 4 days with TRP-2 **peptide** alone or TRP-2 peptide-pulsed **ExA** or **ExAC**. In another group, the mice received a half dose of **ExA** given I.V. and a half dose of **ExAC** injected into the right side tumour (shown as **ExA(I.V.) + ExAC(I.T.)** in the figure). The results (Figure 36 C) showed that ExA and ExAC given I.V. significantly retarded the growth of tumours on both right and left side of the back. More strikingly, however, all tumours on the right (injected) side of the back were completely rejected in 3 out of 5 mice in group ExA(I.V.) + ExAC(I.T.) and grew only very slowly in the other 2 mice after day 21. Interestingly, tumours on the uninjected left side of the back of this group were also rejected in 3 mice, leaving the other 2 mice with slowly-growing tumours. These findings imply that the ExA(I.V.) + ExAC(I.T.) injection scheme effectively activated tumour antigen-specific CD8 T cells (and possibly also other effector cells) in the injected tumour and caused some of these cells to migrate and attack the other tumour. One caveat of this experiment is that the **ExAC** vesicle

preparations were not depleted of unbound CpG. In future experiments it will be important to assess the effects of injecting the tumours with **ExAC** devoid of free CpG**.**

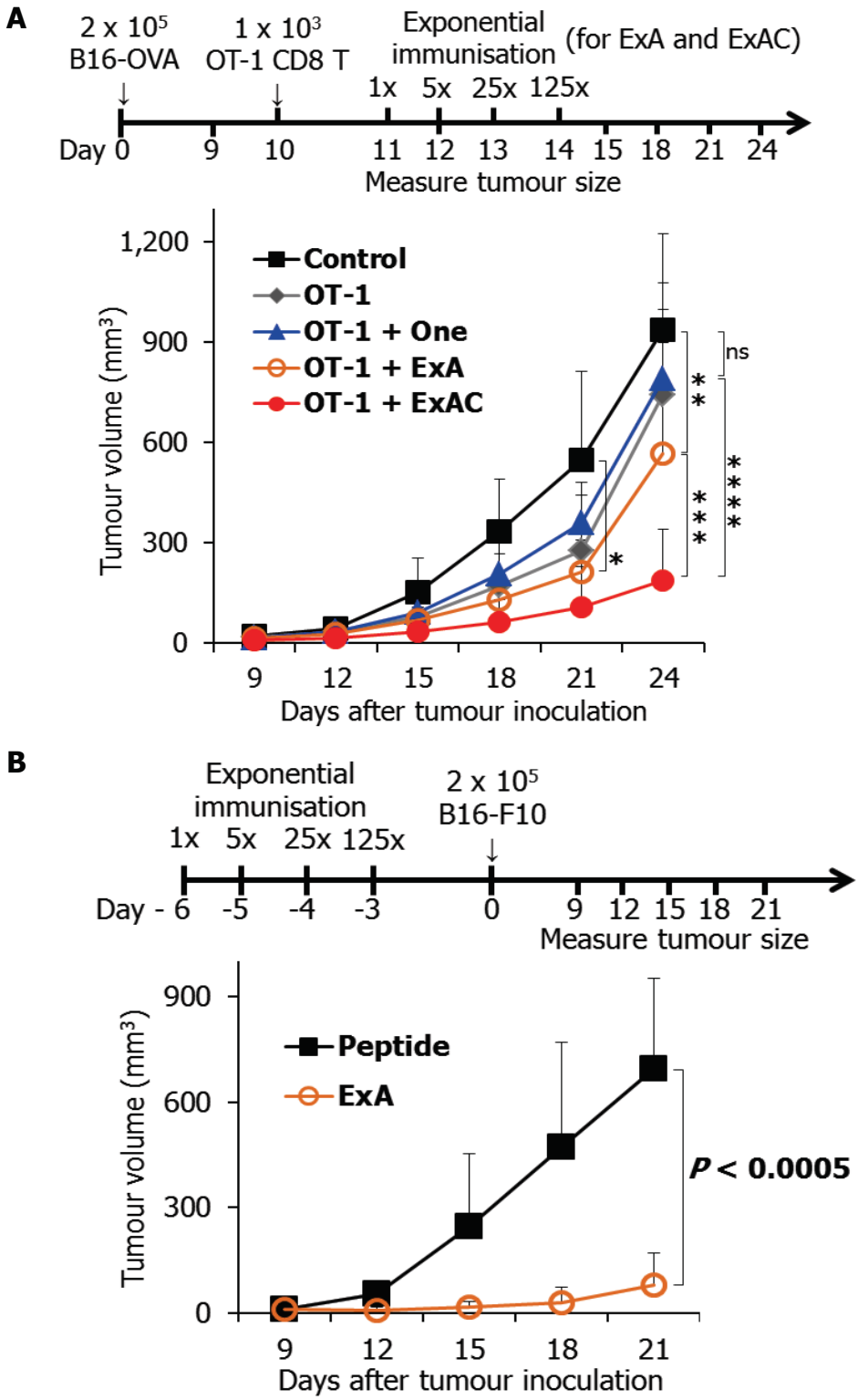

Figure 36 (Continued below)

C

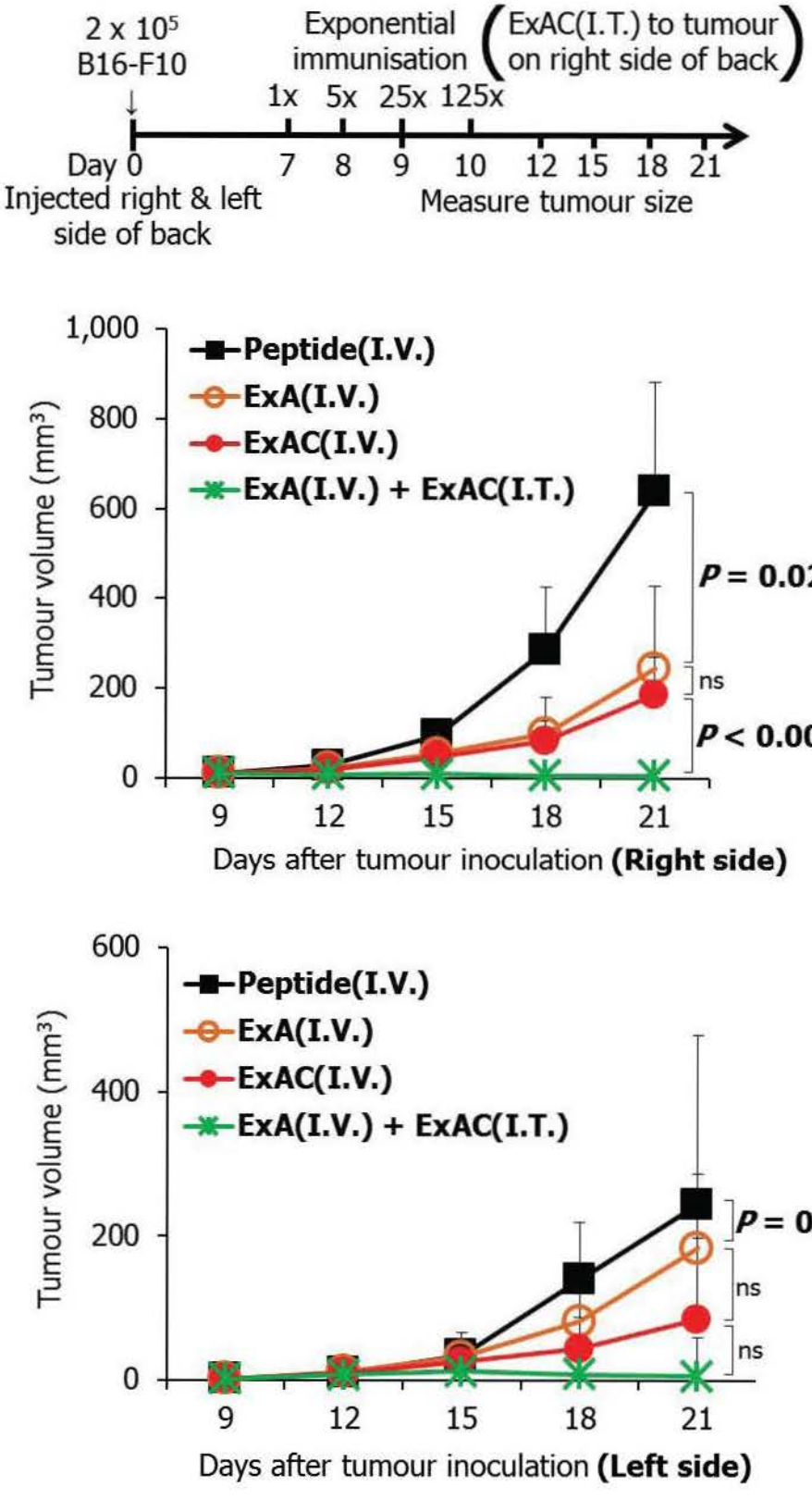

Figure 36 (Continued below)

Figure 36. Anti-tumour effects of nano-vesicles given daily in exponential doses.

A) C57BL/6 mice were injected subcutaneously on the back with 2 x 10^5 B16-OVA tumour cells on day 0. 10 days later, tumour-bearing mice were injected I.V. with 1 x 10^3 OT-1 CD8 T cells. On the following 4 days (day 11 – day 14), these mice were injected with SIINFEKL peptide-pulsed vesicles using the conditions **One**, **ExA** or **ExAC** described in Figure 35. **Control** group received tumour cells only and **OT-1** group received both tumour cells and OT-1 CD8 T cells without vesicles.

B) As shown in the scheme, C57BL/6 mice were injected I.V. in exponential daily doses with a total of 10 nmol TRP-2 peptide alone (**Peptide**) or 10 nmol TRP-2 peptide-pulsed vesicles (total 156 μg) prepared from syngeneic LPS-activated BMDCs; the vesicles were incubated with αCD9 (total 15.6 μg) before injection (**ExA)**. On day 0 (6 days after the first day of immunisation), all mice were injected subcutaneously on the back with 2 x 10^5 B16-F10 tumour cells.

C) C57BL/6 mice were injected subcutaneously on both right and left side of the back with 2 x 10^5 B16-F10 tumour cells on day 0. Starting from day 7, tumour-bearing mice were injected I.V. in exponential daily doses with a total of 10 nmol TRP-2 **peptide** alone or 10 nmol TRP-2 peptide-pulsed **ExA** or **ExAC** (using the same dose of vesicles, αCD9 and CpG as in A). For group **ExA(I.V.) + ExAC(I.T.)**, 10 nmol TRP-2 pulsed 156 μg vesicles were incubated with 15.6 μg αCD9, and then equally divided into two: One half was directly injected I.V. as ExA(I.V.); and another half was further incubated with 80 μg CpG ODN 1668 and then injected into tumour on right side of back of the same mouse.

Tumour sizes were measured with a calliper every 3 days. Tumour volumes were calculated as: π/6 × Length × Width × Height. Tumour growth curves (n = 5) represent mean and SD. The data are from one experiment. **P* < 0.02; ***P* = 0.06; ****P* = 0.03; *****P* = 0.0002; ns, not significant.

3.3.3 Summary and conclusion

Measuring immunogenicity of membrane vesicles *in vivo* showed close similarities with the *in vitro* data but also some interesting differences. As *in vitro,* expression of a high density of co-stimulatory molecules was found to be highly important for the immunogenicity of membrane vesicles *in vivo*. However, in marked contrast to the *in vitro* data, nano-vesicles were far more immunogenic than vesicle-aggregates *in vivo*. Possible reasons for this difference will be mentioned in the General Discussion. After I.V. injection, nano-vesicles were preferentially taken up by $CD11c^+$ DCs residing in the spleen, which resulted in *in situ* activation of antigen-specific CD8 T cells. After activation, CD8 T cells proliferated vigorously in the spleen but some of the proliferating cells left the spleen and migrated to lymph nodes and presumably also to other sites in the body via the bloodstream. When nano-vesicles were injected in a single I.V. dose, delayed injection of T cells showed that immunogenicity of the vesicles declined over a period of a few days, as shown by a decrease in the intensity of donor cell proliferation and effector cell generation. These results imply that CD8 T cells need prolonged antigen presentation for optimal immune responses. Indeed, multiple injections of nano-vesicles considerably increased both the extent of CD8 T cell proliferation and expansion and the differentiation of these cells into effector populations. With regard to further enhancing vesicle immunogenicity, coating vesicles with αCD9 and/or CpG and injecting the vesicles in exponential doses dramatically improved CD8 T cell responses and, importantly, led to strong CTL function in addition to prominent IFNγ synthesis. Effector function applied not only to cytolysis of antigen-specific target cells in an *in vivo* CTL assay but also to retardation or rejection of tumours, in both preventive and therapeutic mouse models.

4 General Discussion

4.1 Research outcome

CD8 T cells are not only important for protecting the host from pathogenic infections, but also play a critical role in the control of malignancy. Blocking negative regulators of CD8 T cell responses and using genetically-engineered T cells are now producing encouraging clinical results which can be further improved by combination with other therapies (Maus et al., 2014; Postow et al., 2015). By inducing tumour antigen-specific immune responses, vaccines are a promising candidate for cancer treatment (Mellman et al., 2011). However, the effects of the currently available cancer vaccines are only limited, including the first US FDA-approved therapeutic DC-based cancer vaccine, Sipuleucel-T, and also DC-derived exosomes. Although the efficacy of these reagents can be improved by modulation of DC maturation and the use of adjuvants (Anguille et al., 2014; Chaput et al., 2004; Viaud et al., 2010), the intrinsic drawbacks associated with the use of live cell-based therapy and the low yields of exosomes limit their application and potential. In this respect, our group has previously proved that, after loading with specific peptide, membrane vesicles prepared from disrupted DC2.4 cells have much higher yields and immunogenicity than exosomes secreted from the same cells (Kovar et al., 2006). Therefore, membrane vesicles obtained from normal DCs could serve as an effective cancer vaccine.

The broad aim of this thesis was to prepare highly immunogenic membrane vesicles in large quantities from natural APCs, namely BMDCs, and use them to stimulate CD8 T cells for cancer immunotherapy. I addressed this objective by optimising BMDC culture conditions to get bulk populations of BMDCs for subsequent use for membrane vesicle preparation. Many factors were examined and optimised to achieve both high yields and strong immunogenicity of membrane vesicles.

In initial experiments, I confirmed the need for costimulatory molecules on

membrane vesicles by studies with transfected *Drosophila* aAPCs expressing MHC I alone or along with B7-1 and ICAM-1 co-stimulatory molecules. These experiments showed that the immunogenicity of aAPCs for naïve CD8 T cells was retained after fixation with paraformaldehyde or, to a more limited extent, even after heat-killing the cells. More importantly, immunogenicity also applied to membrane vesicles from aAPCs, though only when the APCs expressed a high density of costimulatory molecules. These findings, plus the previous work with DC2.4 cells, suggested that immunogenic vesicles could be prepared from normal DCs, with the proviso that these cells could be prepared in large numbers and be fully mature.

To provide bulk populations of mature DCs for membrane vesicle preparation, I devised a new BMDC culture method by modifying several steps in the standard BMDC culture method reported by Inaba et al (Inaba et al., 1992; Inaba et al., 2009). Compared to Inaba's method, the new method increased the yield of mature BMDCs by about 60 fold, leading to a recovery of about 3 x 10^8 mature BMDCs from a single mouse donor. Modifications such as reducing the initial cell density, inclusion of non-adherent cells at early stages of culture and adherent cells at the end of culture were all found critical for the improvement in cell yields. Low-density cell culture was found to be especially important for keeping BMDCs immature and able to proliferate throughout the 10 day culture period. In this respect, it has been reported with spleen cells that culturing immature DCs at a high concentration induces spontaneous maturation of DCs (Vremec et al., 2011) followed by death by apoptosis as the result of down-regulating Bcl-2 (Hou and Van Parijs, 2004). In the new BMDC method, the large number of proliferating immature BMDCs generated in the cultures can be induced to become mature by overnight stimulation with TLR ligands before harvesting the cells. Overall, the new method allows high cell yields with tight control of BMDC maturation. This method has similarities with the protocol of Lutz et al. (Lutz et al., 1999) except that these workers discarded adherent cells at the end of culture; their yields of mature BMDCs were 2-3 fold lower than in the new method described here and the proportion

of cells in their cultures with a mature B7-2^{hi} phenotype was lower, i.e. ~50% compared with ~75% B7-2^{hi} cells and ~75% B7-1^{hi} cells in the current method; note that Lutz et al did not phenotype their cells for B7-1 at the maturation stage.

With regard to IL-4, there are several reports that adding a mixture of GMCSF and IL-4 to BMDC cultures increases DC maturation (Labeur et al., 1999; Lutz et al., 2002; Lutz et al., 2000) and is widely used for generating human DC from peripheral blood monocytes (Nair et al., 2012; Sallusto and Lanzavecchia, 1994). Although this finding was confirmed here, adding IL-4 plus GMCSF throughout culture had the disadvantage of inducing early DC maturation, thereby leading to poor cell yields and cell death. Cell viability was high early in culture (day 6 or 7) but the proportion CD11c^{+} DCs at this stage is low, which often necessitates enrichment of DCs with anti-CD11c magnetic microbeads (Hou and Van Parijs, 2004). By day 10 of culture, however, total cell yields are low and a large proportion of the cells are non-viable. Therefore, adding IL-4 is contraindicated for generating mature DCs in long-term BMDC cultures. Nevertheless, for GMCSF cultures, my preliminary experiments showed that high yields of viable mature DCs were obtained on day 10 when IL-4 was added late in culture, i.e. on day 8, followed by LPS on day 9. Moreover, late addition of IL-4 increased the proportion of mature DCs on day 10 to ~90 % B7-1^{hi} cells and 75% B7-2^{hi} cells. As yet, I have not used IL-4-treated BMDCs to prepare membrane vesicles.

Having succeeded in preparing large number of mature BMDCs from GMCSF-based cultures, I optimised the steps required to prepare membrane vesicles from these cells, modifying the protocol of Kovar et al. (Kovar et al., 2006). These experiments confirmed that, to be immunogenic, the peptide-loaded vesicles had to express a high density of co-stimulatory molecules. Thus, although vesicles from immature BMDC did induce naïve CD8 T cell proliferation, responses were much higher with vesicles from mature BMDC. Likewise, with aAPCs, peptide-pulsed vesicles prepared from aAPCs expressing MHC I alone completely failed to induce naïve CD8 T cell proliferation. Nevertheless, these

vesicles did induce mild CD8 T cell activation, as indicated by low but significant CD69 up-regulation. Such activation may reflect T-T interaction as the result of CD8 T cells binding vesicles via TCRs and then presenting TCR-bound pMHC to neighbouring T cells together with ICAM-1 and possibly also B7-2 (Taylor et al., 2004) on the T cells. This activation was not seen with intact aAPCs expressing MHC I alone, presumably because the large size of intact aAPCs precludes antigen presentation via T-T interaction. Vesicles from dead BMDCs were totally non-immunogenic, presumably reflecting degradation of the stimulatory ligands on these cells (Magner and Tomasi, 2005). Overall, these findings highlighted the importance of co-stimulation in membrane vesicle immunogenicity, which is in line with previous reports with exosomes (Pitt et al., 2014; Segura et al., 2005; Utsugi-Kobukai et al., 2003).

During the process of optimising membrane vesicle preparation, many factors were found to affect both yields and the immunogenicity of vesicles. Surprisingly, some procedures often recommended for effective cell lysis were found detrimental to vesicle immunogenicity. These included homogenizing cells at a high concentration and using a tight-fitting Dounce homogenizer. Under these conditions, vigorous disruption of cells causes the release of proteolytic enzymes that degrade proteins, including those involved in antigen presentation and co-stimulation. In this respect, vesicles prepared with prolonged mild homogenization expressed pan-cadherin (plasma membrane protein) and β-2-microglobulin (an MHC I component), whereas vesicles prepared following strong cell disruption showed little or no expression of pan-cadherin or β-2-microglobulin. Interestingly, these vesicles did express Calnexin (ER protein) and COX IV (mitochondria protein), perhaps because these latter proteins were less sensitive to proteases in the cell lysates (Graham, 2002).

At the end stage of preparing membrane vesicles, I had particular problems in resuspending the pellet after utracentrifugation. Thus, after vigorous pipeting and/or homogenization of the pellet, the resuspended vesicles consisted mostly of large micrometre-sized vesicle-aggregates. Among many approaches tried, sonication of the pellet proved to be a highly effective method for dispersing

the aggregates into nano-vesicles. Freezing-thawing caused the nano-particles to re-aggregate but these could be dispersed by subsequent sonication. An important finding was that, in aggregated form, the vesicles could be analysed for expression of surface markers by conventional flow cytometry (BD FACS Canto II). This approach indicated that the vesicles expressed a high density of the stimulatory molecules present on mature BMDCs, notably MHC I, B7-1, B7-2 and ICAM-1.

It may be noted that the approach of examining markers on aggregated vesicles is much simpler than other published flow cytometry-based methods for nano-vesicle analysis. By conventional flow cytometry, the smallest sized particles that can be measured are about 0.5 μm. Therefore, nano-vesicles such as exosomes need to be first coated on to microbeads to be analysed by flow cytometry (Naslund et al., 2013). More sophisticated flow cytometry machines equipped with small particle detectors (e.g. BD Influx and BD LSR II SORP) can directly detect exosome-sized vesicles. However, because of high sensitivity and "noise" particles present in the buffer, this approach necessitates relatively complicated steps to discriminate fluorescently-labeled vesicles from nonfluorescent noise (van der Vlist et al., 2012).

With regard to immunogenicity, there was a striking difference in the size of the vesicles required to stimulate CD8 T cell responses, depending on whether responses were measured *in vitro* or *in vivo.* Under *in vitro* conditions in the absence of APCs, aggregated vesicles plus specific peptide were strongly stimulatory for naïve 2C and OT-1 CD8 T cells and induced these cells to proliferate and synthesize perforin and granzyme-B. Significantly, such stimulation required that the vesicles expressed a high density of costimulatory molecules. Thus, vesicle aggregates prepared from mature BMDCs were much more immunogenic than vesicles from immature BMDCs. The strong immunogenicity of vesicle aggregates expressing a high density of MHC I and costimulatory molecules presumably reflects presentation of these ligands in cross-linked form, similar to the situation with paraformaldehyde-fixed mature APCs (Figure 5) or contact with a mixture of cross-linked anti-CD28 and anti-

CD3 mAbs in plastic dishes or on large latex beads (Levine et al., 1997). These findings refer to vesicles in the form of large aggregates. However, when vesicle aggregates were dispersed into nano-particles by sonication, these small vesicles were totally nonstimulatory for CD8 T cells *in vitro.* This finding is in line with the observation that the immunogenicity of antigen/mAb expressed on latex beads declines abruptly when the beads are smaller than 3 μm (Luxembourg et al., 1998; Mescher, 1992). Significantly, however, peptide-loaded nano-vesicles did become immunogenic for CD8 T cells *in vitro* with addition of spleen cells as APCs. Under these conditions, the vesicles presumably bind to APCs and are presented to T cells in cross-linked form. In this respect, exosomes are also poorly stimulatory for specific T cells *in vitro* unless exosomes are cross-liked to latex beads or the cultures also contain mature DCs (Thery et al., 2002; Vincent-Schneider et al., 2002). Whether antigen presentation in these situations involves formation of an immunological synapse between T cells and APCs is unclear (Grakoui et al., 1999).

In marked contrast to culture *in vitro*, aggregated vesicles displayed only limited immunogenicity when injected I.V. into mice. This finding probably reflects that, after injection, the aggregates became trapped in capilliary networks in the lung and liver (Kutscher et al., 2010), resulting in only limited localization of the vesicles in spleen. In sharp contrast, injection of the vesicles in the form of nano-particles led to conspicuous stimulation of CD8 T cells in the spleen, presumably because their small size allowed these vesicles to pass through the capiliary network of the lung. Based on the *in vitro* studies, the strong immunogenicity of the nano-vesicles *in vivo* is likely to reflect uptake of the vesicles by host APCs. Although definitive data on this issue are not yet available, examining spleen sections soon after vesicle injection indicated that the vesicles lodged initially in the marginal zone of the spleen. At 3 hours after injection of PKH26-labelled vesicles, flow cytometry showed that in spleen the vesicles were associated almost entirely with $CD11c^+$ cells, presumably DCs. Although the localization of these cells was not established, the data support a model where the vesicles were initially taken up in the marginal zone by

immature DCs which then migrated to the PALS for presentation to T cells. Further studies will be needed assess this model. Why the vesicles bound selectively to $CD11c^+$ cells is unclear. For exosomes, their uptake after injection is much higher on $CD8\alpha^+$ DCs than $CD8\alpha^-$ DCs and correlates with higher expression of LFA-1 on the $CD8\alpha^+$ subset, implying that exosomes may bind to DCs largely through LFA-1/ICAM-1 interaction (Segura et al., 2007). Whether this scenario applies to nano-vesicles will require future investigation.

Since nano-vesicles were immunogenic *in vivo* without injection of adjuvant, the DCs presenting bound vesicles in the T cell zones of the spleen were presumably non-activated and therefore expressed only a low density of costimulatory molecules. Hence, for T cell stimulation, costimulation would have to be provided largely by the vesicles themselves rather than by the host DCs. In direct support of this prediction, peptide-loaded nano-vesicles prepared from mature BMDCs were much more immunogenic *in vivo* than those from immature BMDCs. These data thus correlated closely with the *in vitro* findings. Future studies with host mice lacking costimulatory molecules would address whether costimulation by host APCs plays any role in stimulation by APC-bound vesicles.

Based on studies in which vesicles were injected at various times before T cells, the vesicles remained immunogenic for several days after injection. This finding is surprising because one might expect the bound vesicles to be rapidly degraded and/or internalized. It remains possible, however, that after internalization the stimulatory components on the vesicles are recycled to the cell surface, as has been reported previously for pMHC on exosomes (Montecalvo et al., 2008). This issue could be addressed by examining the fate of vesicles binding to DCs *in vitro.*

Since nano-vesicles lodged only in spleen and not LNs after I.V. injection, the immune response of CD8 T cells presumably began largely in the spleen and then led to migration of proliferating T cells to other sites, including LNs. With injection of vesicles in a single dose, proliferation and expansion of the responding CD8 T cells continued for 3 days and then declined. The

proliferating CD8 T cells displayed prominent IFNγ synthesis, though only with injection of a high dose of vesicles. The surprising finding was that by day 14 after injection the responding T cells had almost entirely disappeared from both spleen and LNs, even after vesicle injection at a high dose. This finding contrasts with typical immune responses of CD8 T cells where ~5 - 10% of the responding cells survive to form long-lived memory cells (Williams and Bevan, 2007). Why immunization with vesicles failed to induce memory cell generation is unclear. One possibility is that, despite the high density of costimulatory molecules on the vesicles, overall exposure of the responding cells to costimulation was insufficient for memory cell generation. However, in addition to costimulation, it is known that effective generation of CD8 T memory cells requires exposure to proinflammatory cytokines, namely IL-12 or type I IFN (Arens and Schoenberger, 2010; Xiao et al., 2009). Hence the inability of vesicle injection to lead to memory generation might reflect that the vesicles failed to cause DC activation. This model would explain why prominent memory generation occurred when the injected vesicles were coated with a known activator of DCs, namely CpG (see below).

Various approaches were tried to improve the immunogenicity of the vesicles. As mentioned earlier, Johansen et al. showed that injecting peptide and CpG ODN in exponentially increasing doses significantly improved effector CD8 T cell expansion (Johansen et al., 2008). In my hands, vesicles were clearly more immunogenic when given in multiple doses rather than in a single high dose. Also, exponential doses were more effective than equal doses. Nevertheless, far stronger proliferative responses and more prominent generation of effector cells occurred when the vesicles were coated with CpG and/or αCD9. As mentioned above, CpG is known to improve APC function by activating these cells, leading to increased expression of costimulatory molecules and synthesis of pro-inflammatory cytokines. Coating the vesicles with αCD9 may work in the same way. Thus, it has been shown that, during infection, antibody-coated pathogens can undergo Fc-dependent internalization by phagocytes and induce activation of these cells via TRIM21 (McEwan et al.,

2013). Whether αCD9 augments vesicle immunogenicity via Fc binding to APCs has yet to be tested directly. Nevertheless, in preliminary experiments it is of interest that the results observed with αCD9 were also seen with mAbs specific for other markers on the vesicles, namely CD47 and PD-L1 (data not shown).

Future studies may show that membrane vesicles coated with CpG, αCD9 or other stimulants can be used as vaccines against infectious agents. Thus, in size, expression of repetitive surface epitopes and PAMPS, the coated membrane vesicles described here show close similarities with viruses and virus-like particles (Bachmann and Jennings, 2010). As discussed below, however, these vesicles may be especially useful for cancer immunotherapy.

Although my data on cancer immunotherapy are still preliminary, it is encouraging that, in mice with B16-OVA tumours, I.V. injection of OVA peptide-loaded vesicles coated with aCD9 and CpG considerably enhanced retardation of tumour growth by OT-1 CD8 T cells, despite injecting these cells in only very low doses (1 x 10^3/mouse). The results were even more striking in a non-transgenic model involving growth of highly-malignant B16-F10 tumour cells. Here, I.V. injection of vesicles loaded with aCD9, CpG and TRP-2 peptide considerably slowed tumour growth, presumably through stimulation of endogenous tumour-reactive CD8 T cells. Interestingly, the anti-tumour response was most prominent when the loaded vesicles were injected both I.V. and into the tumour itself. In this situation, tumour rejection or stabilization of tumour growth applied not only to the injected tumour but also to the uninjected contralateral tumour. This finding is in agreement with reports that tumour rejection in mice can be enhanced by intra-tumour injection of CpG (Shirota et al., 2012; Zoglmeier et al., 2011); such injection overcomes inhibition by myeloid suppressor cells.

Though preliminary, these data suggest that injection of peptide-loaded vesicles from mature BMDCs could be useful for clinical cancer immunotherapy, and might be preferable to injection of exosomes. As mentioned earlier, the results of clinical trials with exosomes have been disappointing, perhaps because these trials have involved exosomes prepared from immature DCs;

hence, these exosomes presumably expressed only a low density of costimulatory molecules (Viaud et al., 2010). Also, even with mature DCs in mice, prior studies with DC2.4 cells showed that, at least *in vitro*, exosomes shed by these cells were much less immunogenic than membrane vesicles prepared from the cells (Kovar et al. 2006). Therefore, especially when loaded with APC-activating agents such as aCD9 and CpG, membrane vesicles from mature BMDCs might be much better cancer therapeutic mediators than exosomes. However, evaluating this approach will first require extensive additional studies in mice.

4.2 Future directions

The results described in this thesis raise a number of questions which need to be addressed in future experiments.

BMDC culture. Although the new method described here for generating mature BMDCs gave high cell yields, the cells eventually stopped growing presumably due to overcrowding of the cultures. Hence, even higher cells yields might be obtained if the initial cell density in the cultures was decreased even further. If this were successful, it may be possible to apply my method to obtaining large numbers of DCs from precursor cells in blood, including human blood, and use these cells to prepare membrane vesicles for clinical studies. It will also be important to further investigate the capacity of IL-4 to induce DC maturation when added late in culture. In particular, I will test whether the immunogenicity of membrane vesicles from BMDCs can be improved by maturing these cells with a mixture of IL-4 and LPS. This has yet to be studied.

Fate of membrane vesicles. Despite the evidence that membrane vesicles are taken up largely by $CD11c^+$ cells *in vivo*, it will be important to obtain detailed information on which particular cells bind the vesicles, including defined subsets of DCs and also macrophages and B cells. These studies may shed light on whether transport of I.V.-injected vesicles from the marginal zone of the spleen to the PALS reflects direct transport by DCs or some form of cell-cell transfer of antigen (Liu et al., 2007; Martinez-Pomares and Gordon, 2012;

Naslund et al., 2013). A related question is how the vesicles remain in immunogenic form for several days *in vivo* after injection. Initially, this question will be addressed by following the fate of fluorochrome-labelled vesicles after binding to spleen cell suspensions *in vitro*. It should be noted that all of my data involved I.V. injection of vesicles. I also plan to study whether injection of vesicles subcutaneously leads to vesicle localization and T cell stimulation in the draining LNs.

Further improvements to the immunogenicity of membrane vesicles. Although the vesicles were much more immunogenic when coated with CpG and/or mAbs specific for CD9 and other markers on the vesicles, namely CD47 and PD-L1, further experiments are needed to establish the mechanisms involved in the adjuvant effect of these agents. In view of the encouraging clinical results observed with the use of αPD-L1 in cancer immunotherapy, it will be of interest to further examine the effect of coating vesicles with αPD-L1, especially in anti-tumour models. Since DCs expressing high level of FcRs (Guilliams et al., 2014), DC-derived vesicles could also be coated with immunostimulatory mAbs (e.g. αCTLA-4, αPD-1, α4-1BB, αCD40) by the interaction of Fc and FcRs. These studies can be extended to various tumour models, and combined with injection of IL-2/mAb complexes to further augment CD8 T cell expansion (Boyman et al., 2006). Here, it will be especially important to determine whether the vesicles can be used to treat tumours that metastasise to the lungs and other sites. In the case of coating vesicles with CpG, my studies involved CpG ODN 1668, which is known to stimulate several cell types, especially B cells (Heit et al., 2004; Krieg et al., 1995). This could explain the splenomegaly and lower than expected CD8 T cell recoveries found at day 6 in the recipients of CpG-coated vesicles. Studies with other CpG ODNs (Marshall et al., 2005) might resolve this problem and induce more potent antigen-specific CD8 T cell responses.

5 References

Andre, F.E., Booy, R., Bock, H.L., Clemens, J., Datta, S.K., John, T.J., Lee, B.W., Lolekha, S., Peltola, H., Ruff, T.A.*, et al.* (2008). Vaccination greatly reduces disease, disability, death and inequity worldwide. Bulletin of the World Health Organization *86*, 140-146.

Andreola, G., Rivoltini, L., Castelli, C., Huber, V., Perego, P., Deho, P., Squarcina, P., Accornero, P., Lozupone, F., Lugini, L.*, et al.* (2002). Induction of lymphocyte apoptosis by tumor cell secretion of FasL-bearing microvesicles. J Exp Med *195*, 1303-1316.

Anguille, S., Smits, E.L., Lion, E., van Tendeloo, V.F., and Berneman, Z.N. (2014). Clinical use of dendritic cells for cancer therapy. The Lancet. Oncology *15*, e257-267.

Aoshi, T., Zinselmeyer, B.H., Konjufca, V., Lynch, J.N., Zhang, X., Koide, Y., and Miller, M.J. (2008). Bacterial entry to the splenic white pulp initiates antigen presentation to CD8+ T cells. Immunity *29*, 476-486.

Appay, V., Douek, D.C., and Price, D.A. (2008). CD8+ T cell efficacy in vaccination and disease. Nat Med *14*, 623-628.

Arens, R., and Schoenberger, S.P. (2010). Plasticity in programming of effector and memory CD8 T-cell formation. Immunol Rev *235*, 190-205.

Bachmann, M.F., Beerli, R.R., Agnellini, P., Wolint, P., Schwarz, K., and Oxenius, A. (2006). Long-lived memory CD8+ T cells are programmed by prolonged antigen exposure and low levels of cellular activation. Eur J Immunol *36*, 842-854.

Bachmann, M.F., and Jennings, G.T. (2010). Vaccine delivery: a matter of size, geometry, kinetics and molecular patterns. Nat Rev Immunol *10*, 787-796.

Baitsch, L., Fuertes-Marraco, S.A., Legat, A., Meyer, C., and Speiser, D.E. (2012). The three main stumbling blocks for anticancer T cells. Trends in immunology *33*, 364-372.

Baumgaertner, P., Jandus, C., Rivals, J.P., Derre, L., Lovgren, T., Baitsch, L., Guillaume, P., Luescher, I.F., Berthod, G., Matter, M.*, et al.* (2012). Vaccination-

induced functional competence of circulating human tumor-specific CD8 T-cells. Int J Cancer *130*, 2607-2617.

Behm, C.A., and Ovington, K.S. (2000). The role of eosinophils in parasitic helminth infections: insights from genetically modified mice. Parasitol Today *16*, 202-209.

Belz, G.T., and Nutt, S.L. (2012). Transcriptional programming of the dendritic cell network. Nat Rev Immunol *12*, 101-113.

Belz, G.T., Smith, C.M., Eichner, D., Shortman, K., Karupiah, G., Carbone, F.R., and Heath, W.R. (2004). Cutting edge: conventional CD8 alpha+ dendritic cells are generally involved in priming CTL immunity to viruses. J Immunol *172*, 1996-2000.

Blander, J.M., and Medzhitov, R. (2006). Toll-dependent selection of microbial antigens for presentation by dendritic cells. Nature *440*, 808-812.

Blander, J.M., and Sander, L.E. (2012). Beyond pattern recognition: five immune checkpoints for scaling the microbial threat. Nat Rev Immunol *12*, 215-225.

Blum, J.S., Wearsch, P.A., and Cresswell, P. (2013). Pathways of antigen processing. Annu Rev Immunol *31*, 443-473.

Bonilla, F.A., and Oettgen, H.C. (2010). Adaptive immunity. J Allergy Clin Immunol *125*, S33-40.

Bourquin, C., Anz, D., Zwiorek, K., Lanz, A.L., Fuchs, S., Weigel, S., Wurzenberger, C., von der Borch, P., Golic, M., Moder, S.*, et al.* (2008). Targeting CpG oligonucleotides to the lymph node by nanoparticles elicits efficient antitumoral immunity. J Immunol *181*, 2990-2998.

Boyman, O., Kovar, M., Rubinstein, M.P., Surh, C.D., and Sprent, J. (2006). Selective stimulation of T cell subsets with antibody-cytokine immune complexes. Science *311*, 1924-1927.

Boyman, O., and Sprent, J. (2012). The role of interleukin-2 during homeostasis and activation of the immune system. Nat Rev Immunol *12*, 180-190.

Bromley, S.K., Thomas, S.Y., and Luster, A.D. (2005). Chemokine receptor CCR7 guides T cell exit from peripheral tissues and entry into afferent lymphatics. Nat Immunol *6*, 895-901.

Cai, Z., Brunmark, A., Jackson, M.R., Loh, D., Peterson, P.A., and Sprent, J. (1996). Transfected Drosophila cells as a probe for defining the minimal requirements for stimulating unprimed CD8+ T cells. Proc Natl Acad Sci U S A *93*, 14736-14741.

Cai, Z., Kishimoto, H., Brunmark, A., Jackson, M.R., Peterson, P.A., and Sprent, J. (1997a). Requirements for peptide-induced T cell receptor downregulation on naive CD8+ T cells. J Exp Med *185*, 641-651.

Cai, Z., Kishimoto, H., Brunmark, A., Jackson, M.R., Peterson, P.A., and Sprent, J. (1997b). Requirements for peptide-induced T cell receptor downregulation on naive CD8+ T cells. J Exp Med *185*, 641-651.

Chaplin, D.D. (2006). 1. Overview of the human immune response. J Allergy Clin Immunol *117*, S430-435.

Chaplin, D.D. (2010). Overview of the immune response. J Allergy Clin Immunol *125*, S3-23.

Chaput, N., Schartz, N.E., Andre, F., Taieb, J., Novault, S., Bonnaventure, P., Aubert, N., Bernard, J., Lemonnier, F., Merad, M.*, et al.* (2004). Exosomes as potent cell-free peptide-based vaccine. II. Exosomes in CpG adjuvants efficiently prime naive Tc1 lymphocytes leading to tumor rejection. J Immunol *172*, 2137-2146.

Cho, J.H., Kim, H.O., Kim, K.S., Yang, D.H., Surh, C.D., and Sprent, J. (2013). Unique features of naive CD8+ T cell activation by IL-2. J Immunol *191*, 5559-5573.

Clayton, A., Mitchell, J.P., Court, J., Mason, M.D., and Tabi, Z. (2007). Human tumor-derived exosomes selectively impair lymphocyte responses to interleukin-2. Cancer Res *67*, 7458-7466.

Coffman, R.L., Sher, A., and Seder, R.A. (2010). Vaccine adjuvants: putting innate immunity to work. Immunity *33*, 492-503.

Curtsinger, J.M., Johnson, C.M., and Mescher, M.F. (2003a). CD8 T cell clonal expansion and development of effector function require prolonged exposure to antigen, costimulation, and signal 3 cytokine. J Immunol *171*, 5165-5171.

Curtsinger, J.M., Lins, D.C., and Mescher, M.F. (2003b). Signal 3 determines

tolerance versus full activation of naive CD8 T cells: dissociating proliferation and development of effector function. J Exp Med *197*, 1141-1151.

de Saint Basile, G., Menasche, G., and Fischer, A. (2010). Molecular mechanisms of biogenesis and exocytosis of cytotoxic granules. Nat Rev Immunol *10*, 568-579.

den Haan, J.M., and Bevan, M.J. (2002). Constitutive versus activation-dependent cross-presentation of immune complexes by CD8(+) and CD8(-) dendritic cells in vivo. J Exp Med *196*, 817-827.

Di Bonito, P., Grasso, F., Mochi, S., Petrone, L., Fanales-Belasio, E., Mei, A., Cesolini, A., Laconi, G., Conrad, H., Bernhard, H.*, et al.* (2009). Anti-tumor CD8+ T cell immunity elicited by HIV-1-based virus-like particles incorporating HPV-16 E7 protein. Virology *395*, 45-55.

Dominguez-Villar, M., Baecher-Allan, C.M., and Hafler, D.A. (2011). Identification of T helper type 1-like, Foxp3+ regulatory T cells in human autoimmune disease. Nat Med *17*, 673-675.

Dunn, G.P., Old, L.J., and Schreiber, R.D. (2004). The immunobiology of cancer immunosurveillance and immunoediting. Immunity *21*, 137-148.

Dustin, M.L. (2014). The Immunological Synapse. Cancer immunology research *2*, 1023-1033.

Eggermont, L.J., Paulis, L.E., Tel, J., and Figdor, C.G. (2014). Towards efficient cancer immunotherapy: advances in developing artificial antigen-presenting cells. Trends in biotechnology *32*, 456-465.

Fifis, T., Gamvrellis, A., Crimeen-Irwin, B., Pietersz, G.A., Li, J., Mottram, P.L., McKenzie, I.F., and Plebanski, M. (2004). Size-dependent immunogenicity: therapeutic and protective properties of nano-vaccines against tumors. J Immunol *173*, 3148-3154.

Fridman, W.H., Pages, F., Sautes-Fridman, C., and Galon, J. (2012). The immune contexture in human tumours: impact on clinical outcome. Nat Rev Cancer *12*, 298-306.

Fujii, S., Liu, K., Smith, C., Bonito, A.J., and Steinman, R.M. (2004). The linkage of innate to adaptive immunity via maturing dendritic cells in vivo requires CD40

ligation in addition to antigen presentation and CD80/86 costimulation. J Exp Med *199*, 1607-1618.

Fujii, S., Shimizu, K., Smith, C., Bonifaz, L., and Steinman, R.M. (2003). Activation of natural killer T cells by alpha-galactosylceramide rapidly induces the full maturation of dendritic cells in vivo and thereby acts as an adjuvant for combined CD4 and CD8 T cell immunity to a coadministered protein. J Exp Med *198*, 267-279.

Futreal, P.A., Coin, L., Marshall, M., Down, T., Hubbard, T., Wooster, R., Rahman, N., and Stratton, M.R. (2004). A census of human cancer genes. Nat Rev Cancer *4*, 177-183.

Galon, J., Costes, A., Sanchez-Cabo, F., Kirilovsky, A., Mlecnik, B., Lagorce-Pages, C., Tosolini, M., Camus, M., Berger, A., Wind, P.*, et al.* (2006). Type, density, and location of immune cells within human colorectal tumors predict clinical outcome. Science *313*, 1960-1964.

Gastpar, R., Gehrmann, M., Bausero, M.A., Asea, A., Gross, C., Schroeder, J.A., and Multhoff, G. (2005). Heat shock protein 70 surface-positive tumor exosomes stimulate migratory and cytolytic activity of natural killer cells. Cancer Res *65*, 5238-5247.

Gehrmann, U., Naslund, T.I., Hiltbrunner, S., Larssen, P., and Gabrielsson, S. (2014). Harnessing the exosome-induced immune response for cancer immunotherapy. Semin Cancer Biol *28*, 58-67.

Germain, R.N. (2002). T-cell development and the CD4-CD8 lineage decision. Nat Rev Immunol *2*, 309-322.

Goronzy, J.J., and Weyand, C.M. (2013). Understanding immunosenescence to improve responses to vaccines. Nat Immunol *14*, 428-436.

Graham, J.M. (2002). Homogenization of mammalian cultured cells. ScientificWorldJournal *2*, 1630-1633.

Grakoui, A., Bromley, S.K., Sumen, C., Davis, M.M., Shaw, A.S., Allen, P.M., and Dustin, M.L. (1999). The immunological synapse: a molecular machine controlling T cell activation. Science *285*, 221-227.

Greenwald, R.J., Freeman, G.J., and Sharpe, A.H. (2005). The B7 family

revisited. Annu Rev Immunol *23*, 515-548.

Guilliams, M., Bruhns, P., Saeys, Y., Hammad, H., and Lambrecht, B.N. (2014). The function of Fcgamma receptors in dendritic cells and macrophages. Nat Rev Immunol *14*, 94-108.

Hammer, G.E., and Ma, A. (2013). Molecular control of steady-state dendritic cell maturation and immune homeostasis. Annu Rev Immunol *31*, 743-791.

Hao, S., Bai, O., Yuan, J., Qureshi, M., and Xiang, J. (2006). Dendritic cell-derived exosomes stimulate stronger CD8+ CTL responses and antitumor immunity than tumor cell-derived exosomes. Cell Mol Immunol *3*, 205-211.

Harding, C.V., and Song, R. (1994). Phagocytic processing of exogenous particulate antigens by macrophages for presentation by class I MHC molecules. J Immunol *153*, 4925-4933.

Heit, A., Huster, K.M., Schmitz, F., Schiemann, M., Busch, D.H., and Wagner, H. (2004). CpG-DNA aided cross-priming by cross-presenting B cells. J Immunol *172*, 1501-1507.

Hou, W.S., and Van Parijs, L. (2004). A Bcl-2-dependent molecular timer regulates the lifespan and immunogenicity of dendritic cells. Nat Immunol *5*, 583-589.

Hsu, C.J., Hsieh, W.T., Waldman, A., Clarke, F., Huseby, E.S., Burkhardt, J.K., and Baumgart, T. (2012). Ligand mobility modulates immunological synapse formation and T cell activation. PloS one *7*, e32398.

Huang, J.F., Yang, Y., Sepulveda, H., Shi, W., Hwang, I., Peterson, P.A., Jackson, M.R., Sprent, J., and Cai, Z. (1999). TCR-Mediated internalization of peptide-MHC complexes acquired by T cells. Science *286*, 952-954.

Huber, M.L., Haynes, L., Parker, C., and Iversen, P. (2012). Interdisciplinary critique of sipuleucel-T as immunotherapy in castration-resistant prostate cancer. J Natl Cancer Inst *104*, 273-279.

Huppa, J.B., and Davis, M.M. (2003). T-cell-antigen recognition and the immunological synapse. Nat Rev Immunol *3*, 973-983.

Hwang, I., Huang, J.F., Kishimoto, H., Brunmark, A., Peterson, P.A., Jackson, M.R., Surh, C.D., Cai, Z., and Sprent, J. (2000). T cells can use either T cell

receptor or CD28 receptors to absorb and internalize cell surface molecules derived from antigen-presenting cells. J Exp Med *191*, 1137-1148.

Hwang, I., Shen, X., and Sprent, J. (2003). Direct stimulation of naive T cells by membrane vesicles from antigen-presenting cells: distinct roles for CD54 and B7 molecules. Proc Natl Acad Sci U S A *100*, 6670-6675.

Inaba, K., Inaba, M., Romani, N., Aya, H., Deguchi, M., Ikehara, S., Muramatsu, S., and Steinman, R.M. (1992). Generation of large numbers of dendritic cells from mouse bone marrow cultures supplemented with granulocyte/macrophage colony-stimulating factor. J Exp Med *176*, 1693-1702.

Inaba, K., Swiggard, W.J., Steinman, R.M., Romani, N., Schuler, G., and Brinster, C. (2009). Isolation of dendritic cells. Curr Protoc Immunol *Chapter 3*, Unit 3 7.

Irvine, D.J., and Doh, J. (2007). Synthetic surfaces as artificial antigen presenting cells in the study of T cell receptor triggering and immunological synapse formation. Semin Immunol *19*, 245-254.

Irvine, D.J., Swartz, M.A., and Szeto, G.L. (2013). Engineering synthetic vaccines using cues from natural immunity. Nature materials *12*, 978-990.

Jenkins, M.K., Pardoll, D.M., Mizuguchi, J., Chused, T.M., and Schwartz, R.H. (1987). Molecular events in the induction of a nonresponsive state in interleukin 2-producing helper T-lymphocyte clones. Proc Natl Acad Sci U S A *84*, 5409-5413.

Jennings, G.T., and Bachmann, M.F. (2007). Designing recombinant vaccines with viral properties: a rational approach to more effective vaccines. Current molecular medicine *7*, 143-155.

Johansen, P., Storni, T., Rettig, L., Qiu, Z., Der-Sarkissian, A., Smith, K.A., Manolova, V., Lang, K.S., Senti, G., Mullhaupt, B.*, et al.* (2008). Antigen kinetics determines immune reactivity. Proc Natl Acad Sci U S A *105*, 5189-5194.

Josefowicz, S.Z., Lu, L.F., and Rudensky, A.Y. (2012). Regulatory T cells: mechanisms of differentiation and function. Annu Rev Immunol *30*, 531-564.

Josien, R., Li, H.L., Ingulli, E., Sarma, S., Wong, B.R., Vologodskaia, M., Steinman, R.M., and Choi, Y. (2000). TRANCE, a tumor necrosis factor family member, enhances the longevity and adjuvant properties of dendritic cells in

vivo. J Exp Med *191*, 495-502.

Jung, S., Unutmaz, D., Wong, P., Sano, G., De los Santos, K., Sparwasser, T., Wu, S., Vuthoori, S., Ko, K., Zavala, F.*, et al.* (2002). In vivo depletion of CD11c+ dendritic cells abrogates priming of CD8+ T cells by exogenous cell-associated antigens. Immunity *17*, 211-220.

Kaech, S.M., and Cui, W. (2012). Transcriptional control of effector and memory CD8+ T cell differentiation. Nat Rev Immunol *12*, 749-761.

Kaech, S.M., Tan, J.T., Wherry, E.J., Konieczny, B.T., Surh, C.D., and Ahmed, R. (2003). Selective expression of the interleukin 7 receptor identifies effector CD8 T cells that give rise to long-lived memory cells. Nat Immunol *4*, 1191-1198.

Kaisho, T., and Akira, S. (2006). Toll-like receptor function and signaling. J Allergy Clin Immunol *117*, 979-987; quiz 988.

Karre, K., Ljunggren, H.G., Piontek, G., and Kiessling, R. (1986). Selective rejection of H-2-deficient lymphoma variants suggests alternative immune defence strategy. Nature *319*, 675-678.

Kim, J.H., Kang, T.H., Noh, K.H., Bae, H.C., Kim, S.H., Yoo, Y.D., Seong, S.Y., and Kim, T.W. (2009). Enhancement of dendritic cell-based vaccine potency by anti-apoptotic siRNAs targeting key pro-apoptotic proteins in cytotoxic CD8(+) T cell-mediated cell death. Immunol Lett *122*, 58-67.

Koch, U., and Radtke, F. (2011). Mechanisms of T cell development and transformation. Annual review of cell and developmental biology *27*, 539-562.

Kourtis, I.C., Hirosue, S., de Titta, A., Kontos, S., Stegmann, T., Hubbell, J.A., and Swartz, M.A. (2013). Peripherally administered nanoparticles target monocytic myeloid cells, secondary lymphoid organs and tumors in mice. PloS one *8*, e61646.

Kovacsovics-Bankowski, M., Clark, K., Benacerraf, B., and Rock, K.L. (1993). Efficient major histocompatibility complex class I presentation of exogenous antigen upon phagocytosis by macrophages. Proc Natl Acad Sci U S A *90*, 4942-4946.

Kovacsovics-Bankowski, M., and Rock, K.L. (1995). A phagosome-to-cytosol pathway for exogenous antigens presented on MHC class I molecules. Science

267, 243-246.

Kovar, M., Boyman, O., Shen, X., Hwang, I., Kohler, R., and Sprent, J. (2006). Direct stimulation of T cells by membrane vesicles from antigen-presenting cells. Proc Natl Acad Sci U S A *103*, 11671-11676.

Krieg, A.M., Yi, A.K., Matson, S., Waldschmidt, T.J., Bishop, G.A., Teasdale, R., Koretzky, G.A., and Klinman, D.M. (1995). CpG motifs in bacterial DNA trigger direct B-cell activation. Nature *374*, 546-549.

Kurts, C., Robinson, B.W., and Knolle, P.A. (2010). Cross-priming in health and disease. Nat Rev Immunol *10*, 403-414.

Kushnir, N., Streatfield, S.J., and Yusibov, V. (2012). Virus-like particles as a highly efficient vaccine platform: diversity of targets and production systems and advances in clinical development. Vaccine *31*, 58-83.

Kushwah, R., and Hu, J. (2010). Dendritic cell apoptosis: regulation of tolerance versus immunity. J Immunol *185*, 795-802.

Kutscher, H.L., Chao, P., Deshmukh, M., Singh, Y., Hu, P., Joseph, L.B., Reimer, D.C., Stein, S., Laskin, D.L., and Sinko, P.J. (2010). Threshold size for optimal passive pulmonary targeting and retention of rigid microparticles in rats. Journal of controlled release : official journal of the Controlled Release Society *143*, 31-37.

Labeur, M.S., Roters, B., Pers, B., Mehling, A., Luger, T.A., Schwarz, T., and Grabbe, S. (1999). Generation of tumor immunity by bone marrow-derived dendritic cells correlates with dendritic cell maturation stage. J Immunol *162*, 168-175.

Lahoud, M.H., Ahmet, F., Zhang, J.G., Meuter, S., Policheni, A.N., Kitsoulis, S., Lee, C.N., O'Keeffe, M., Sullivan, L.C., Brooks, A.G.*, et al.* (2012). DEC-205 is a cell surface receptor for CpG oligonucleotides. Proc Natl Acad Sci U S A *109*, 16270-16275.

Lanier, L.L. (2013). Shades of grey--the blurring view of innate and adaptive immunity. Nat Rev Immunol *13*, 73-74.

Levine, B.L., Bernstein, W.B., Connors, M., Craighead, N., Lindsten, T., Thompson, C.B., and June, C.H. (1997). Effects of CD28 costimulation on long-

term proliferation of CD4+ T cells in the absence of exogenous feeder cells. J Immunol *159*, 5921-5930.

Li, G.B., and Lu, G.X. (2010). Adherent cells in granulocyte-macrophage colony-stimulating factor-induced bone marrow-derived dendritic cell culture system are qualified dendritic cells. Cell Immunol *264*, 4-6.

Liu, C., Yu, S., Zinn, K., Wang, J., Zhang, L., Jia, Y., Kappes, J.C., Barnes, S., Kimberly, R.P., Grizzle, W.E., and Zhang, H.G. (2006). Murine mammary carcinoma exosomes promote tumor growth by suppression of NK cell function. J Immunol *176*, 1375-1385.

Liu, K., Waskow, C., Liu, X., Yao, K., Hoh, J., and Nussenzweig, M. (2007). Origin of dendritic cells in peripheral lymphoid organs of mice. Nat Immunol *8*, 578-583.

Lou, Y., Liu, C., Lizee, G., Peng, W., Xu, C., Ye, Y., Rabinovich, B.A., Hailemichael, Y., Gelbard, A., Zhou, D.*, et al.* (2011). Antitumor activity mediated by CpG: the route of administration is critical. J Immunother *34*, 279-288.

Lutz, M.B., Kukutsch, N., Ogilvie, A.L., Rossner, S., Koch, F., Romani, N., and Schuler, G. (1999). An advanced culture method for generating large quantities of highly pure dendritic cells from mouse bone marrow. Journal of immunological methods *223*, 77-92.

Lutz, M.B., and Rossner, S. (2007). Factors influencing the generation of murine dendritic cells from bone marrow: the special role of fetal calf serum. Immunobiology *212*, 855-862.

Lutz, M.B., Schnare, M., Menges, M., Rossner, S., Rollinghoff, M., Schuler, G., and Gessner, A. (2002). Differential functions of IL-4 receptor types I and II for dendritic cell maturation and IL-12 production and their dependency on GM-CSF. J Immunol *169*, 3574-3580.

Lutz, M.B., Suri, R.M., Niimi, M., Ogilvie, A.L., Kukutsch, N.A., Rossner, S., Schuler, G., and Austyn, J.M. (2000). Immature dendritic cells generated with low doses of GM-CSF in the absence of IL-4 are maturation resistant and prolong allograft survival in vivo. Eur J Immunol *30*, 1813-1822.

Luxembourg, A.T., Brunmark, A., Kong, Y., Jackson, M.R., Peterson, P.A., Sprent,

J., and Cai, Z. (1998). Requirements for stimulating naive CD8+ T cells via signal 1 alone. J Immunol *161*, 5226-5235.

Magner, W.J., and Tomasi, T.B. (2005). Apoptotic and necrotic cells induced by different agents vary in their expression of MHC and costimulatory genes. Molecular immunology *42*, 1033-1042.

Manolova, V., Flace, A., Bauer, M., Schwarz, K., Saudan, P., and Bachmann, M.F. (2008). Nanoparticles target distinct dendritic cell populations according to their size. Eur J Immunol *38*, 1404-1413.

Marin-Muller, C., Li, M., Chen, C., and Yao, Q. (2009). Current understanding and potential immunotherapy for HIV-associated squamous cell carcinoma of the anus (SCCA). World J Surg *33*, 653-660.

Marshall, J.D., Fearon, K.L., Higgins, D., Hessel, E.M., Kanzler, H., Abbate, C., Yee, P., Gregorio, J., Cruz, T.D., Lizcano, J.O.*, et al.* (2005). Superior activity of the type C class of ISS in vitro and in vivo across multiple species. DNA and cell biology *24*, 63-72.

Martinez-Pomares, L., and Gordon, S. (2012). CD169+ macrophages at the crossroads of antigen presentation. Trends in immunology *33*, 66-70.

Masopust, D., and Schenkel, J.M. (2013). The integration of T cell migration, differentiation and function. Nat Rev Immunol *13*, 309-320.

Maus, M.V., Fraietta, J.A., Levine, B.L., Kalos, M., Zhao, Y., and June, C.H. (2014). Adoptive immunotherapy for cancer or viruses. Annu Rev Immunol *32*, 189-225.

McEwan, W.A., Tam, J.C., Watkinson, R.E., Bidgood, S.R., Mallery, D.L., and James, L.C. (2013). Intracellular antibody-bound pathogens stimulate immune signaling via the Fc receptor TRIM21. Nat Immunol *14*, 327-336.

McHeyzer-Williams, M., Okitsu, S., Wang, N., and McHeyzer-Williams, L. (2012). Molecular programming of B cell memory. Nat Rev Immunol *12*, 24-34.

Meeks, M., and Bush, A. (2000). Primary ciliary dyskinesia (PCD). Pediatric pulmonology *29*, 307-316.

Melenhorst, J.J., and Barrett, A.J. (2011). Tumor vaccines and beyond. Cytotherapy *13*, 8-18.

Mellman, I., Coukos, G., and Dranoff, G. (2011). Cancer immunotherapy comes of age. Nature *480*, 480-489.

Menges, M., Baumeister, T., Rossner, S., Stoitzner, P., Romani, N., Gessner, A., and Lutz, M.B. (2005). IL-4 supports the generation of a dendritic cell subset from murine bone marrow with altered endocytosis capacity. Journal of leukocyte biology *77*, 535-543.

Mescher, M.F. (1992). Surface contact requirements for activation of cytotoxic T lymphocytes. J Immunol *149*, 2402-2405.

Miga, A.J., Masters, S.R., Durell, B.G., Gonzalez, M., Jenkins, M.K., Maliszewski, C., Kikutani, H., Wade, W.F., and Noelle, R.J. (2001). Dendritic cell longevity and T cell persistence is controlled by CD154-CD40 interactions. Eur J Immunol *31*, 959-965.

Miller, J.C., Brown, B.D., Shay, T., Gautier, E.L., Jojic, V., Cohain, A., Pandey, G., Leboeuf, M., Elpek, K.G., Helft, J.*, et al.* (2012). Deciphering the transcriptional network of the dendritic cell lineage. Nat Immunol *13*, 888-899.

Min-Oo, G., Kamimura, Y., Hendricks, D.W., Nabekura, T., and Lanier, L.L. (2013). Natural killer cells: walking three paths down memory lane. Trends in immunology *34*, 251-258.

Montecalvo, A., Shufesky, W.J., Stolz, D.B., Sullivan, M.G., Wang, Z., Divito, S.J., Papworth, G.D., Watkins, S.C., Robbins, P.D., Larregina, A.T., and Morelli, A.E. (2008). Exosomes as a short-range mechanism to spread alloantigen between dendritic cells during T cell allorecognition. J Immunol *180*, 3081-3090.

Moon, J.J., Chu, H.H., Pepper, M., McSorley, S.J., Jameson, S.C., Kedl, R.M., and Jenkins, M.K. (2007). Naive CD4(+) T cell frequency varies for different epitopes and predicts repertoire diversity and response magnitude. Immunity *27*, 203-213.

Mount, A.M., Smith, C.M., Kupresanin, F., Stoermer, K., Heath, W.R., and Belz, G.T. (2008). Multiple dendritic cell populations activate CD4+ T cells after viral stimulation. PloS one *3*, e1691.

Mueller, S.N., Gebhardt, T., Carbone, F.R., and Heath, W.R. (2013). Memory T cell subsets, migration patterns, and tissue residence. Annu Rev Immunol *31*,

137-161.

Nair, S., Archer, G.E., and Tedder, T.F. (2012). Isolation and generation of human dendritic cells. Curr Protoc Immunol *Chapter 7*, Unit7 32.

Nakayamada, S., Takahashi, H., Kanno, Y., and O'Shea, J.J. (2012). Helper T cell diversity and plasticity. Curr Opin Immunol *24*, 297-302.

Naslund, T.I., Gehrmann, U., Qazi, K.R., Karlsson, M.C., and Gabrielsson, S. (2013). Dendritic cell-derived exosomes need to activate both T and B cells to induce antitumor immunity. J Immunol *190*, 2712-2719.

Neefjes, J., Jongsma, M.L., Paul, P., and Bakke, O. (2011). Towards a systems understanding of MHC class I and MHC class II antigen presentation. Nat Rev Immunol *11*, 823-836.

Obar, J.J., Khanna, K.M., and Lefrancois, L. (2008). Endogenous naive CD8+ T cell precursor frequency regulates primary and memory responses to infection. Immunity *28*, 859-869.

Oelke, M., Maus, M.V., Didiano, D., June, C.H., Mackensen, A., and Schneck, J.P. (2003). Ex vivo induction and expansion of antigen-specific cytotoxic T cells by HLA-Ig-coated artificial antigen-presenting cells. Nat Med *9*, 619-624.

Ohkura, N., Kitagawa, Y., and Sakaguchi, S. (2013). Development and maintenance of regulatory T cells. Immunity *38*, 414-423.

Oldenhove, G., Bouladoux, N., Wohlfert, E.A., Hall, J.A., Chou, D., Dos Santos, L., O'Brien, S., Blank, R., Lamb, E., Natarajan, S.*, et al.* (2009). Decrease of Foxp3+ Treg cell number and acquisition of effector cell phenotype during lethal infection. Immunity *31*, 772-786.

Overwijk, W.W., and Restifo, N.P. (2001). B16 as a mouse model for human melanoma. Curr Protoc Immunol *Chapter 20*, Unit 20 21.

Pages, F., Galon, J., Karaschuk, G., Dudziak, D., Camus, M., Lazar, V., Camilleri-Broet, S., Lagorce-Pages, C., Lebel-Binay, S., Laux, G.*, et al.* (2005). Epstein-Barr virus nuclear antigen 2 induces interleukin-18 receptor expression in B cells. Blood *105*, 1632-1639.

Parham, P., and Janeway, C. (2009). The immune system, 3rd edn (London ; New York: Garland Science).

Parkin, J., and Cohen, B. (2001). An overview of the immune system. Lancet *357*, 1777-1789.

Pearce, E.J., and Everts, B. (2015). Dendritic cell metabolism. Nat Rev Immunol *15*, 18-29.

Pfeifer, J.D., Wick, M.J., Roberts, R.L., Findlay, K., Normark, S.J., and Harding, C.V. (1993). Phagocytic processing of bacterial antigens for class I MHC presentation to T cells. Nature *361*, 359-362.

Pitt, J.M., Charrier, M., Viaud, S., Andre, F., Besse, B., Chaput, N., and Zitvogel, L. (2014). Dendritic cell-derived exosomes as immunotherapies in the fight against cancer. J Immunol *193*, 1006-1011.

Pooley, J.L., Heath, W.R., and Shortman, K. (2001). Cutting edge: intravenous soluble antigen is presented to CD4 T cells by CD8- dendritic cells, but cross-presented to CD8 T cells by CD8+ dendritic cells. J Immunol *166*, 5327-5330.

Postow, M.A., Callahan, M.K., and Wolchok, J.D. (2015). Immune Checkpoint Blockade in Cancer Therapy. J Clin Oncol.

Prakken, B., Wauben, M., Genini, D., Samodal, R., Barnett, J., Mendivil, A., Leoni, L., and Albani, S. (2000). Artificial antigen-presenting cells as a tool to exploit the immune 'synapse'. Nat Med *6*, 1406-1410.

Prlic, M., Hernandez-Hoyos, G., and Bevan, M.J. (2006). Duration of the initial TCR stimulus controls the magnitude but not functionality of the CD8+ T cell response. J Exp Med *203*, 2135-2143.

Provinciali, M. (2009). Immunosenescence and cancer vaccines. Cancer Immunol Immunother *58*, 1959-1967.

Quezada, S.A., and Peggs, K.S. (2013). Exploiting CTLA-4, PD-1 and PD-L1 to reactivate the host immune response against cancer. British journal of cancer *108*, 1560-1565.

Radbruch, A., Muehlinghaus, G., Luger, E.O., Inamine, A., Smith, K.G., Dorner, T., and Hiepe, F. (2006). Competence and competition: the challenge of becoming a long-lived plasma cell. Nat Rev Immunol *6*, 741-750.

Ramirez-Olivencia, G., Valencia-Ortega, M.E., Martin-Carbonero, L., Moreno-Celda, V., and Gonzalez-Lahoz, J. (2009). [Malignancies in HIV infected patients:

study of 139 cases]. Med Clin (Barc) *133*, 729-735.

Reddy, S.T., van der Vlies, A.J., Simeoni, E., Angeli, V., Randolph, G.J., O'Neil, C.P., Lee, L.K., Swartz, M.A., and Hubbell, J.A. (2007). Exploiting lymphatic transport and complement activation in nanoparticle vaccines. Nat Biotechnol *25*, 1159-1164.

Reizis, B., Bunin, A., Ghosh, H.S., Lewis, K.L., and Sisirak, V. (2011). Plasmacytoid dendritic cells: recent progress and open questions. Annu Rev Immunol *29*, 163-183.

Rosenberg, S.A. (2004). Development of effective immunotherapy for the treatment of patients with cancer. Journal of the American College of Surgeons *198*, 685-696.

Rosenberg, S.A., Yannelli, J.R., Yang, J.C., Topalian, S.L., Schwartzentruber, D.J., Weber, J.S., Parkinson, D.R., Seipp, C.A., Einhorn, J.H., and White, D.E. (1994). Treatment of patients with metastatic melanoma with autologous tumor-infiltrating lymphocytes and interleukin 2. J Natl Cancer Inst *86*, 1159-1166.

Sahin, U., Tureci, O., and Pfreundschuh, M. (1997). Serological identification of human tumor antigens. Curr Opin Immunol *9*, 709-716.

Sallusto, F., and Lanzavecchia, A. (1994). Efficient presentation of soluble antigen by cultured human dendritic cells is maintained by granulocyte/macrophage colony-stimulating factor plus interleukin 4 and downregulated by tumor necrosis factor alpha. J Exp Med *179*, 1109-1118.

Sallusto, F., Lanzavecchia, A., Araki, K., and Ahmed, R. (2010). From vaccines to memory and back. Immunity *33*, 451-463.

Satpathy, A.T., Wu, X., Albring, J.C., and Murphy, K.M. (2012). Re(de)fining the dendritic cell lineage. Nat Immunol *13*, 1145-1154.

Schmid, D.A., Irving, M.B., Posevitz, V., Hebeisen, M., Posevitz-Fejfar, A., Sarria, J.C., Gomez-Eerland, R., Thome, M., Schumacher, T.N., Romero, P.*, et al.* (2010). Evidence for a TCR affinity threshold delimiting maximal CD8 T cell function. J Immunol *184*, 4936-4946.

Schreiber, R.D., Old, L.J., and Smyth, M.J. (2011). Cancer immunoediting: integrating immunity's roles in cancer suppression and promotion. Science *331*,

1565-1570.

Segura, E., Guerin, C., Hogg, N., Amigorena, S., and Thery, C. (2007). CD8+ dendritic cells use LFA-1 to capture MHC-peptide complexes from exosomes in vivo. J Immunol *179*, 1489-1496.

Segura, E., Nicco, C., Lombard, B., Veron, P., Raposo, G., Batteux, F., Amigorena, S., and Thery, C. (2005). ICAM-1 on exosomes from mature dendritic cells is critical for efficient naive T-cell priming. Blood *106*, 216-223.

Shirota, Y., Shirota, H., and Klinman, D.M. (2012). Intratumoral injection of CpG oligonucleotides induces the differentiation and reduces the immunosuppressive activity of myeloid-derived suppressor cells. J Immunol *188*, 1592-1599.

Slifka, M.K., and Whitton, J.L. (2000). Antigen-specific regulation of T cell-mediated cytokine production. Immunity *12*, 451-457.

Sofra, V., Mansour, S., Liu, M., Gao, B., Primpidou, E., Wang, P., and Li, S. (2009). Antigen-loaded ER microsomes from APC induce potent immune responses against viral infection. Eur J Immunol *39*, 85-95.

Speiser, D.E., Utzschneider, D.T., Oberle, S.G., Munz, C., Romero, P., and Zehn, D. (2014). T cell differentiation in chronic infection and cancer: functional adaptation or exhaustion? Nat Rev Immunol *14*, 768-774.

Sprent, J., Miller, J.F., and Mitchell, G.F. (1971). Antigen-induced selective recruitment of circulating lymphocytes. Cell Immunol *2*, 171-181.

Sprent, J., and Surh, C.D. (2011). Normal T cell homeostasis: the conversion of naive cells into memory-phenotype cells. Nat Immunol *12*, 478-484.

Starr, T.K., Jameson, S.C., and Hogquist, K.A. (2003). Positive and negative selection of T cells. Annu Rev Immunol *21*, 139-176.

Steinman, R.M., and Cohn, Z.A. (1973). Identification of a novel cell type in peripheral lymphoid organs of mice. I. Morphology, quantitation, tissue distribution. J Exp Med *137*, 1142-1162.

Storni, T., Ruedl, C., Schwarz, K., Schwendener, R.A., Renner, W.A., and Bachmann, M.F. (2004). Nonmethylated CG motifs packaged into virus-like particles induce protective cytotoxic T cell responses in the absence of systemic side effects. J Immunol *172*, 1777-1785.

Tan, C., and Gery, I. (2012). The unique features of Th9 cells and their products. Critical reviews in immunology *32*, 1-10.

Tangye, S.G., Ma, C.S., Brink, R., and Deenick, E.K. (2013). The good, the bad and the ugly - TFH cells in human health and disease. Nat Rev Immunol *13*, 412-426.

Taylor, P.A., Lees, C.J., Fournier, S., Allison, J.P., Sharpe, A.H., and Blazar, B.R. (2004). B7 expression on T cells down-regulates immune responses through CTLA-4 ligation via T-T interactions [corrections]. J Immunol *172*, 34-39.

Thery, C., Duban, L., Segura, E., Veron, P., Lantz, O., and Amigorena, S. (2002). Indirect activation of naive CD4+ T cells by dendritic cell-derived exosomes. Nat Immunol *3*, 1156-1162.

Thery, C., Ostrowski, M., and Segura, E. (2009). Membrane vesicles as conveyors of immune responses. Nat Rev Immunol *9*, 581-593.

Turvey, S.E., and Broide, D.H. (2010). Innate immunity. J Allergy Clin Immunol *125*, S24-32.

Utsugi-Kobukai, S., Fujimaki, H., Hotta, C., Nakazawa, M., and Minami, M. (2003). MHC class I-mediated exogenous antigen presentation by exosomes secreted from immature and mature bone marrow derived dendritic cells. Immunol Lett *89*, 125-131.

van den Boorn, J.G., and Hartmann, G. (2013). Turning tumors into vaccines: co-opting the innate immune system. Immunity *39*, 27-37.

van der Vlist, E.J., Nolte-'t Hoen, E.N., Stoorvogel, W., Arkesteijn, G.J., and Wauben, M.H. (2012). Fluorescent labeling of nano-sized vesicles released by cells and subsequent quantitative and qualitative analysis by high-resolution flow cytometry. Nature protocols *7*, 1311-1326.

Viaud, S., Thery, C., Ploix, S., Tursz, T., Lapierre, V., Lantz, O., Zitvogel, L., and Chaput, N. (2010). Dendritic cell-derived exosomes for cancer immunotherapy: what's next? Cancer Res *70*, 1281-1285.

Vincent-Schneider, H., Stumptner-Cuvelette, P., Lankar, D., Pain, S., Raposo, G., Benaroch, P., and Bonnerot, C. (2002). Exosomes bearing HLA-DR1 molecules need dendritic cells to efficiently stimulate specific T cells. Int Immunol *14*,

713-722.

Vremec, D., O'Keeffe, M., Wilson, A., Ferrero, I., Koch, U., Radtke, F., Scott, B., Hertzog, P., Villadangos, J., and Shortman, K. (2011). Factors determining the spontaneous activation of splenic dendritic cells in culture. Innate immunity *17*, 338-352.

Wakim, L.M., and Bevan, M.J. (2011). Cross-dressed dendritic cells drive memory CD8+ T-cell activation after viral infection. Nature *471*, 629-632.

Whiteside, T.L. (2010). Immune responses to malignancies. J Allergy Clin Immunol *125*, S272-283.

Wieckowski, E.U., Visus, C., Szajnik, M., Szczepanski, M.J., Storkus, W.J., and Whiteside, T.L. (2009). Tumor-derived microvesicles promote regulatory T cell expansion and induce apoptosis in tumor-reactive activated CD8+ T lymphocytes. J Immunol *183*, 3720-3730.

Williams, L.A., Egner, W., and Hart, D.N. (1994). Isolation and function of human dendritic cells. International review of cytology *153*, 41-103.

Williams, M.A., and Bevan, M.J. (2004). Shortening the infectious period does not alter expansion of CD8 T cells but diminishes their capacity to differentiate into memory cells. J Immunol *173*, 6694-6702.

Williams, M.A., and Bevan, M.J. (2007). Effector and memory CTL differentiation. Annu Rev Immunol *25*, 171-192.

Wolchok, J.D., Kluger, H., Callahan, M.K., Postow, M.A., Rizvi, N.A., Lesokhin, A.M., Segal, N.H., Ariyan, C.E., Gordon, R.A., Reed, K.*, et al.* (2013). Nivolumab plus ipilimumab in advanced melanoma. The New England journal of medicine *369*, 122-133.

Wong, P., and Pamer, E.G. (2003). Feedback regulation of pathogen-specific T cell priming. Immunity *18*, 499-511.

Xiao, Z., Casey, K.A., Jameson, S.C., Curtsinger, J.M., and Mescher, M.F. (2009). Programming for CD8 T cell memory development requires IL-12 or type I IFN. J Immunol *182*, 2786-2794.

Xu, Y., Zhan, Y., Lew, A.M., Naik, S.H., and Kershaw, M.H. (2007). Differential development of murine dendritic cells by GM-CSF versus Flt3 ligand has

implications for inflammation and trafficking. J Immunol *179*, 7577-7584.
Yang, J., Sundrud, M.S., Skepner, J., and Yamagata, T. (2014). Targeting Th17 cells in autoimmune diseases. Trends in pharmacological sciences *35*, 493-500.
Yewdell, J.W. (2010). Designing CD8+ T cell vaccines: it's not rocket science (yet). Curr Opin Immunol *22*, 402-410.
Yi, H.J., and Lu, G.X. (2012). Adherent and non-adherent dendritic cells are equivalently qualified in GM-CSF, IL-4 and TNF-alpha culture system. Cell Immunol *277*, 44-48.
Zippelius, A., Batard, P., Rubio-Godoy, V., Bioley, G., Lienard, D., Lejeune, F., Rimoldi, D., Guillaume, P., Meidenbauer, N., Mackensen, A.*, et al.* (2004). Effector function of human tumor-specific CD8 T cells in melanoma lesions: a state of local functional tolerance. Cancer Res *64*, 2865-2873.
Zitvogel, L., Regnault, A., Lozier, A., Wolfers, J., Flament, C., Tenza, D., Ricciardi-Castagnoli, P., Raposo, G., and Amigorena, S. (1998). Eradication of established murine tumors using a novel cell-free vaccine: dendritic cell-derived exosomes. Nat Med *4*, 594-600.
Zoglmeier, C., Bauer, H., Norenberg, D., Wedekind, G., Bittner, P., Sandholzer, N., Rapp, M., Anz, D., Endres, S., and Bourquin, C. (2011). CpG blocks immunosuppression by myeloid-derived suppressor cells in tumor-bearing mice. Clin Cancer Res *17*, 1765-1775.